AD NUMBER

AD063539

NEW LIMITATION CHANGE

TO

Approved for public release, distribution unlimited

FROM

Distribution authorized to U.S. Gov't. agencies and their contractors; Administrative/Operational Use; 1954. Other requests shall be referred to Office of the Chief of Research and Development, Department of the Army, Washington, DC 20310.

AUTHORITY

OCRD D/A memo dtd 28 Mar 1968

FC

Final Report
Office of Ordnance Research Contract
DA-30-069-ORD-459

Internal Friction of Metal Single Crystals

School of Engineering
Columbia University
New York 27, N. Y.

TABLE OF CONTENTS

Section I

Introduction

During the period of this contract, studies of the internal friction of single crystals were made. The principle investigator was Dr. T. A. Read, Professor of Metallurgy, and the chief contributors were H. Birnbaum, D. Frankl, M. Levy, M. Metzger, S. Shapiro, and S. Zirinsky, members of the scientific staff, Metallurgy Department, Columbia University.

The work was chiefly designed to utilize the internal friction measurements as a tool for the examination of the properties of single crystals. The investigations can be divided into several phases; the investigation of the effect of thermal treatment on single crystals (M. Levy, M. Metzger, S. Shapiro), the investigation of the effect of torsional deformation (H. Birnbaum, M. Levy), the investigation of the effect of X-Ray irradiation on Sodium Chloride single crystals (D. Frankl), and the investigation of the temperature dependence of the elastic moduli of Au-Cd crystals.

Section 2

Experimental Procedure

The internal friction measurements were all made by the composite piezoelectric oscillator method[41], using as transducer a Straubel-cut quartz rod having contacting electrodes of chemically deposited silver and electroplated gold. The specimen and transducer were cemented together under light finger pressure with either phenyl salicylate applied at room temperature or a beeswax-rosin mixture applied at about 70°C. The assembly was suspended in a vacuum chamber by fine horizontal wires engaging small transverse nicks located at the displacement node of the quartz, these suspensions serving also as electrical contacts.

The specimens were adjusted in length so as to have, within a few tenths of one percent in most cases, the same resonant frequencies as the transducers with which they were used. Under these conditions, since the systems were very nearly perfectly elastic, the amplitude distribution was quite closely a sinusoidal half-wave in each part of the composite oscillator.

The equivalent series electric circuit constants of the composite oscillator were measured at room temperature near the fundamental resonance frequency--about 70 to 80 KC for the five transducers used--by a capacitance bridge fed from a stable variable frequency transitron type oscillator. From the equivalent constants, the decrement and maximum strain amplitude are calculated by the formulae given in general form by Read[2] and reducing in the present case of one half wavelength in each part of the composite oscillator to

$$\Delta = \frac{4R}{Kf_0M} - \frac{M_0\Delta_q}{M} \tag{1}$$

$$U = \frac{(1.25K)^{1/2}}{f_0L}\ \frac{E}{R} \times 10^3 \tag{2}$$

where

Δ = Ratio of energy dissipated per half cycle in the specimen to energy stored in the specimen; Δ is used throughout as the measure of the internal friction and is called the "decrement".

R = equivalent resistance of the composite oscillator, in ohms.

K = 8 x ratio of equivalent inductance to mass of the composite oscillator, in henries/gm. This is a constant for a given transducer, provided that the specimen and transducer frequencies are properly matched.

f_o = resonant frequency of the composite oscillator, in $sec.^{-2}$

M = mass of the specimen, in gms.

U = maximum strain amplitude in the specimen

L = length of the specimen, in cm.

E = RMS voltage applied to the transducer

Subscript q denotes quantity for the transducer.

The formulae (1) and (2) are derived on the assumption that the specimen is a homogeneous anelastic body, by equating the appropriate mechanical energy terms to the corresponding electrical energy terms, the electric current being the displacement current in the transducer. Actually, since the dissipation is observed to vary with the strain amplitude, and since the latter in turn varies along the length of the specimen rod, the specimen is, in effect, an inhomogeneous material under the conditions of measurement. However, it has been shown by Nowick[7] that, under conditions of negligible dissipative coupling of higher modes of vibration, formulae

of the type (1) and (2) are applicable. In the present work we assume, in view of the low values of the decrement observed, that these conditions are fulfilled.

The quantities M_q, $\mathcal{E}_q$, and K are determined for each transducer, the latter by means of the variation of impedance with frequency near resonance. Each point on an internal friction curve is then obtained from measurements of the resistance at resonance, by means of the bridge, and of the applied voltage, by means of a Ballantine vacuum-tube voltmeter.

The range of measurements was limited in all cases by the available driving voltage. In the earlier measurements, this limit was about 2.5 volts, but later the signal generator was modified to raise this to 4.0 volts, about the maximum to which the bridge resistors could safely be subjected.

Also measured in some cases were small but significant changes in the Young's modulus of the specimen with changes in driving voltage; the resulting shifts in resonant frequency were measured by means of a small calibrated tuning condenser in the tank circuit of the signal generator.

Section 3

Effect of Annealing on the Internal Friction of Copper and Aluminum Single Crystals

Results

A. Copper Crystals

1. Effect of impurity content

Fig. 1 shows the curves of internal friction versus maximum strain amplitude for four single crystals of differing nickel content following an anneal for 24 hours at 1050°C. The curves for these crystals show that the decrement and the strain amplitude dependence of the 99.999% copper sample are the greatest, and that both decrease as the impurity content is increased to 0.10 atomic percent nickel.

It may be noted from Fig. 1 that the lowest measured decrement was of the order of 10^{-4} observed for the sample with greatest content. In all subsequent measurements made in this investigation, for similar previous histories, the lowest decrements were always observed in samples of highest impurity content. After long period high temperature anneals this decrement was approximately 10^{-4}. On the other hand, even after long high temperature anneals, the decrement of the highest purity samples was 5×10^{-4} to 5×10^{-3} in agreement with previous work on highest purity copper[7].

2. Effects of thermal history

In previous investigations it has been observed that the strain amplitude dependent internal friction is sensitive to the previous thermal history of the samples. However, the only conclusion which may be drawn from the available information is that the internal friction of an annealed crystal is lower than that of a freshly grown crystal. Even though the dislocation pattern may be stabilized by sufficient annealing at a given temperature, the concentration of solute atoms near the dislocations and the concentration of vacancies in the crystal may be altered by annealing at different temperatures. In order to study these processes, an investigation was made of

the effect on the internal friction of annealing the single crystals at various temperatures.

First, the samples were annealed under vacuum of 10^{-5}mm. Hg for 96 hours at 1000°C and cooled at a rate of 75°C/hr. to room temperature. In all cases, this long time treatment resulted in the lowest and flattest curves of decrement versus strain amplitude obtained for the particular crystal, see Fig. 2, curve A. Subsequent anneals at 1000°C produced insignificant changes from these results.

Figs. 2, 3, 4, 5, 6, 7 show the results for anneals at 250°C and 450°C following the high temperature anneals. Cooling to room temperature was done at approximately the same rate as from the high temperature. The 250°C anneal produced little change from the starting curves. However, annealing at 450°C always increased the level of internal friction. In addition, there was usually a marked increase in the strain amplitude dependence. Following this, annealing for 24 hours at 1000°C and slowly cooling to room temperature nearly recovered the original high temperature annealing curve. Examples are shown in Figs. 2 and 5. On some occasions, annealing for 24 hours at 250°C and slowly cooling to room temperature was effective in lowering the internal friction after an anneal at 450°C, see Figs. 3 and 7.

In order to determine if this behavior of internal friction with annealing temperature was a function solely of the annealing temperature, samples were inserted into the furnace directly at either 450°C or 250°C for 24 hours, or taken first to 900°C for 24 hours, then slowly cooled to either 250°C, 450°C, or 750°C, held for 20 hours and slowly cooled to room temperature. Typical results are shown in Figs. 6 and 7. The behavior of the internal friction with annealing temperature was the same in both cases and must then have been a function solely

of the final annealing temperature. Fig. 8 is a cross plot of the data of Fig. 7. This behavior was observed regardless of the impurity content of the specimen.

A general characteristic of the results following all thermal treatments was that the internal friction decreased with time. Ordinarily it was slow, amounting to only several percent over a day. The greatest decreases usually were observed in samples containing the most nickel. Figs. 2, 4, and 5 illustrate this decrease following a 450°C anneal and slowly cooling to room temperature. The 99.999% sample shows a slight decrease, whereas the crystals with .08 atomic percent Ni and 0.10 atomic percent Ni show large decreases.

B. Aluminum Crystals

The decrements of the aluminum single crystals varied between 10^{-5} and 10^{-4}. Even in the as grown condition and after cutting and polishing, the decrements were only rarely above 10^{-4}. Subsequent anneals near the melting point always resulted in a reduction of the internal friction. In general, reproducibility in results obtained with aluminum crystals was better than that obtained using copper single crystals. In spite of the fact that the aluminum single crystals showed some handling effects whereas the copper single crystals showed little or no handling effects, these effects in aluminum disappeared quickly even at room temperature. It was also found for the heat treatments used, that little difference appeared in the behavior of crystals of the two different purities used. Typical results for a crystal in the as grown condition are shown in Fig. 9.

The samples were annealed at 640°C, and slowly cooled to room temperature, air cooled to room temperature, or water quenched to room temperature. Results for three crystals are shown in Figs. 9, 10 and 11. It will be noted that the greatest strain amplitude dependence was observed when the samples were cooled slowly to room temperature. The air cooled behavior showed less amplitude dependence. In

contrast, following water quenching, the samples exhibited low, very flat curves of internal friction vs. strain amplitude.

The samples were then quenched from 550°C, 450°C, and 350°C after being annealed at these temperatures for 24 hours. In order to erase the effects of previous treatments the samples were first annealed at 640°C for a day then very slowly cooled to the final annealing temperatures. Typical results for this series of thermal treatments are shown in Fig. 12. The striking feature of these curves is that the level of internal friction increases as the quenching temperature is reduced.

Following quenching from 640°C, several samples were given short time anneals at various temperatures from 175°C to 640°C. They were all air cooled from the annealing temperatures. These results are shown in Fig. 13. It is to be noted that as the annealing temperature was raised, the internal friction at room temperature became more strain amplitude dependent and increased in level until the annealing temperatures reached 525°C. For temperatures of 525°C and 640°C the internal friction, however, was reduced in level and showed a smaller strain amplitude dependence.

Discussion

A. Copper Single Crystals

Cottrell[24] has shown that the energy of elastic interaction of a solute atom with an edge dislocation for distances greater than several atom spacings from the dislocation line is given by:

$$V = \frac{4}{3}\,\frac{(1+\nu)}{(1-\nu)}\; G\, r_a^{3} b\, \frac{\sin\alpha}{r}\quad\left(\frac{r_b - r_a}{r_a}\right)$$

where

V = the interaction energy

ν = Poisson's ratio $\doteq$ 0.33 for copper[38]

G = the shear modulus $\doteq 4 \times 10^{11}$ dynes/cm^2 for copper[38]

r_a = atomic radius of the solvent atom = 1.28 Å for copper[39]

r_b = atomic radius of the solute atom = 1.24 Å for nickel[39]

b = strength of the dislocation $\doteq$ 2.5 Å

α = angle from the slip plane of the dislocation

r = distance from the center of the dislocation

Substitution of these values yields approximately $\frac{0.10}{r(\text{Å})}$ ev. for the energy of interaction of a nickel atom with an edge dislocation in copper. The concentration of nickel atoms in the vicinity of the dislocations is given by $C_{oe}^{\,V/kT}$ where C_o is the overall concentration of nickel atoms, V is the interaction energy given above, k is the Boltzmann constant and T is the absolute temperature o. These relations indicate that nickel atoms preferentially segregate in the vicinity of dislocations in the crystals, and that the concentration of nickel atoms at any given distance from the dislocation lines will be directly proportional to the overall nickel concentration in the crystal. In order for the dislocations to move

freely under the applied stress, either the solute atoms must diffuse with the dislocations, or the dislocations must be torn free of the solute atoms. Since the measurements of internal friction were all made at room temperature, where the diffusion rate of nickel in copper is extremely low[40], the solute atoms remain essentially fixed during a cycle of vibration.

The observations shown in Fig. 1 are qualitatively completely consistent with these conclusions. Since no hysteresis in the decrement versus strain amplitude curves were observed when the strain amplitude was increased, then decreased, it is evident that the dislocations were not torn free of their impurity atmospheres. Thus, as the nickel content increased, the level and the strain amplitude dependence of the internal friction decreased showing that the mobility of the dislocations had been reduced by the addition of nickel. Evidence for the low interaction energy of nickel atoms with dislocations in copper is also given in these results, for it is seen that only the crystal containing 0.10 atomic percent nickel exhibited the low, flat decrement versus strain amplitude curve characteristic of crystals in which the dislocations have been thoroughly pinned.

An analysis of the data of Fig. 1 also shows that the decrement for a given strain amplitude is proportional to C_0^{-x} where C_0 is the overall atom fraction of nickel atoms and x varies between 0.35 and 0.6. Koehler, in his theoretical treatment found the decrement to be proportional to C_0^{-4}, while Weertman obtained the decrement to be proportional to $C_0^{-14/9}$. The comparison would indicate that the nature of impurity atom pinning of dislocations is as yet not clearly understood.

An analysis of the results obtained in the study of the effects of thermal history on the internal friction may also be made assuming the solute atoms distribute according to the Boltzman relation. However, in order to insure that such an analysis is valid, it must first be established that the configuration of the

dislocations is not altered by the thermal treatments. Therefore, before any sequence of annealing treatments was made, the crystals were all annealed for long periods at 900°C - 1000°C. Subsequent annealing for 24 hours at these temperatures produced only minor changes in the internal friction. In addition, the results obtained did not depend on the exact manner in which the crystals were taken to the annealing temperatures of interest. No differences were observed whether the crystals were inserted directly at the desired annealing temperature or first inserted at 900°C and then slowly cooled to the final annealing temperature. These observations indicate that the dislocation configuration did remain unaltered during the thermal treatments and that the observed effects of thermal history are to be associated with other imperfections present.

If a Boltzmann distribution of impurity atoms is assumed, the equilibrium concentration of impurity atoms near dislocations would be the least at the highest annealing temperature. As the crystal is cooled, impurity atoms diffuse to the dislocations. However, at some point in the cooling process the rate of diffusion will be insufficient to maintain the equilibrium concentration of impurity atoms at the dislocation. Thus, on subsequent annealing at lower temperatures the impurity atom distribution would more closely approach the equilibrium distribution for these temperatures.

Some of the effects observed in the copper single crystals may be attributed to this type of behavior. The internal friction following annealing at 450°C was always lower than that after annealing at 750°C. Annealing at 250°C always yielded a lower internal friction than annealing at 450°C. But by the same argument, the highest internal friction should have been observed after annealing at 900°C, whereas, the lowest internal friction was always observed after the 900°C anneal. This behavior suggests that a second mechanism may operate at the high temperature.

B. Aluminum Single Crystals

The results obtained on the aluminum single crystal also cannot be accounted for on the basis of the solute atom dislocation interaction outlined above. It is to be expected that the highest concentration of impurity atoms near dislocations would exist after the crystals had been cooled to room temperature at the lowest rate, and, therefore, that the internal friction would be lower and less strain amplitude dependent for a slowly cooled crystal than for a crystal which had been cooled rapidly. However, it was observed that when the crystals were slowly cooled to room temperature, they exhibited higher and more strain amplitude dependent internal friction than when they were rapidly cooled to room temperature. The results obtained after annealing and quenching from various temperatures also show a reverse effect. On the basis of a Boltzmann distribution, it is to be expected that the impurity atom concentrations near the dislocations would increase as the annealing temperature was decreased. The increased concentration would result in a lowering of the internal friction. However, the observations showed that the lower the temperature at which the samples were annealed, the higher was the internal friction.

After being cooled rapidly from 640°C the aluminum single crystals were annealed at various low temperatures for short times. Here, the initial state was a high temperature state. In this case one would expect that during the low temperature anneals, impurity atoms would diffuse into the dislocations and reduce the level and strain amplitude dependence of the internal friction. However, just the opposite was observed, for as the annealing temperature was raised from 175°C to 420°C the internal friction increased and became more strain amplitude dependent. When the annealing temperature was raised to 520°C, the internal friction and strain amplitude dependence began to decrease, and both decreased further when the samples were annealed at 640°C. The maximum in internal friction with annealing

temperature again appeared as it had in copper. These results also indicate that another mechanism must operate at the higher temperatures.

Since the results obtained in this investigation cannot be simply accounted for on the basis of the solute atom dislocation interaction generally assumed, it is necessary to examine more carefully the conditions existing within materials having the face-centered cubic structure. The dislocations in crystals of this structure may be separated into two groups. The first includes those dislocations which exist in aggregates forming the subgrain boundaries in the crystals, while the second comprises those dislocations existing within the subgrains. The latter are probably mainly responsible for the energy dissipation within a vibrating solid. On the basis of the Read-Shockley dislocation model of a low angle grain boundary, the boundaries would consist of linear arrays of edge dislocations and, as has been noted earlier, it is likely that principally extended dislocations exist within the subgrains. Suzuki has suggested, the strain field about an extended dislocation in a face-centered cubic crystal is considerably weaker than the field about a screw or edge dislocation. Therefore, the interaction energy of solute atoms with dislocations which form the subgrain boundaries in a crystal will be much greater than the interaction energy of solute atoms with the extended dislocations within subgrains. Thus, under equilibrium conditions, the concentration of solute atoms within subgrains would decrease as the temperature was lowered. Cooling rapidly from any annealing temperature would leave more solute atoms within the subgrains than would cooling slowly. The concentration of impurity atoms at the dislocations within the subgrains would be greatest for the most rapid cooling, and the internal friction of a crystal would, therefore, be lower and less strain amplitude dependent after the crystal had been cooled rapidly than it would be after the crystal had been cooled slowly to room temperature. In a series of

observations in which a crystal was rapidly cooled from various annealing temperatures, the internal friction would decrease as the annealing temperature was raised. These conclusions are all consistent with the results obtained for the aluminum single crystals.

The results shown in Fig. 13 for the effects of low temperature annealing on a sample which had previously been quenced from a high temperature are also consistent with the above ideas. At the low temperatures, impurities diffuse away from the dislocations within the subgrains, some of the excess impurity atoms diffusing into the dislocations which form the subgrain walls of the crystal. As a result, the internal friction measured at room temperature increases. After the crystal had been annealed at the higher temperature, the internal friction was observed to decrease, i.e., the internal friction reached a maximum with annealing temperature in the neighborhood of 500°C. At the higher temperature of annealing impurity atoms diffuse out of the subgrain boundaries to increase the concentration within the subgrains. On cooling, more impurity atoms are available for pinning the mobile dislocations existing within the subgrains, and the internal friction is reduced.

The results obtained for the variation of room temperature internal friction of copper single crystals with annealing treatment are consistent with those obtained for aluminum. Essentially, the same behavior was observed except that for copper the behavior was found even when the crystals were cooled slowly from the annealing temperatures.

As previously discussed for the results on the aluminum crystals, the existence of two preferential sites for solute atoms in a crystal leads to a decrease with temperature of the concentration of solute atoms in the regions within the subgrains. Cooling slowly from any given annealing temperature will result in a concentration of impurity atoms in these regions corresponding to an equilibrium temperature

somewhat lower than the annealing temperature, this "equilibrium temperature" depending on the diffusion rates of the impurity atoms. For slower diffusing elements it will be closer to the annealing temperature than for rapidly diffusing atoms. During the process of cooling to room temperature, some of the solute atoms in these regions will diffuse into the dislocations within the subgrains. The greatest concentration exists after annealing at the highest temperature, so that the most solute atom pinning is exhibited after annealing at the highest temperature, 900°C. Thus, the internal friction following a 900°C anneal is lower and less amplitude dependent than that following a 750°C anneal.

Since the concentration within the subgrains decays exponentially with temperature, the concentration of solute atoms at 450°C is not very different from the concentration at 750°C. However, a greater proportion of the impurity atoms available for pinning the dislocations within the subgrains diffuse into these dislocations at 450°C than at 750°C. The internal friction after annealing at 450°C is lower than the internal friction after annealing at 750°C. A similar interpretation holds for the relation between the internal frictions following a 250°C and 450°C anneal. Thus, a maximum in the internal friction with annealing temperature may be expected.

Results for the effects of annealing temperature and cooling rate from the annealing temperature on the stress strain curves of zinc single crystals have been reported by Li, Washburn, and Parker[43]. In the range of temperature investigated, it was found that the room temperature yield stress increased as the annealing temperature was raised. Increasing the cooling rate from a given temperature of anneal also increased the yield strength of the crystal. These observations showed that the effects were not altered by the intentional addition of small amounts of either copper or nitrogen to the zinc crystals, but did seem to be affected by the subgrain structure of the crystals. It may be concluded that the dislocations producing slip were more difficult to move when the annealing

temperature was raised or the cooling rate from the annealing temperature was increased. There is then a general parallelism between observations of Li, Washburn and Parker, and those of the present investigation.

Effect of quenching copper crystals from high temperature

An unusual effect was obtained when the copper crystals were quenched in water to room temperature after being annealed for 24 hours at 1050°C. This behavior is shown in Fig. 14 to 18. During approximately the first hour after quenching, the internal friction decreased and thereafter, it increased. Even after 24 hours the internal friction showed no signs of leveling off. This behavior was observed in all crystals regardless of purity. On but one occasion was a different behavior observed following the quench. In this case, shown in Fig. 14, the internal friction decreased in approximately six hours to a stable value.

For the annealing treatment, the samples were sealed under vacuum in fused silica tubes. In order to quench the specimens, it was necessary to break the tubes under water. In the one test in which the internal friction did not rise with time, the quench was noticeably slower due to difficulty in cracking the tube. This would indicate that the internal friction rise after approximately one hour is to be associated with a rapid quench.

The shapes of the curves of internal friction vs. time following the quench suggest that two processes take place simultaneously. The effect of one process is to decrease the internal friction with time, while the other produces an increase of the internal friction with time. Since the samples were quenched from near 1000°C, an excess of vacancies was present over the equilibrium vacancy concentration at room temperature. The excess vacancies, after forming pairs, could diffuse rapidly to screw dislocations forming jogs on the dislocations. The jogs, acting as pinning points, would reduce the mobility of the dislocations and thus lower the internal friction.

The second process which results in an increase of the internal friction with time may be due to stresses introduced by the inhomogeneous rapid cooling. As these stresses are relieved, the dislocations become more mobile, so that the internal friction would increase with time.

V. BIBLIOGRAPHY

1. C. Zener, "Elasticity and Anelasticity of Metals", Univ. of Chic. Press (1948)

2. T. A. Read, Phys. Rev. 58, 371 (1940)

3. T. A. Read and E. P. T. Tyndall, J. Appl. Phys. 17, 713 (1946)

4. I. H. Swift and J. E. Richardson, J. Appl. Phys. 18, 417 (1947)

5. A. S. Newick, "Pittsburgh Symposium on Plastic Deformation of Crystalline Solids", Mellon Inst. (1950)

6. J. Marx and J. S. Keehler, ibid.

7. J. Weertman and J. S. Keehler, J. Appl. Phys. 24, 624 (1953)

8. G. I. Taylor, Proc. Roy. Soc. A 145, 362, 388, 405 (1934)

9. A. H. Cottrell, "Dislocations and Plastic Flow in Crystals", Oxford Univ. Press, Lond. (1953)

10. F. C. Frank, "Pittsburgh Symposium on Plastic Deformation of Crystalline Solids", Mellon Inst. (1950)

11. A. R. Verma, S. Amelinckx, Nature 167, 939 (1951)

12. A. J. Forty, Phil. Mag. 42, 670 (1951)

13. A. J. Forty, Phil. Mag. 43, 481 (1952)

14. A. J. Forty, Phil. Mag. 44, (1953)

15. A. H. Cottrell, Chap. 5 of B. Chalmers "Progress in Metal Physics IV", Interscience Publishers Inc., N.Y. (1953)

16. W. T. Read, Jr., Dislocations in Crystals", McGraw-Hill Co., Inc., N.Y. (1953)

17. F. C. Frank, Physics 15, 131 (1949)

18. A. E. H. Love, "Mathematical Theory of Elasticity", 4th Ed., pp. 221 ff., Dover Publications, N.Y. (1944)

19. J. M. Burgers, Proc. Roy. Acad. Sci. Amsterdam 42, 293, 378 (1939)

20. R. W. Cahn, Rep. Conf. on Strength of Solids, Phys. Soc. Lond., p. 30 (1948)

21. W. T. Read, Jr. and W. Sheckley, "Pittsburgh Symposium on Plastic Deformation of Crystalline Solids", Mellon Inst. (1950)

22. K. T. Aust and B. Chalmers, Proc. Roy. Soc. A 204, 359 (1950)

23. P. Lacombe, Rep. Conf. on Strength of Solids, Phys. Soc. Lond., p. 91 (1948)

24. A. H. Cottrell, "Bristol Conference on the Strength of Solids", p. 30, Phys. Soc. Lond., (1948)

25. H. Suzuki, Sci. Rep., Tohoku Univ., A 4, 455 (1952)

26. R. D. Heidenreich and W. Sheckley, Report on Strength of Solids, Phys. Soc. Lond., p. 57 (1948)

27. J. O. Linde, B. Lindell and C. H. Stade, Ark. for Fys. 2, 89 (1950)

28. P. Tury and S. Krausz, Nature 138, 331 (1936)

29. P. Bartlett and G. Diennes, Phys. Rev. 89, 848 (1953)

30. J. S. Koehler, "Imperfections in Nearly Perfect Crystals", John Wiley and Sons, Inc., N.Y. (1952)

31. J. D. Eshelby, Proc. Roy. Soc. Lond. A 297, 396 (1949)

32. F. Seitz, "Pittsburgh Symposium on Plastic Deformation of Crystalline Solids", Mellon Inst. (1950)

33. F. R. N. Nabarro, Proc. Roy. Soc. A 209, 279 (1951)

34. A. S. Newick, Chap. I of B. Chalmers "Progress in Metal Physics IB", Interscience Publishers Inc., N.Y. (1953)

35. J. Weertman, private communication to T. A. Read.

36. H. H. Kellogg, private communication

37. S. L. Quimby, Phys. Rev. 25, 558 (1925)

38. E. Schmid and W. Boas, "Plasticity of Crystals" (1935): English trans. publ. by F. A. Hughes and Co. Ltd., Lond. (1950)

39. W. Hume-Rothery, "The Structure of Metals and Alloys", Inst. Metals Monograph and Report Series, No. 1, 1944

40. C. J. Smithells, "Metals Reference Book", Interscience Publishers Inc., N.Y. (1949)

41. C. H. Li, J. Washburn and E. R. Parker, J. Met. 5, 1223 (953)

An investigation was made to determine the effect of solute atoms on the internal friction due to dislocation scources. It has been suggested by Cottrell that solute atoms will interact elastically with dislocations in crystals. Due to this interaction, the mobility of dislocations would be reduced by the presence of solute atoms. It is commonly assumed that the strain amplitude dependent internal friction originates from the movement of dislocations in the crystal. Therefore, it is to be expected that solute atoms would reduce the internal friction.

The investigation was carried out using 99.999 percent cadmium single crystals and alloy single crystals containing up to 0.01 atomic percent mercury. All crystals were grown by the Bridgman technique.

X-ray Laue patterns were taken of all crystals to obtain the crystal orientations. It was observed that the Laue spots were very sharp, indicating a low imperfection density.

The samples were all annealed near the melting point and then slowly cooled to room temperature to determine a reference level of internal friction. The crystals were then reannealed near the melting point and quenched in water at room temperature. After this thermal treatment, the internal friction of the sample of highest purity showed no change with time. The level of internal friction was approximately that after the crystal had been slowly cooled to room temperature. However, the decrements of all samples containing mercury decreased with time. This difference in behavior attributed to the presence of the mercury atoms. At the high temperature these impurity atoms are nearly uniformly distributed throughout the crystall lattice. After quenching to room temperature, the mercury atoms diffuse to dislocation sites to reduce the dislocation mobilities. The data was shown to agree with the relation derived by Zener for the diffusion of solute atoms into a cylindrical precipitate.

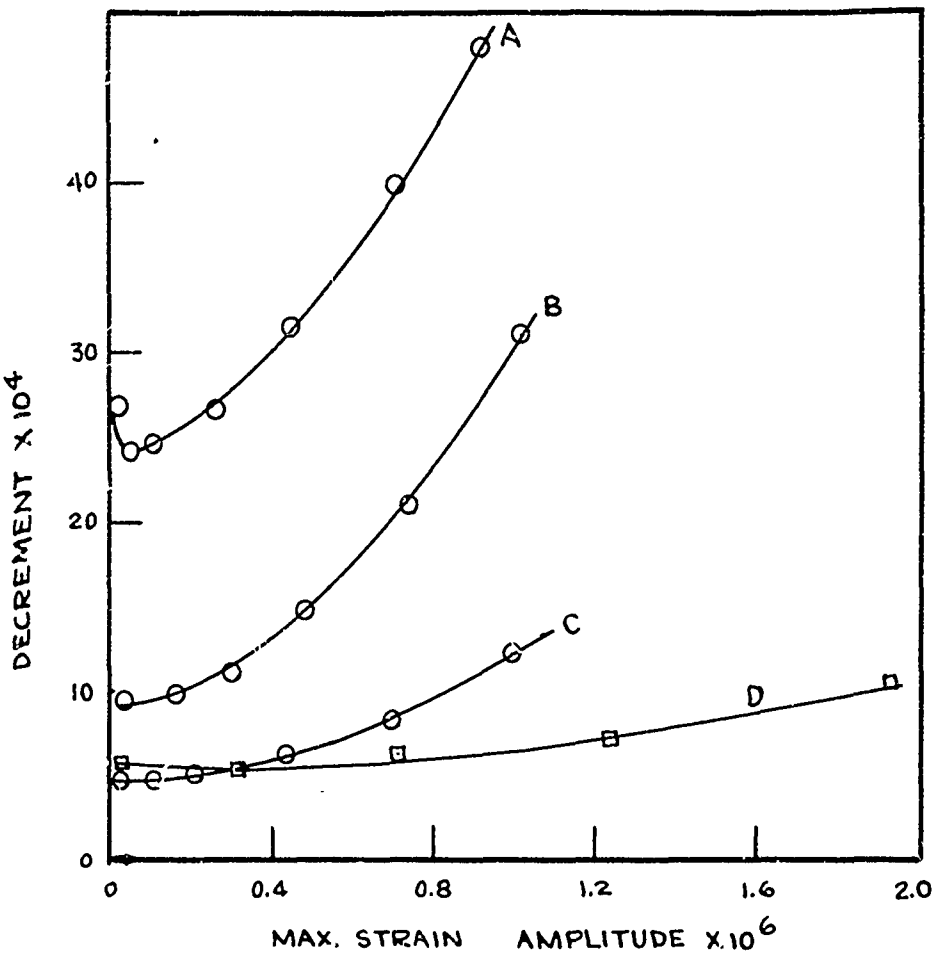

FIGURE 1

Effect of nickel content on the internal friction of copper base single crystals..

A. 99.999 per cent copper

B.. 0.01 atomic per cent nickel

C.. 0.08 atomic per cent nickel

D.. 0.10 atomic per cent nickel

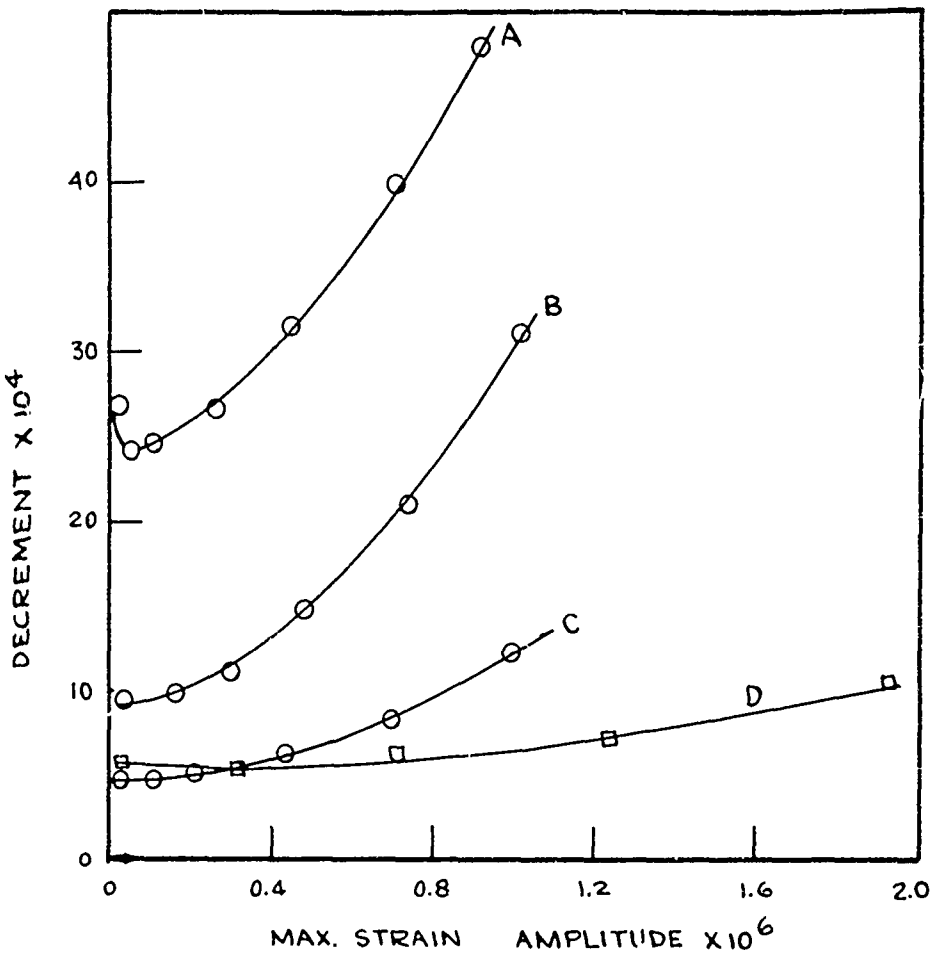

FIGURE 1

Effect of nickel content on the internal friction of copper base single crystals..

A. 99.999 per cent copper

B. 0.01 atomic per cent nickel

C. 0.08 atomic per cent nickel

D. 0.10 atomic per cent nickel

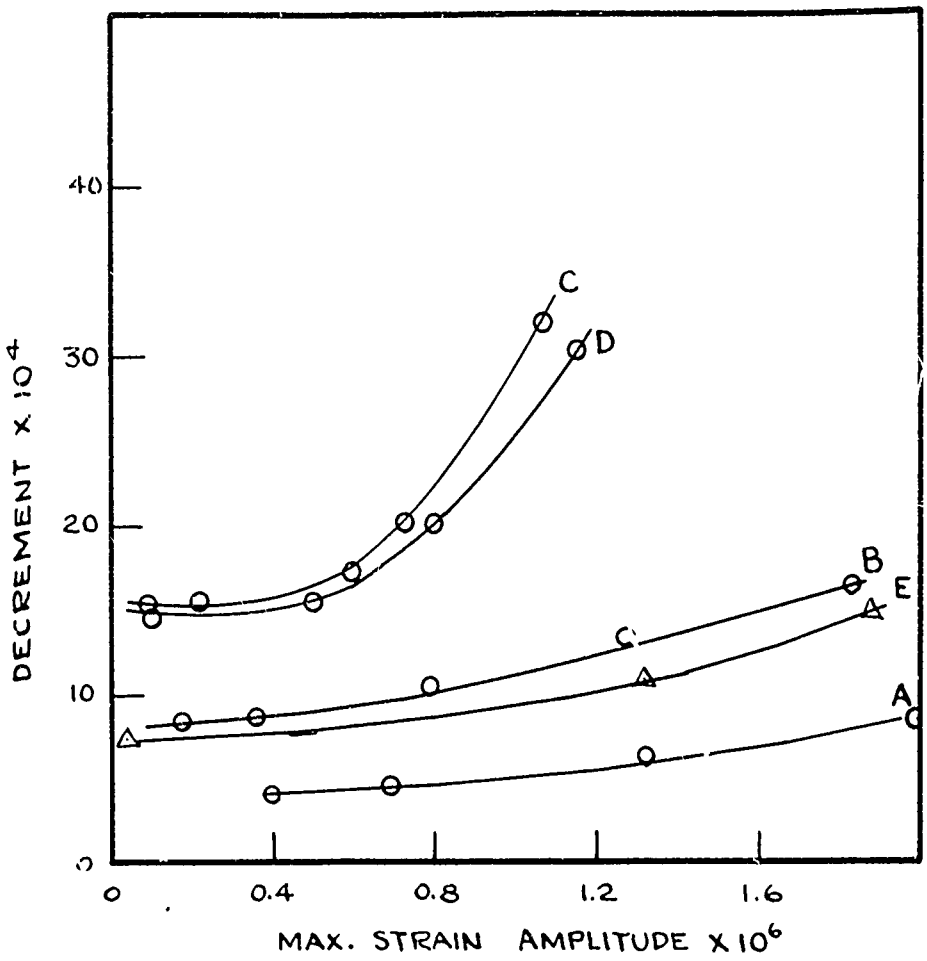

FIGURE 2

Effect of annealing temperature on the internal friction of a 99.999 per cent copper single crystal. Tests made in order indicated.

A. 96 hours at 1000°C.

B. 40 hours at 250°C.

C. 40 hours at 450°C.

D. 20 hours at 25°C.

E. 24 hours at 1000°C.

Crystal cooled to room temperature at the rate of 75°C per hour in all tests.

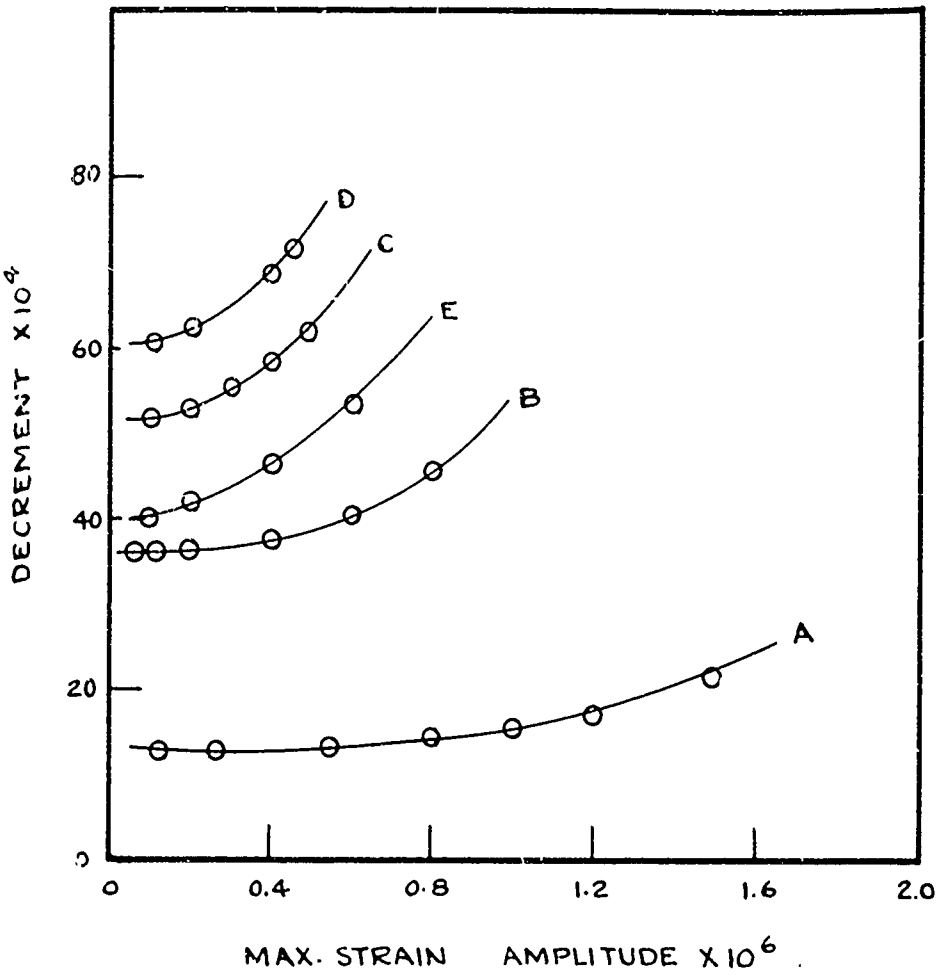

FIGURE 3

Effect of annealing temperature on the internal friction of 99.999 percent copper single crystal.. Tests made in order indicated..

A.. 24 hours at 250°C..

B.. 24 hours at 450°C..

C.. Additional 48 hours at 450°C..

D.. Additional 24 hours at 450°C.

E.. 24 hours at 250°C.

Crystal cooled to room temperature at the rate of 75°C per hour in all tests.

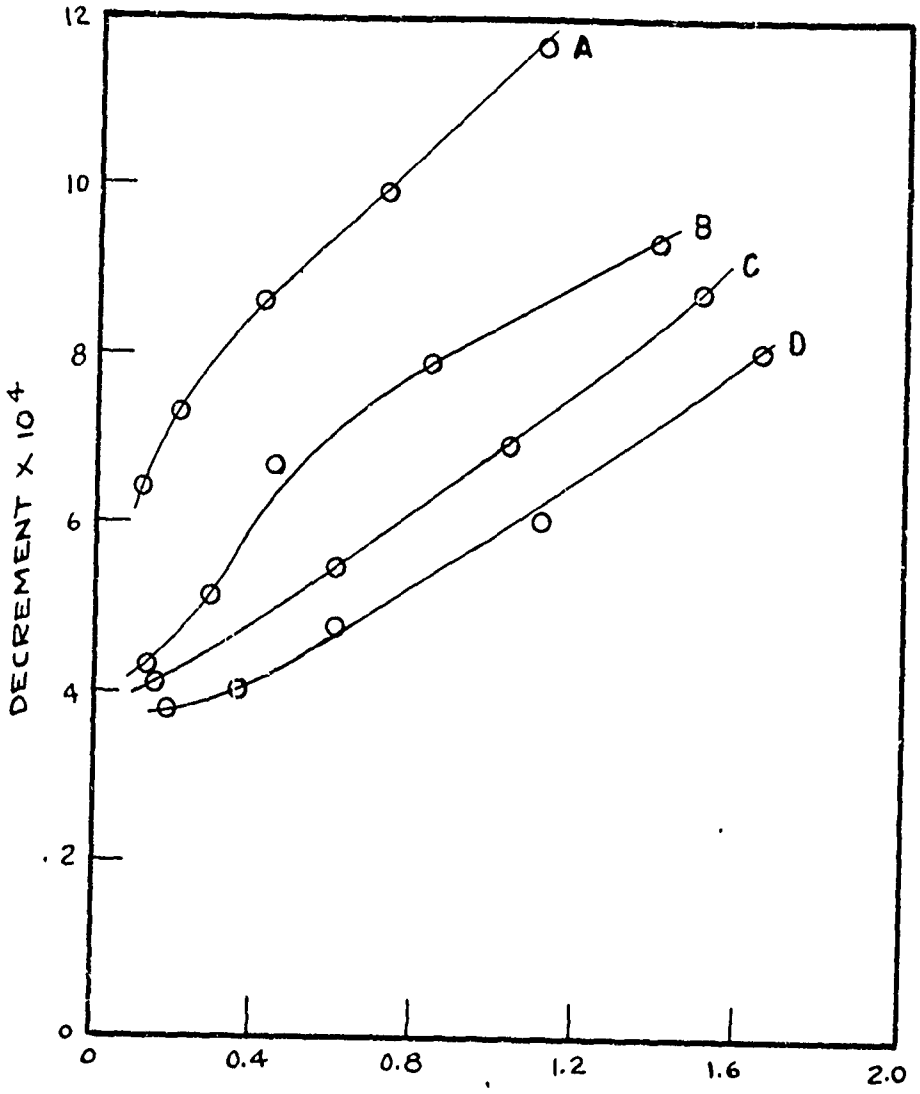

FIGURE 4

Effect of annealing temperature on the internal friction of a copper single crystal containing 0.08 atomic percent nickel.. Tests made in order indicated..

A.. 24 hours at 250°C..

B.. 40 hours at 450°C..

C.. 15 hours at 25°C..

D.. Additional 25 hours at 25°C..

Crystal cooled to room temperature at the rate of 100°C per hour in all tests.

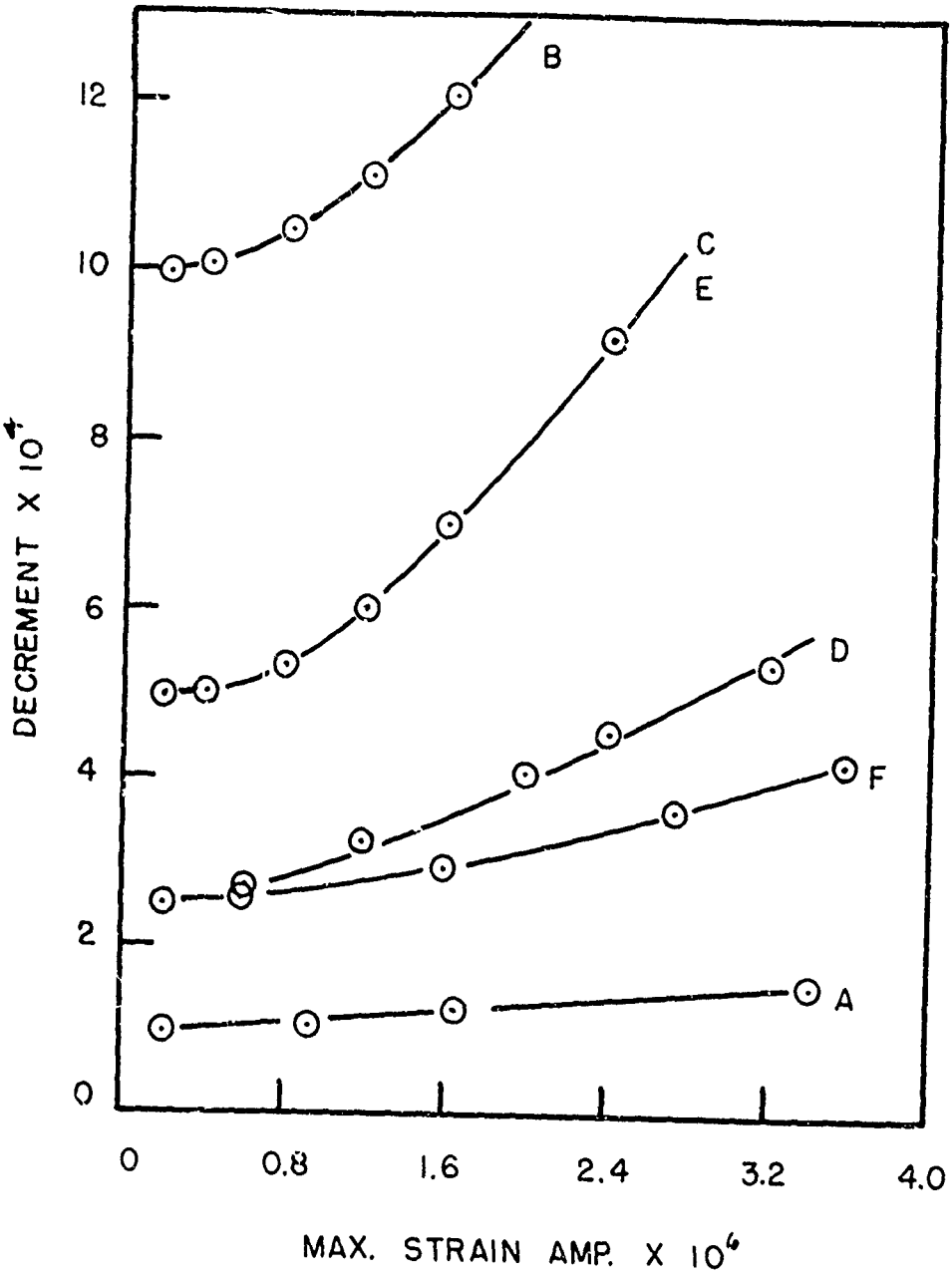

FIGURE 5

Effect of annealing temperature on the internal friction of a copper single crystal containing 0.10 atomic per cent nickel. Tests made in order indicated.

A. 28 hours at 900°C. D. 21 hours at 900°C.

B. 40 hours at 450°C. E. 1½ hours at 450°C.

C. 15 hours at 250°C. F. 21 hours at 900°C.

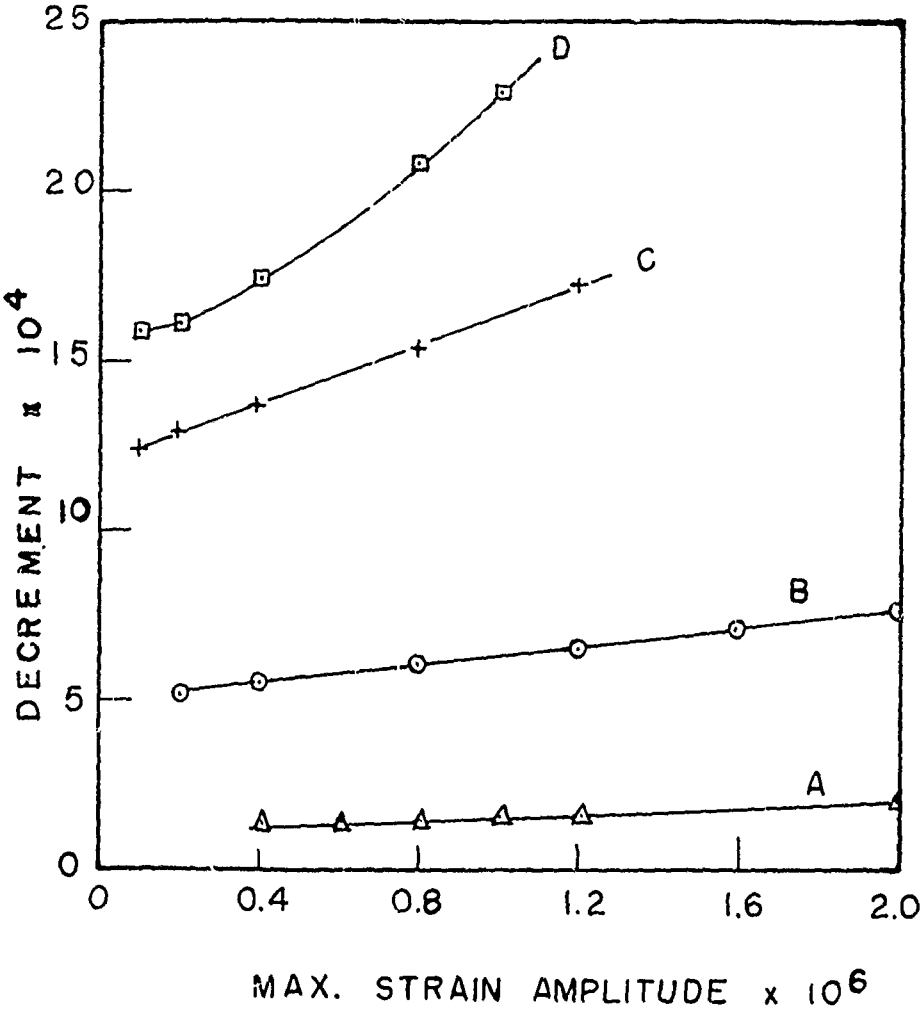

FIGURE 6

Effect of annealing temperature on the internal friction of a copper single crystal containing 0.10 atomic per cent nickel. Tests made in order indicated.

A. 24 hours at 250°C.

B. 24 hours at 450°C.

C. Additional 24 hours at 450°C.

D. Additional 48 hours at 450°C.

Crystal cooled to room temperature at the rate of 75°C per hour in all tests.

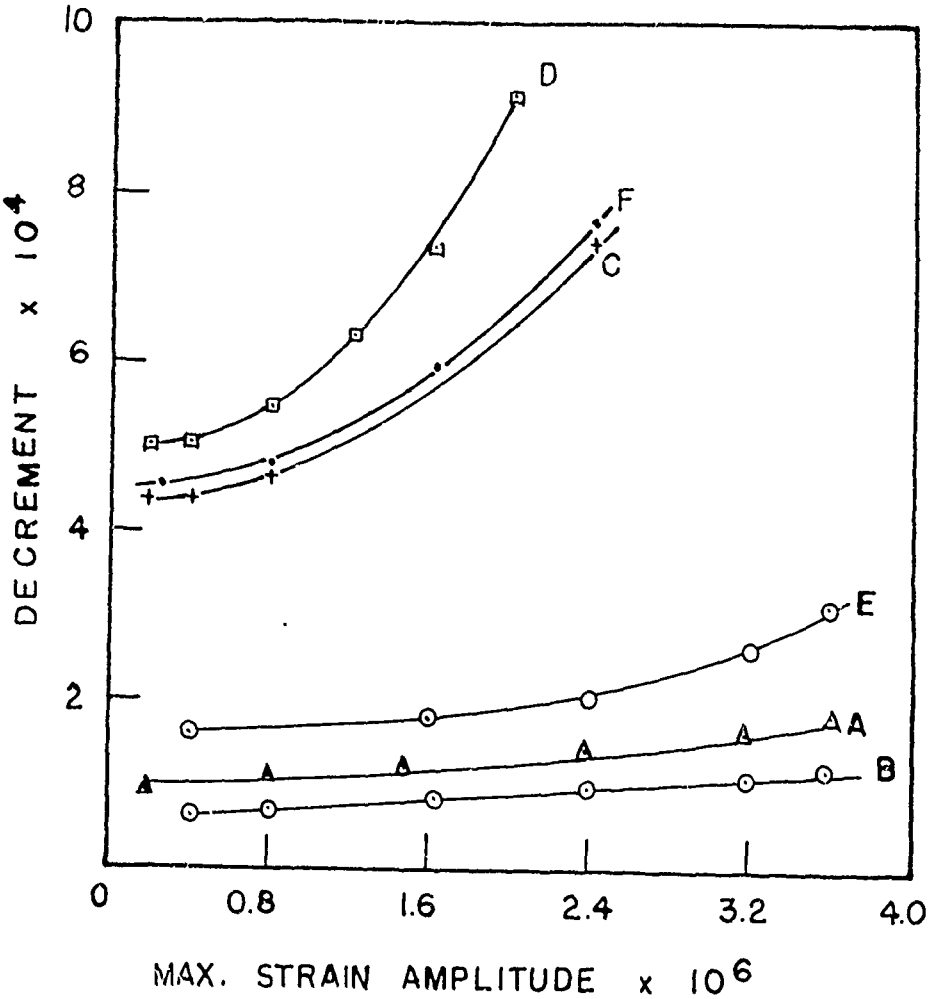

FIGURE 7

Effect of annealing on the internal friction of a copper single crystal containing 0.10 atomic per cent nickel. Crystal annealed 24 hours at 900°C and cooled at the rate of 100°C per hour to the final annealing temperature.

A. 24 hours at 900°C.
B. 24 hours at 250°C.
C. 24 hours at 450°C.
D. 24 hours at 750°C.
E. 24 hours at 250°C.
F. 24 hours at 450°C.

Crystal cooled to room temperature at the rate of 100°C per hour in all tests.

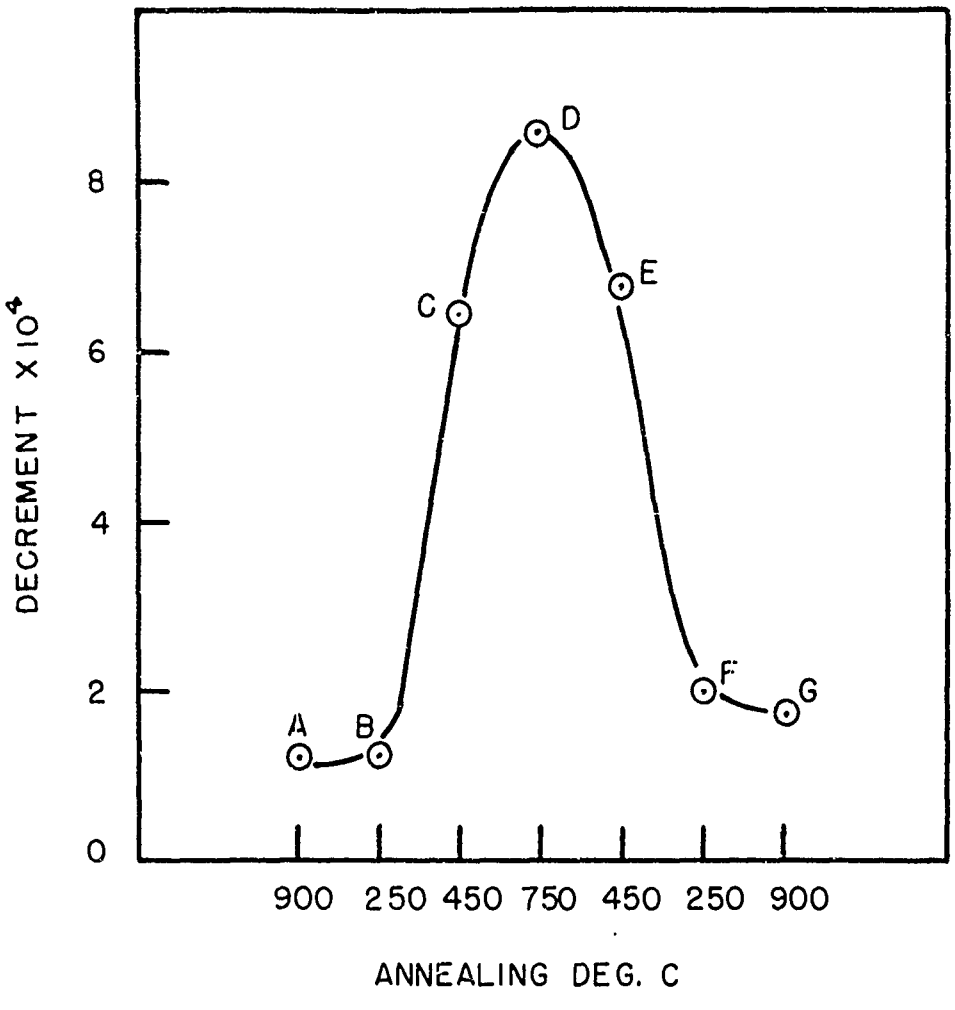

FIGURE 8

Cross-plot of data of figure 7 at the maximum strain amplitude of 2×10^{-6}. Letters indicate order of tests.

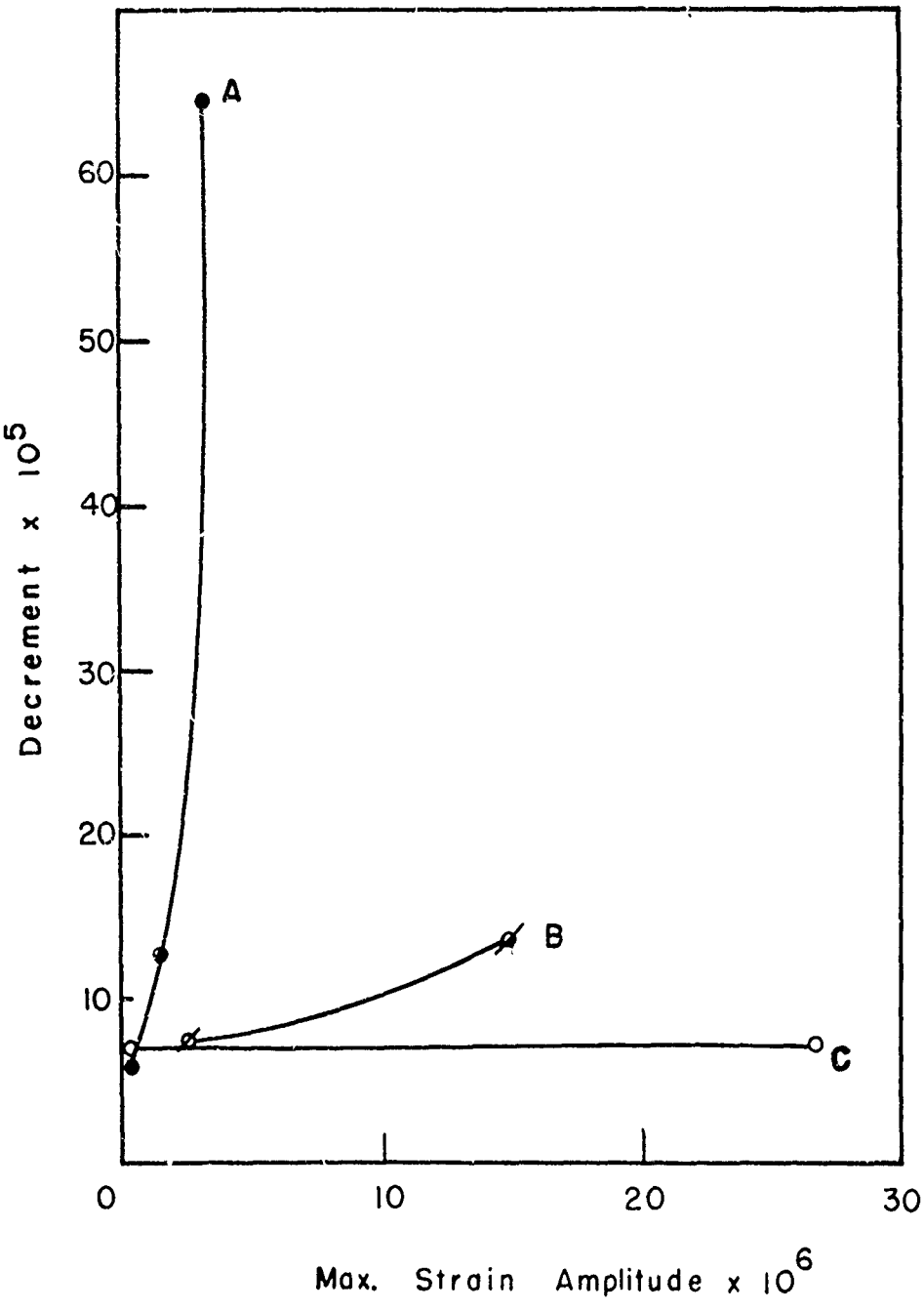
A
B
C
60
50
40
30
20
10
0
10
20
30
Decrement x 10^5
Max. Strain Amplitude x 10^6

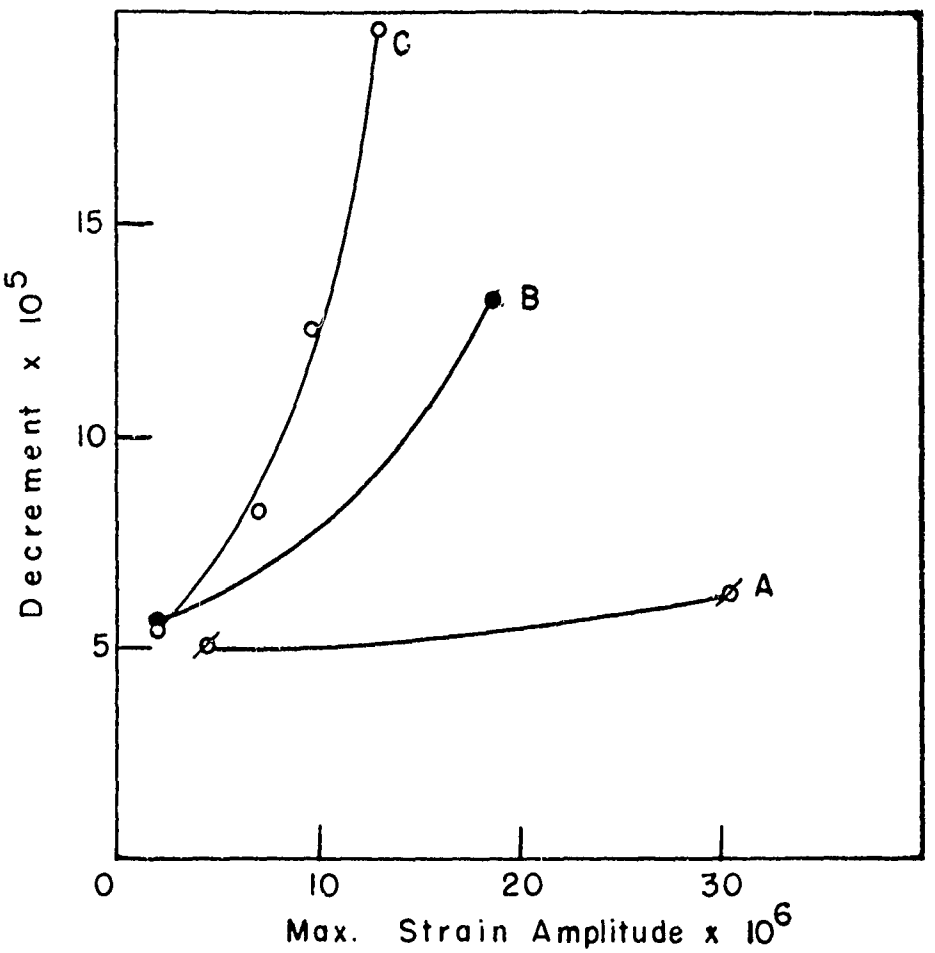

FIGURE 10

Effect of the rate of cooling from the annealing temperature of 640°C on the internal friction of aluminum single crystal Y-4..

A.. Quenched into water at room temperature..

B.. Air cooled to room temperature..

C.. Cooled at the rate of 50°C per hour to room temperature..

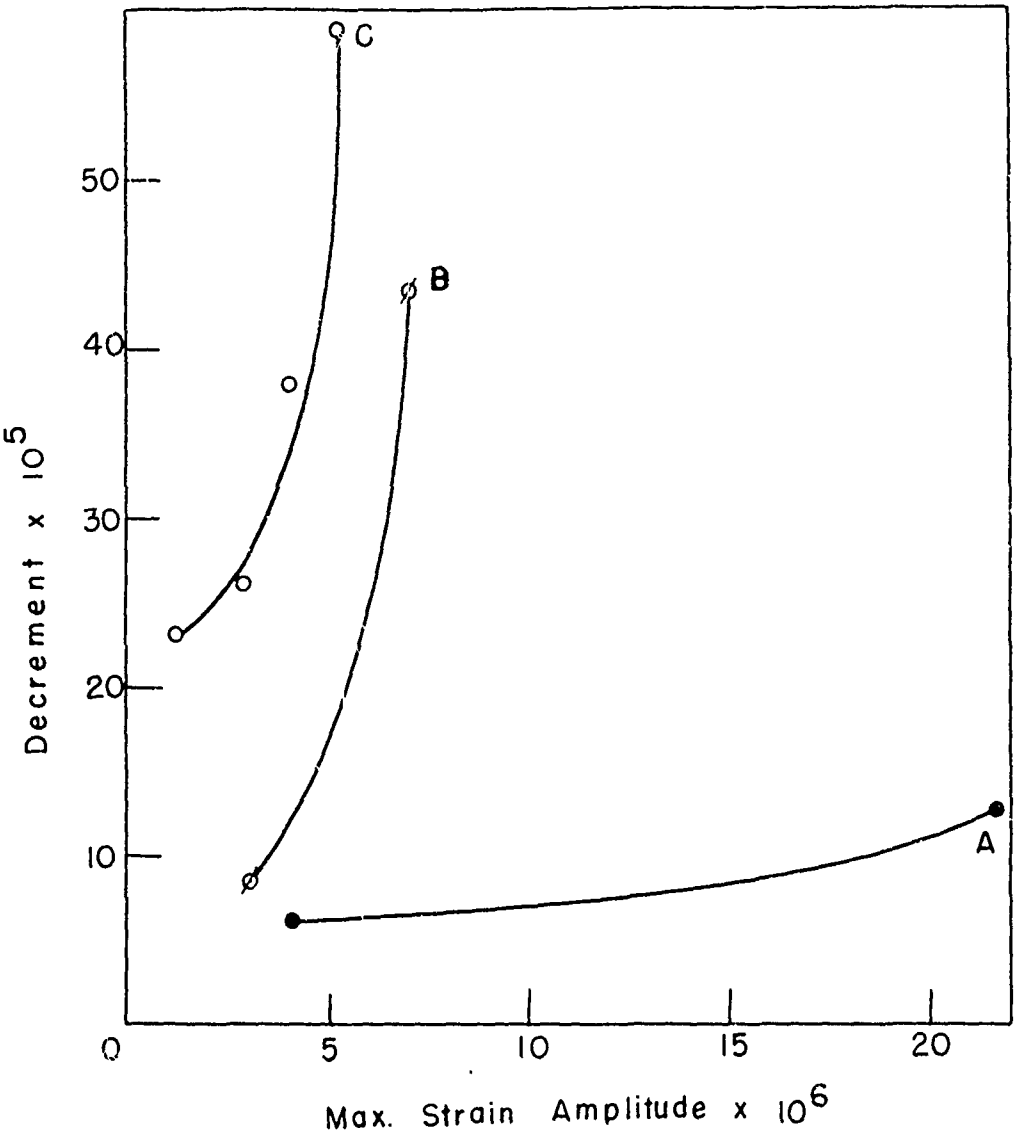

FIGURE 11

Effect of the rate of cooling from the annealing temperature of 640°C on the internal friction of aluminum crystal Y-1.

A. Quenched into water at room temperature.

B. Cooled at the rate of 50°C per hour to room temperature.

C. Cooled to room temperature in 16 days.

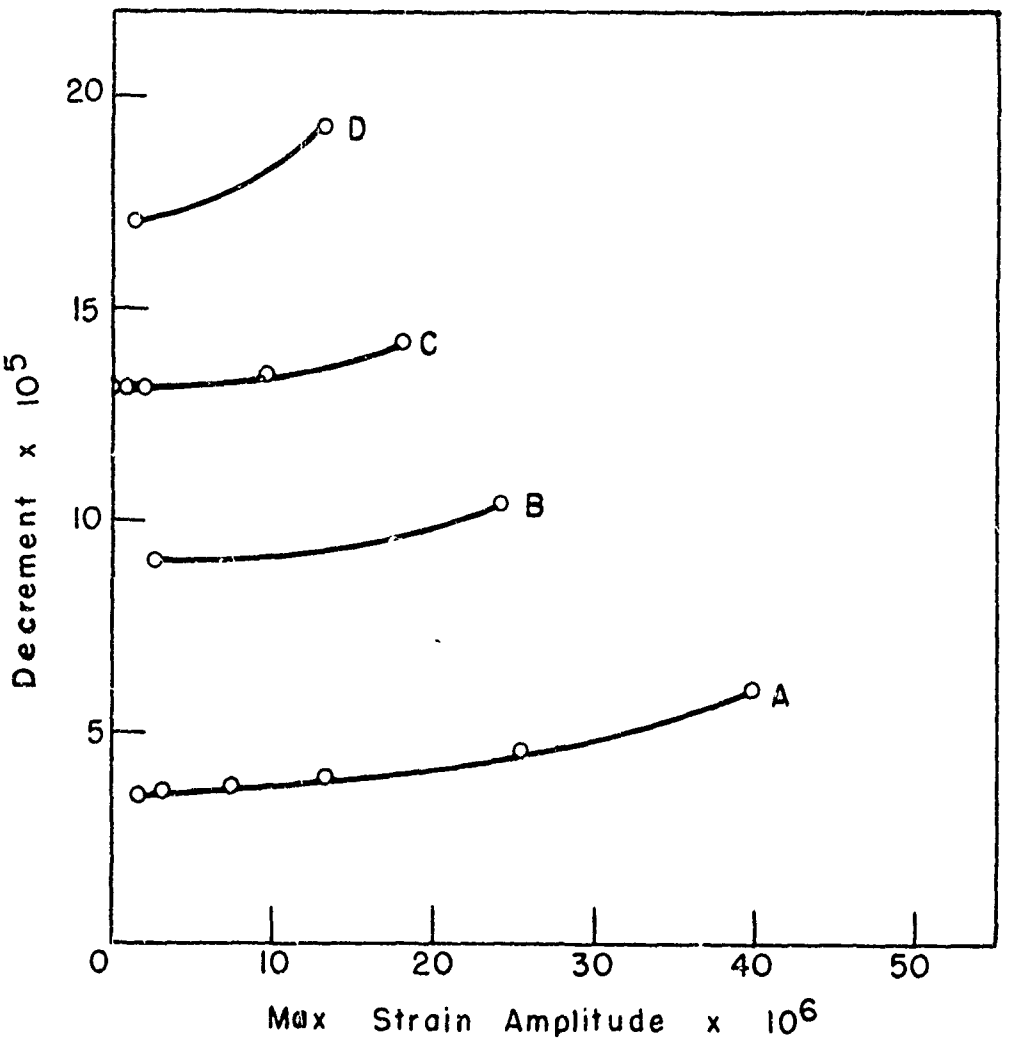

FIGURE 12

Effect of quenching from various annealing temperatures on the internal friction of aluminum single crystal Ia..

A.. Annealed at 640°C..

B.. Annealed at 550°C..

C.. Annealed at 450°C..

D.. Annealed at 350°C..

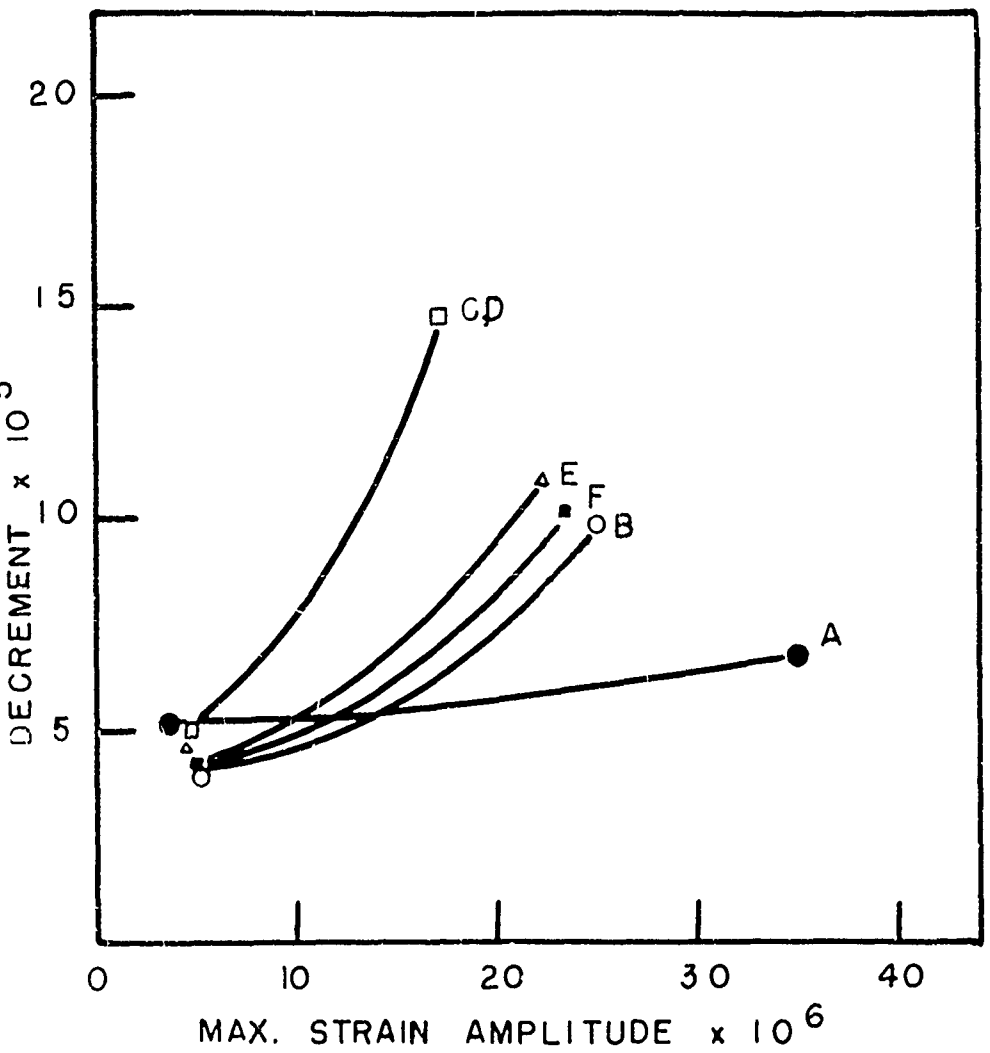

FIGURE 13

Effect of 15 minute anneals at various temperatures on the internal friction of aluminum single crystal Y-4.

A. Initial state: Quenched into water from 640°C.

B. Annealed at 250°C. E. Annealed at 520°C.

C. Annealed at 325°C. F. Annealed at 640°C.

D. Annealed at 425°C.

Crystal air cooled to room temperature after these thermal treatments.

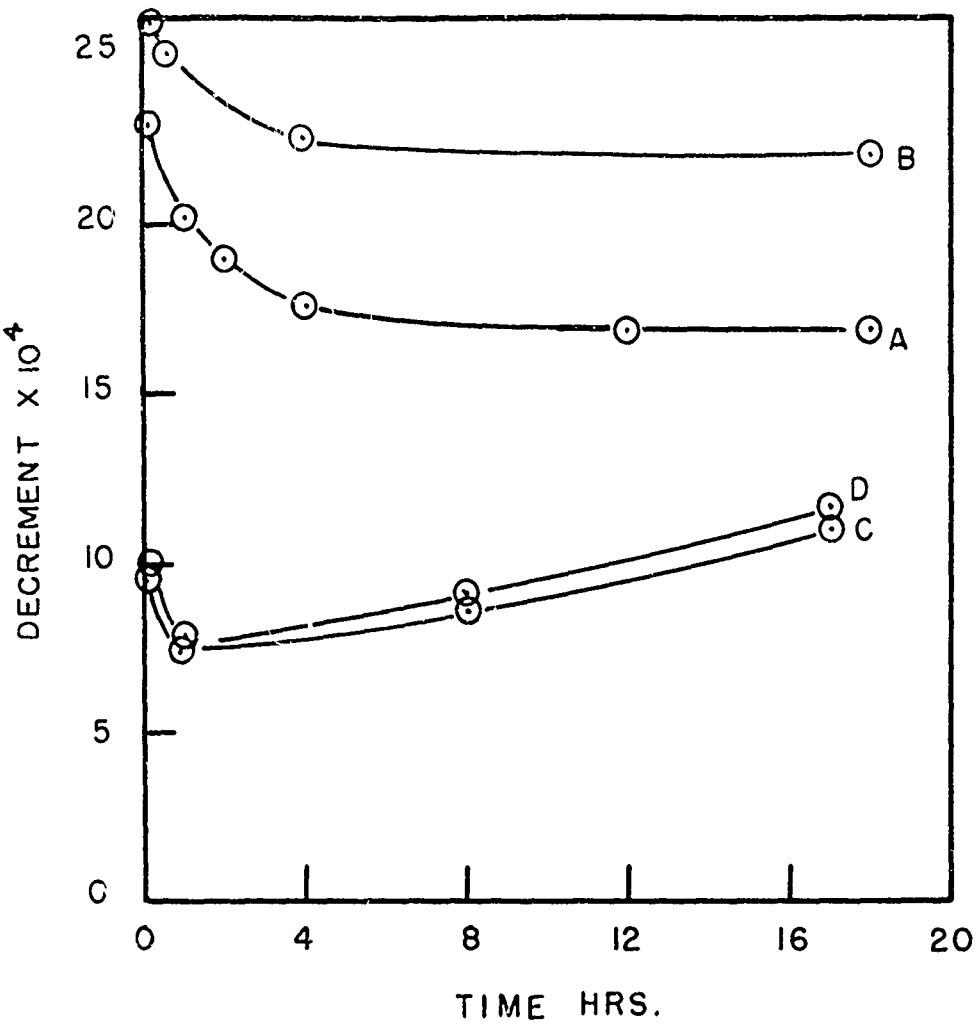

FIGURE 14

Variation with time of the decrement of a 99.999 per cent copper single crystal after being quenched from 1050°C into water at room temperature.

A. Max. strain amplitude, 0.2×10^{-6}

Test 1;slow quench:

B. Max. strain amplitude, 1.0×10^{-6}

C. Max. strain amplitude, 0.2×10^{-6}

Test 2;rapid quench:

D. Max. strain amplitude, 1.0×10^{-6}

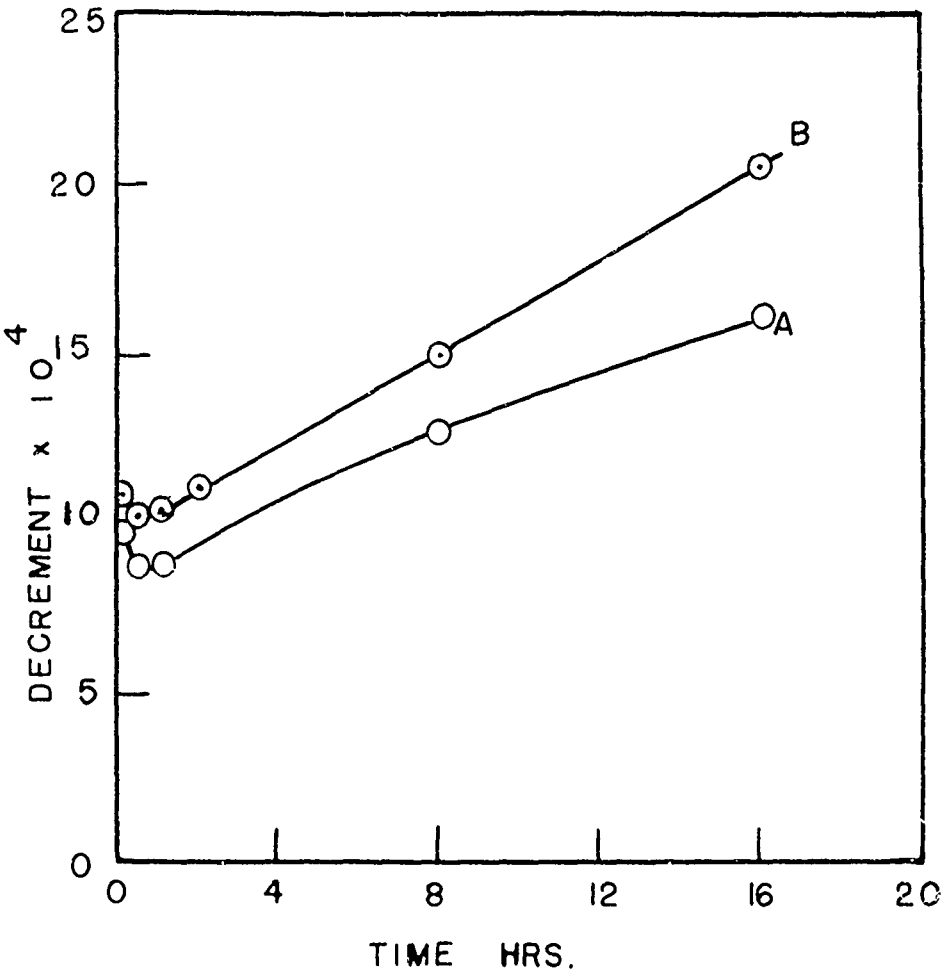

FIGURE 15

Variation with time of the decrement of copper single crystal containing 0.01 atomic per cent nickel after being quenched from 1050°C into water at room temperature.

A. Maximum strain amplitude, 0.2×10^{-6}.

B. Maximum strain amplitude, 1.0×10^{-6}.

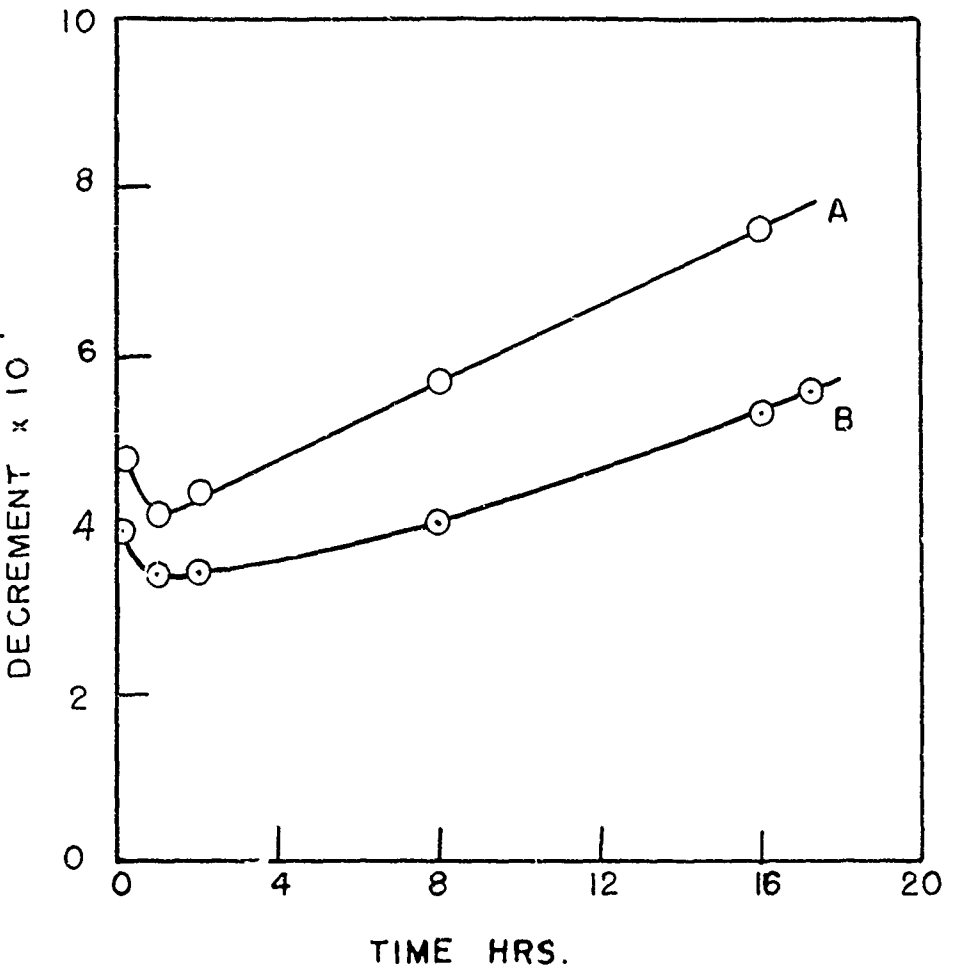

FIGURE 16

Variation with time of the decrement of a copper single crystal containing 0.08 atomic per cent nickel after being quenched from 1050°C into water at room temperature.

B. Maximum strain amplitude, 0.2×10^{-6}.

A. Maximum strain amplitude, 1.0×10^{-6}.

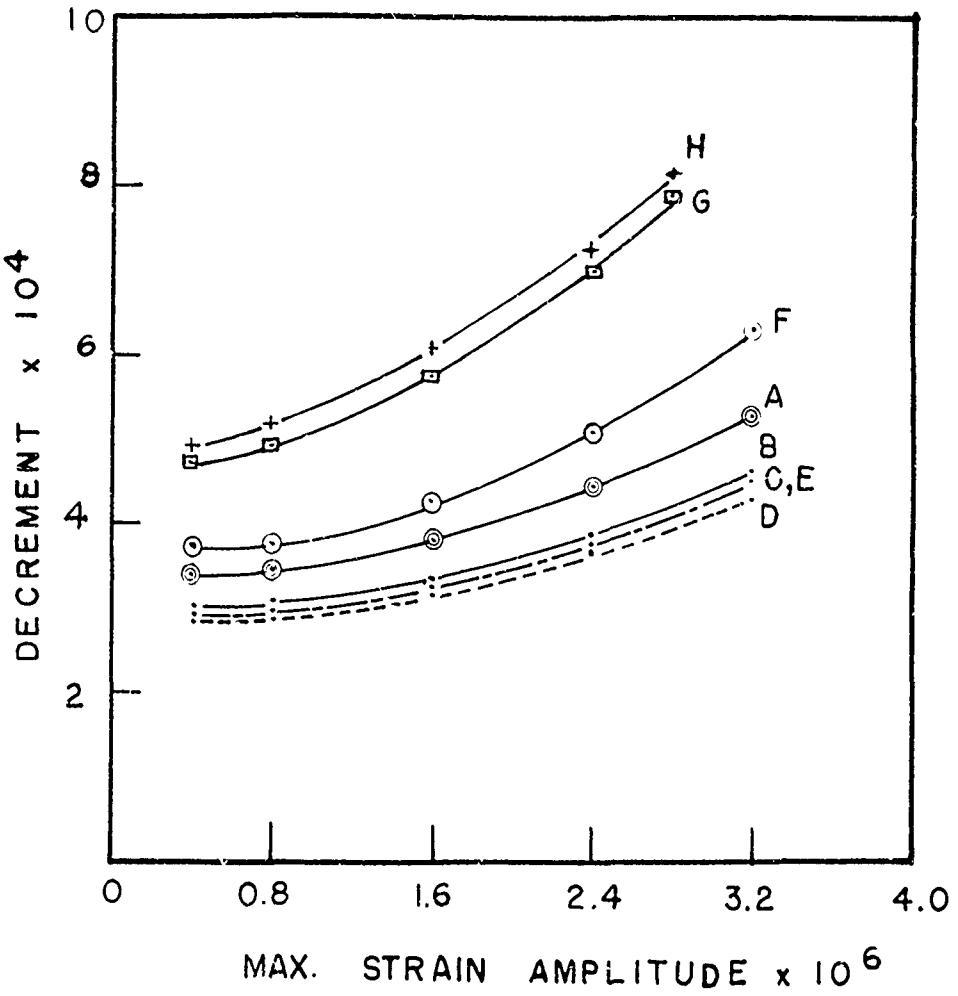

FIGURE 17

Variation of the internal friction with time of a copper single crystal containing 0.10 atomic per cent nickel after being quenched from 1050°C into water at room temperature.

A. 10 minutes.
B. 20 minutes.
C. 30 minutes.
D. 67 minutes.
E. 80 minutes.
F. 8 hours.
G. 15½ hours.
H. 15 3/4 hours.
I. 16⅓ hours.

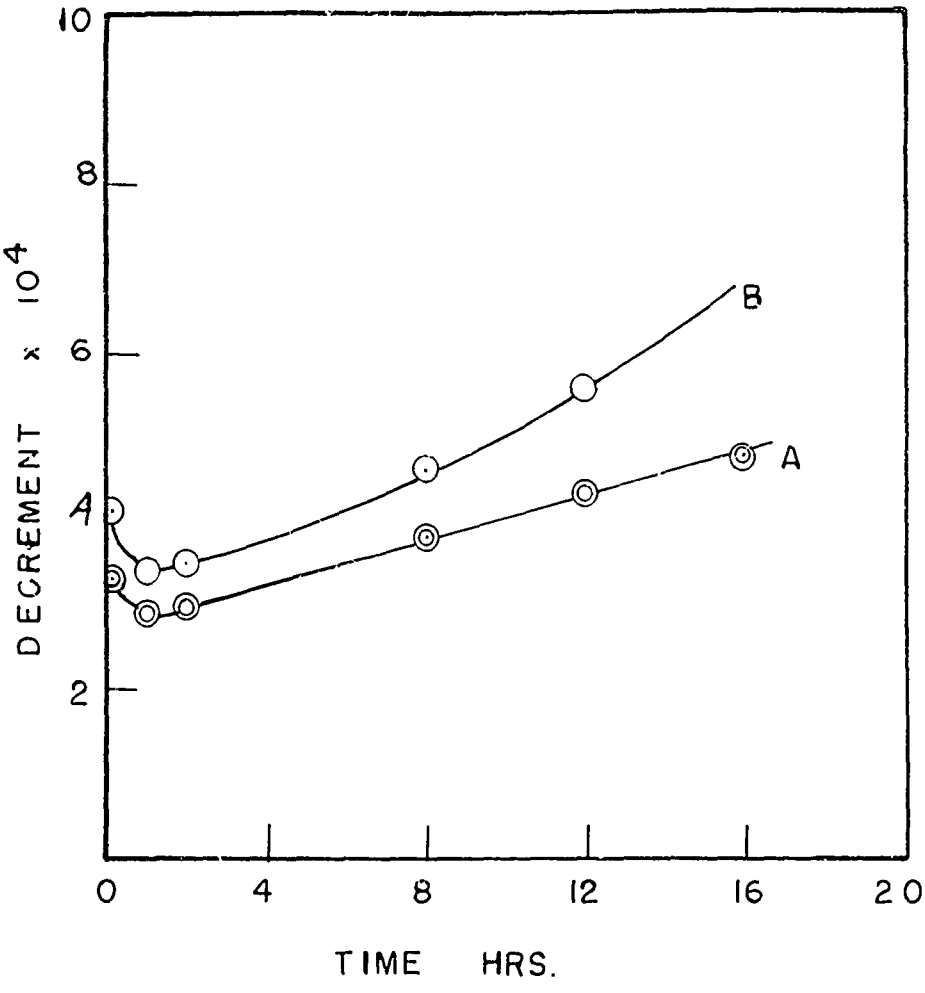

FIGURE 18

Variation with time of the decrement of a copper single crystal containing 0.10 atomic per cent nickel after being quenched from 1050°C into water at room temperature.

A. Maximum strain amplitude, 0.4×10^{-6}.

B. Maximum strain amplitude, 2.0×10^{-6}.

Section 4

Effect of Irradiation on the Internal Friction of Sodium Chloride Single Crystals

THE INTERNAL FRICTION OF ROCKSALT SINGLE CRYSTALS

The internal friction of sodium chloride single crystals measured by the composite oscillator method has been studied by D. R. Frankl, and as the results have been previously reported[1], only the main results shall be summarized. The specific purpose of this investigation was to study the interaction of dislocations with the imperfections introduced in the sodium chloride crystals by X-ray irradiation. It has been previously established[2] that X-ray irradiation of sodium chloride produces F and V centers, the densities of which are functions of the intensities of irradiation. The photo chemical properties of these centers have been studied[3] and their effect on the plastic properties of the ionic crystals have been examined[4]. The present investigation utilized the internal friction measurements as a measure of the dislocation properties after various treatments.

The variation of the decrement with strain amplitude in the ionic crystals is similar to that found in metal crystals[5]. The modulus decrease accompanying the increase in internal with strain amplitude is also qualitatively similar to that observed in metals. The modulus shift is found to be a function of the decrement only and is independent of the strain amplitude required to produce the decrement, thus indicating that the modulus shift and the decrement arise from the same mechanism. In several of the crystals it was observed that a double valued internal friction vs. strain amplitude curve was obtained on increasing the driving voltage to the composite oscillator. On decreasing the driving voltage the initial curve was retraced, ie; only a slight hysteresis loop was observed. This double valued behavior is the result

of a large increase in the damping as the driving voltage is increased. The mechanics of this behavior was not determined although the results indicated that it was associated with cold work.

Mild photochemical irradiation by X-rays resulted in a large decrease in the amplitude dependence of the internal friction. This was proved to be a volume effect by dissolution of the surface and by irradiation through a sodium chloride window. Bleaching of the F and F' centers by exposure to visible light did not result in an increase in the internal friction, thus indicating that the lowering of the decrement was not a result of the direct interaction of the F centers with the dislocations. These results indicate that it is the interaction of the V centers with the dislocations which cause the decrease in internal friction. The irradiation of the crystals causes the formation of positive and negative ion vacancies which are associated in pairs due to the electrical interactions. However the binding energy of an electron to a negative ion vacancy is greater than the binding energy of the vacancy pairs. This allows the negative ion vacancies to trap electrons with the formation of F centers and the freeing of the positive ion vacancies. The positive ion vacancies can form V centers and diffuse to the dislocation lines where they can act as pinning points. The F centers are less mobile and will not diffuse appreciably at room temperature. The pinning of the dislocation by the V centers will cause a decrease in the internal friction. If the irradiation is carried out at -196°C the internal friction is not decreased, thus indicating the necessity of the diffusion of the centers to attain the decrease in decrement. After low temperature irradiation, annealing at room temperature before bleaching causes a large decrease in the internal friction. The effects of coloration may be removed by low temperature anneals.

Several effects of thermal treatments on the internal friction have been noted. High temperature annealing followed by rapid cooling in air resulted in an increase in the decrement and in its amplitude dependence. Following the high temperature anneals, intermediate temperature anneals resulted in a decrease in the decrement. These results indicate that dislocation pinning by some mechanism other than vacancies is operative. This pinning may be due to impurity atoms.

1. Frankl, D. R. Phys. Rev. 58 (1953) 371

2. Esterman, I., Leivo, W. J. Stern, O. Phys. Rev. 75 (1949) 627
   Seitz, F. Rev. of Mod. Phys. (1946) 394
   Markham, J. J. Phys. Rev. 88 (1950) 500

3. Mott, N. F., Gurney, R. W. "Electronic Processes in Ionic Crystals" Oxford Press London

4. Metag, W. Zeits. F. Phys. 78 (1932) 363
   Podschewsky, M. N. Zeits. d. Sowjetunion 8 (1935) 81

5. Read, T. A. Phys. Rev. 58 (1940) 371
   Nowick, A. S. Phys. Rev. 80 (1950) 249

Section 5

Temperature Dependence of the Elastic Constants of Gold Cadmium Alloys

Summary Terminal Report on Temperature Dependence
of Elastic Constants of Gold Cadmium Alloys.

I. A. This work was primarily undertaken to investigate the influence of the temperature dependence of the single crystal elastic constants upon diffusionless phase changes in the above alloy system.

B. A theoretical analysis was presented by Zener[1] whereby the mechanical equivilance of FCC and BCC structures by a simple shear mechanism was shown. This relative thermodynamic stability as a function of temperature was compared and a diffusionless phase change toward thermodynamic stability was obtained by lattice vibrations. Therefore it was predicted that the BCC shear diagnol constant S (110) $[\bar{1}10]$ would change rapidly with temperature becoming relatively much larger approaching the phase transition point. Experimental investigation would be confined to high temperature phase cubic Au Cd alloys, because of their simple structure lending easy interpretation to data, and single crystals can be retained only in the high temperature phase. Alloys of 47.5% Au Cd and 50% Au Cd were selected because of their convenient transformation behavior. Single crystals of arbitrary and controlled orientation were prepared by a modified Bridgeman technique and properly heat treated. Dynamic elastic moduli were obtained with these crystals as a function of temperature (in the high temperature phase only) and prior thermal history. The composite-oscillator technique was used exclusively[2]. The experimental variables for necessary measurement are crystal orientation, specimen

(1) C. Zener, "Elastic and Anelastic properties of Metals. U. Chicago Press Chap. IV.

(2) S. L. Quinsby, Phys. Rev. 25 p. 558 (1925)
L. Balamuth, Phys. Rev. 45 p. 715 (1934)
J. Zacharias, Phys. Rev. 45 p. 116 (1933)

length and diameter (right circular cylinder), specimen mass, temperature dependence of thermal expansion, temperature dependence of longitudinal and torsional resonant frequencies. Details of the technique are explained in the above mentioned references. Suitable quartz crystals were prepared and bonded with metal specimens for resonant frequency measurements. A suitable electronic oscillator had been built for driving the composite oscillator and measurement of resonant frequencies. The natural specimen frequencies were calculated and with the allied measurements, the principal cubic elastic constants were calculated:

$$(a)\quad s'_{33} = 1/E = S_{11} - 2(S_{11} - S_{12} - \tfrac{1}{2} S_{44}) \left[n_1^2 n_2^2 + n_2^2 n_3^2 + n_1^2 n_3^2 \right]$$

where E = axial Young's modulus

S'_{13} = The elastic compliance coefficient in the arbitrary oriented direction of the axis with regard to the crystallographic reference system.

S_{ij} = The crystallographic compliance coefficients

n_i = directional cosines appropriate to following transformation scheme.

	[100] X	[010] Y	[001] Z
X^1	l_1	l_2	l_3
Y^1	m_1	m_2	m_3
Z^1	n_1	n_2	n_3

$$(b)\quad S'_{44} = \frac{1}{G} = S_{44} + 4 (S_{11} - S_{12} - \tfrac{1}{2} S_{44}) \left[n_1^2 n_2^2 + n_1^2 n_3^2 + n_2^2 n_3^2 \right]$$

G = axial torsional modulus

The orientation functions were determined by crystal orientation measurements using the Laue back reflection X-ray technique. Thermal expansion was determined by X-ray lattice parameter measurements and linear dilatometric measurements.

Crystals with [100], [110], [111] axial orientations were necessary for the torsional measurements so as to avoid flexual frequency coupling affects, to yield accurate moduli values.

Some results obtained are indicated as follows:

Table I 47.5 At% Au-Cd
$x10^{-2}$ cm^2/dyne

Temperature°C	S_{11}	$-S_{12}$	S_{uu}	K	$1/E_{111}$	E_{111}/E_{100}	$\frac{2(S_{11}-S_{12})}{S_{uu}}$
50	11.24	5.446	2.363	1.032	0.9024	12.45	14.11
60	10.91	5.289	2.364	1.026	0.9021	12.09	13.70
80	10.35	5.003	2.370	1.023	0.9038	11.45	12.95
100	9.892	4.776	2.383	1.021	0.9076	10.90	12.32
140	9.122	4.393	2.420	1.012	0.9125	9.927	11.17
180	8.536	4.099	2.462	1.014	0.9333	9.146	10.26
220	8.106	3.883	2.510	1.016	0.9503	8.530	9.556
260	7.785	3.722	2.564	1.026	0.9685	8.038	8.974
320	7.365	3.509	2.650	1.041	0.9990	7.372	8.208
360	7.234	3.438	2.709	1.076	1.023	7.073	7.877

Table II 50 At % Au-Cd

Temperature°C							
30	8.919	4.275	2.275	1.110	0.8817	10.12	11.60
40	8.692	4.161	2.280	1.109	0.8832	9.843	11.27
50	8.491	4.060	2.288	1.111	0.8851	9.596	10.97
70	8.148	3.892	2.304	1.091	0.8897	9.165	10.44
100	7.744	3.691	2.334	1.084	0.8984	8.633	9.749
160	7.185	3.412	2.397	1.087	0.9198	7.831	8.842
220	6.787	3.205	2.468	1.134	0.9488	7.180	8.094
230	6.482	3.042	2.547	1.195	0.9817	6.634	7.481
320	6.318	2.951	2.601	1.247	1.006	6.308	7.126
360	6.196	2.882	2 658	1.295	1.030	6.046	6.833

The principal cubic elastic compliance coefficients S_{11}, S_{12}, S_{44} are listed as a function of temperature. All other pertinent elastic properties can be calculated from them[3]. Also listed are the compressibilities, $3(S_{11}+2S_{12})$ and ratios of maximum and minimum crystallographic elastic constants. The last, the ratio of the cubic edge and diagonal shear constants are pertinent to the theoretical consideration previously mentioned. S_{44} should remain fairly constant with temperature charge for BCC lattice while the diagonal shows constant, $2(S_{11} - S_{12})$ should increase sharply approaching the diffusionless phase charge temperature. Qualitative agreement is obtained with theory, but no drastic charge is obtained approaching the phase transformation temperature. Jones[4] has quantitatively shown, for the case of beta brass, that its face diagonal shear constant $S_{110} = 2(S_{11}-S_{12})$ is positive as a result of the stabilizing influence of a positive energy contribution due to the interaction between the fermi energy of the valence electrons and the first (110) Brillouin zone. This is followed in that higher gold contents (lower electron/atom density) show a greater elastic anisotropy and transform at a higher temperature.

Table III - Comparative Elastic Properties

	Beta Brass[5]		47.5 at % Au-Cd		50 at % Au-Cd
Temp. °C	20	-200	annealed 50	quenched from 550°C 28	annealed 30
E_{111}	18.2	23.2	11.1	11.1	11.3
E_{100}	2.44	2.32	0.890	1.10	1.12
$\times 10^{-2}$ cm^2/dyne E_{111}/E_{100}	7.45	8.55	12.5	10.1	10.1
$\frac{2(S_{11}-S_{12})}{S_{44}}$	8.93	10.4	14.1	11.6	11.6

(3) R.F.S. Hearmon, Rev. Mod. Phys. 18 #3 416 (1946)
(4) H. Jones, Phil. Mag. 43, 105 (1952)
(5) Artman, J.A.P. 23 470 (1952)

Table III indicates that the elastic anisotropy for the lowest temperatures measured with beta brass (exomorphous to Au-Cd) is not as great as that for Au-Cd. The brass is stable to lowest available temperatures while the Au-Cd transforms. This lends support to an elastic anisotropy criteria for diffusionless transformation.

Table IV - Calculated and Experimentally[6] determined Compressibilites ($X10^{-2}cm^2/dyne$)

Alloy	$3(S_{11} + 2S_{12})$	Weibbe Eq.	Detirmined	% Diff.
Cu Zn		0.938	0.948	1.0
Cu Zn		0.942	0.913	2.0
55 At% Cu-Zn	0.927	0.924		0.3
51.7 At% Cu-Zn	0.861	0.808		6.0
47.5 At% Au-Cd	1.03	0.998		5.0
50 At% Au-Cd	1.11	1.02		8.5

The above data indicates that the absolute values of the elastic constants are to be considered reliable. Calculated compressibilities are obtained as a small difference of two experimented values and are usually not too accurate.

---

6. F. Weible, Zeits. F. Met. 30 (1938) p. 322

Section 6

Effect of Plastic Deformation on the Internal Friction of Metal Single Crystals

EXPERIMENTAL PROCEDURE

A. SPECIMENS

The specimens used in this investigation were single crystals of aluminum, silver, sodium chloride and copper. The impurity content of the specimen material is given in Table I. The silver and copper crystals were prepared by the Bridgeman technique in a vacuum furnace, using split molds of AEC high purity graphite. The sodium chloride crystals were purchased from the Harshaw Co. The aluminum crystals were prepared by a horizontal Bridgeman technique which utilized the aluminum oxide "skin" as a mold. The orientation of each crystal was obtained by the back reflection Laue technique and is given in Fig. I. The copper and silver specimens were checked for boundaries by etching before the internal friction measurements were taken, while the aluminum crystals were used before etching and were etched subsequent to the internal friction measurement.

B. Internal Friction Measurements

The internal friction measurements were all made by the composite piezoelectric oscillator method[59] utilizing straubel cut quartz crystals with electrodes of evaporated aluminum and chromium. The resonant frequencies of the quartz crystals were in the range of 30 to 80 Kc. The resonant frequencies of the metal crystals were matched to within a few tenths of a percent of the quartz frequencies and are listed in Table II. The crystals were cemented to the quartz by phenyl salicylate or by sauereisen cement which was air dried. The temperature measurements were all made with the sauereisen bond. It was determined that the internal friction was independent of the bonding material.

The composite oscillator assembly was suspended by fine wire supports placed at the displacement node of the quartz. The measurements were all made

in a vacuum chamber. The composite oscillator was excited at the fundamental frequency by a transitron oscillator and the electrical resistance at resonance was measured by a capacitive A.C. bridge. Since the composite oscillator may be considered a RLC electrical circuit, its decrement and strain amplitude may be calculated from the measured resistance at resonance by the relations developed by Read and presented below.

$$M_s \Delta_s + M_q \Delta_q = 4R/K f_c$$

$$U = \frac{\sqrt{1.25K} \times 10^3}{f_c l_s} \times \frac{\mathcal{E}}{R}$$

Δ = decrement, defined as the ration of the energy dissipated per half cycle, to twice the energy stored in the specimen. The decrement is used as a measure of the internal friction.

R = resistance of the composite oscillator at resonance.

f_c = Frequency of composite oscillator.

M = mass

$K = \frac{8L}{M_s + M_q}$

L = inductance of the quartz

l_s = length of the specimen

$\mathcal{E}$ = driving voltage supplied to composite oscillator

U = maximum strain amplitude.

subscripts s and q refer to the specimen and quartz respectively.

The changes in modulus of the specimen were also obtained by measuring the variation of resonant frequency of the composite oscillator and by applying the following relations.

$$\frac{\tan\left(\frac{\pi f_c}{f_s}\right)}{f_c/f_s} = -\frac{M_q}{M_s} \frac{\tan\left(\frac{\pi f_c}{f_q}\right)}{f_c/f_q}$$

$$f_s = \frac{1}{2l_s}\sqrt{E/\rho}$$

where E is the elastic modulus in the crystallographic direction of the length of the specimen.

C. Deformation of Crystals

The specimens were deformed in compression and in torsion. The method of compressive deformation was to place the specimen between the anvils of a micrometer and to use the micrometer for application of the load and for measuring the strain. Specimens Ag 1 and 2 were deformed in compression by axially loading the crystal rather than by compressing it in the micrometer.

The torsional deformation was performed between two axially aligned Jacobs chucks each of which contained a pole piece. The specimen was cemented between these pole pieces using phenol salicylate. Since the amount of torsional deformation was small, the specimens were not bent by lattice plane rotations during the torsional deformation. The strains were measured by using an optical lever arm two meters in length. It was established that the mounting of the crystal in the torsion apparatus and removing it did not affect the internal friction.

D. Torsion Pendulum Measurements

The torsion pendulum experiments were carried out at frequencies of about 1 cps. An inverted torsion pendulum was used to enable the stress on the specimen to be varied without altering the frequency of the measurement. The fixed pin vise was at the bottom of the apparatus while the top pin vise carrying the inertia bar was supported by .004" piano wire which went over a pulley and to a load pan. This apparatus allowed measurements to be performed over a wide range of stress. The vibrational coupling between the piano wire and the torsion pendulum was extremely small as demonstrated by the fact that oscillations of the load pan did not cause any measurable oscillations in the torsion pendulum inertia bar.

The specimens used in these measurements were wires, 0.030" in diameter and 10 inches long. The materials used were OFHC copper of commercial quality, 99.999% copper, and aluminum of the same purity as the specimens used in the high frequency measurements.

Experimental Results

A. Double Valued Behavior

Fig. 2 is typical of the double valued internal friction vs. strain amplitude behavior in sodium chloride. The crystals had been vacuum annealed at 750°C and slowly cooled at the rate of 50°C/hr. to room temperature. It was then heated to 500°C and cooled at 300°/hr. to room temperature. Fig. 2 shows the behavior of the crystal after it had annealed at room temperature. At point I on curve C, the driving voltage was shut off for about 30 seconds before the next driving voltage was applied. This short anneal altered the nature of the curve markedly in that the type II behavior was removed. In every case of double valued behavior found in NaCl, the crystal exhibited a large hysteresis loop as the driving voltage was decreased. This hysteresis was not observed in the crystal initially. This type of behavior combines the features of type I and II behavior in that it exhibits a large hysteresis loop and a double valued behavior as the driving voltage is increased. In Frankl's data the maximum strain amplitude was of the order of 3×10^{-6} while these experiments employed strain amplitude of the order of 14×10^{-4}. This may account for the differences in the observations.

Fig. 3 indicates the nature of the double valued behavior in a silver single crystal. Curve B indicates the double valued behavior obtained after

a torsional deformation of 4×10^{-4} in./in. maximum shear strain in torsion. On annealing at room temperature, the double valued behavior was removed as shown in curve C. On further torsional deformation of 16×10^{-4} in./in. maximum shear strain in torsion and annealing for 70 minutes at room temperature, the double valued behavior was recovered as indicated in curve D. The strain amplitude at which the crystal exhibited the rapid change in decrement increased with the amount of deformation. The behavior in the silver single crystal is characteristic of type II behavior. No hysteresis loop was observed on decreasing the driving voltage.

Fig. 4 indicates the double valued behavior in an aluminum single crystal which is typical of type II behavior. The room temperature curve indicated a large increase of the decrement with strain amplitude. On cooling to -196°C in vacuum, the crystal exhibited a double valued behavior of the decrement with strain amplitude. The double valued behavior was also found at -186°C, -167°C, -147°C. At all these temperatures, no hysteresis loop was observed. On testing at -125°C the specimen no longer exhibited a double valued behavior. The strain amplitudes at which the large increase in decrement occurred decreased as the temperature of testing was increased. On retesting at -196°C the double valued behavior was not obtained, although the amplitude dependence of the decrement was quite large.

B. The Effect of Deformation on the Internal Friction

1. Silver Single Crystals

The effect of torsional deformation on the internal friction of silver single crystals is shown in Fig. 5. Crystal Ag 1 exhibited a large strain amplitude dependence of the decrement in the as grown condition. The initial torsional deformation of 2.93×10^{-4} in./in. maximum shear strain resulted in

a decrease in the strain amplitude dependence of the decrement and an increase in the value of the decrement at low strain amplitudes. Subsequent torsional deformation resulted in no significant changes in the strain amplitude dependence although the level of the decrement was varied. With increasing torsional deformation the decrement increased to a maximum and then decreased as shown in Fig. 5 and 6. The maximum decrement is obtained after a torsional deformation of 17×10^{-3} in./in.

It was found that the decrement decreased with annealing time at 25°C. The relaxation time for this annealing effect appeared to be insensitive to the mode and amount of deformation in the range examined, as shown in Fig. 9. Fig. 10 shows the behavior of crystal Ag 2 on annealing at 25°C after torsional deformation of 15.2×10^{-4} in./in. maximum shear strain. The amplitude dependence of the decrement is not affected by this anneal although the general level of the decrement is decreased.

In the as grown condition crystal Ag 2 exhibited less dependence of the decrement on the strain amplitude than Ag 1. Torsional deformation to a maximum shear strain of 51.2×10^{-4} in./in. did not significantly alter the strain amplitude dependence of the decrement, as shown in Fig. 7. The level of the decrement was increased by the torsional strain. Fig. 8 shows the variation of the decrement with strain at a strain amplitude of 1×10^{-7}.

The effect of plastically straining Ag 1 in torsion followed by compressive stressing is shown in Fig. 11. Large torsional deformation followed by annealing at room temperature caused a decrease in the strain amplitude dependence of the decrement. Compressive stressing increased the value of the decrement and its amplitude dependence. Further torsional deformation did not alter the amplitude dependence appreciably and increased the level of the decrement. The behavior of Ag 2 under alternate torsional and compressive deformation as shown in Fig. 12

was qualitatively similar to that of Ag 1. The amplitude dependence of the decrement of the deformed crystal was markedly less than for the crystal in the as grown condition.

2. Copper Single Crystals

The effect of torsional deformation on the decrement of a copper single crystal containing 0.1% Al. is shown in Fig. 13. The initial torsional deformation of 3.5×10^{-4} in./in. maximum shear strain resulted in a decrease in the decrement. Further torsional deformation resulted in an increase in the decrement reaching a maximum after a deformation of about 55×10^{-4} in./in. maximum shear strain. Further deformation caused a decrease in the decrement as shown in Fig. 14, where the data at a strain amplitude of 2.5×10^{-7} in./in. is plotted.

The behavior of this crystal under alternate torsional and compressive strains is shown in Fig. 15. After torsional deformation of 33.9×10^{-3} in./in., and 9.2×10^{-4} in./in. in compression, the decrement is considerably higher than that of the original crystal. Subsequent torsional deformation of 52×10^{-4} in./in. maximum shear strain resulted in a decrease in the decrement. Further torsional deformation of 17.5×10^{-4} in./in. caused an increase in the decrement.

In the range of strains examined, the deformation did not have any effect on the amplitude dependence of the decrement.

3. Aluminum Single Crystals

The effect of torsional deformation on the internal friction of aluminum single crystals is shown in Fig. 16. The decrement at low strain amplitudes is increased by a torsional strain of 1.71×10^{-4} in./in. maximum shear strain, as is the amplitude dependence of the decrement. Further torsional deformation results in a decrease in the decrement at low strain amplitude and a further increase in the amplitude dependence. The variation of the decrement with

torsional deformation at a strain amplitude of 0.5×10^{-6} in./in. is shown in Fig. 17. For the initially undeformed crystal, the decrement has a maximum value at a torsional deformation of the order of 2×10^{-4} in./in. maximum shear strain. The dependence of the decrement on the strain amplitude increases and then remains constant with increasing torsional deformation.

The internal friction of aluminum single crystals was found to decrease with annealing at 25°C as shown in Fig. 18 and 19. The effects of annealing is most evident at the high strain amplitudes and therefore the annealing results in a decrease in the strain amplitude dependence of the decrement. The final amplitude dependence of the decrement was significantly less than that of the as grown crystal.

The behavior of the crystal under alternate torsional and compressive deformation is shown in Fig. 20. Torsional deformation of 1.71×10^{-4} and 8.89×10^{-4} in./in. maximum shear strain results in an increase and then a decrease in the decrement and an increase in the amplitude dependence. Compressive deformation of 3×10^{-4} in./in. results in an increase in the decrement. Further torsional strain of 3.4×10^{-4} in./in. increased the decrement and the amplitude dependence. On continued torsional deformation the decrement and amplitude dependence decreased. Following this compressive strain of 3×10^{-4} in./in. decreased the decrement and amplitude dependence and subsequent torsional deformation first cause an increase in the decrement and amplitude dependence and then a decrease.

The behavior of the decrement with torsional deformation after compressive strain is shown in Fig. 17. After the crystal was initially deformed 15.7×10^{-4} in./in. maximum shear strain in torsion and 6.0×10^{-4} in./in. in compression, the variation of the decrement with further torsional deformation was studied.

This behavior may be contrasted with that of a crystal which was initially undeformed. Increasing the amount of initial deformation causes the torsional shear strain at which the maximum occurs to be increased and also appears to increase the magnitude of the decrement at the maximum.

The effect of compressional deformation on the internal friction of aluminum single crystals is shown in Fig. 21. Increasing compressional deformation results in increased decrements which reach a maximum at a deformation of the order of 30×10^{-4} in./in. Fig. 22 shows the variation of the decrement with deformation. As shown in Fig. 21 a compressive strain of 40.7×10^{-4} in./in. compressive deformation and torsional strain of 15×10^{-4} in./in. results in a large increase in the decrement at low strain amplitudes and in the amplitude dependence of the decrement. Further torsional deformation of 15×10^{-4} in./in. decreased the level of the decrement at low strain amplitudes and increased the amplitude dependence of the decrement.

The effect of the mode of vibration in the internal friction measurement was determined by matching an aluminum single crystal to a quartz rod oriented so as to vibrate in a torsional mode. Fig. 23 shows the behavior of this crystal as affected by plastic deformation. Compressive deformation up to 6×10^{-4} in./in. caused an increase in the value of the decrement at low strain amplitudes and an increase in the amplitude dependence of the decrement. Subsequent torsional deformation up to 7.0×10^{-4} in./in. maximum shear strain caused a further increase in both the value of the decrement at low strain amplitudes and the amplitude dependence of the decrement.

4. The Effect of Deformation in Internal Friction As Measured by the Torsion Pendulum

The behavior of the internal friction of copper specimens as affected by stress and plastic deformation is shown in Table I and Fig. 24. The high purity

specimen H. P. Cu 4, showed a decrease in the decrement as the tensile stress was increased followed by a small increase as the stress was further increased. Torsional strain increased the decrement following which further tensile stress caused a slight decrease in the decrement. After the torsional strain, the decrement exhibited a dependence on the strain amplitude of measurement, decreasing as the torsional strain amplitude decreased. The maximum torsional strain used during the measurement was of the order of 5×10^{-5} in./in.

The behavior of the OFHC copper with deformation is shown in Table III and in Figs. 25 and 26. The decrement increased with torsional strain to a maximum at about 39.3×10^{-4} in./in. maximum shear strain in torsion. Further torsional deformation caused a decrease in the internal friction. The effect of tensile stress during the internal friction measurement was to cause an initial decrease in the decrement to a minimum occurring at about 1600 g/mm^2 tensile stress and a subsequent increase in the decrement as the tensile stress was increased. These measurements were made with the tensile stress applied to the specimen. Alternate application of torsional strain and tensile stress to the OFHC specimens caused a behavior which was consistent with the above results as shown in Table I. The torsional strain caused an increase in the decrement and the tensile stress caused a decrease.

The effect of torsional deformation and tensile stress on the aluminum specimens is shown in Table IV. It is seen that the polycrystalline and single crystal material exhibited similar behavior indicating a qualitative independence of the behavior on the presence of grain boundaries. The decrement of a well annealed aluminum wire showed an initial increase with increased tensile stress. Short time anneals at 25°C caused large decreases in the value of the decrement after stressing. The measurements were made while the wires were under tensile stress. Torsional strain caused the decrement of the aluminum to increase and

to exhibit a dependence on the torsional strain amplitude of the internal friction measurement similar to that found in the HP Cu 4. This amplitude dependence of the internal friction was removed by a 24 hour anneal at 25°C.

In the single crystal specimen, after a tensile stress of 286 g/mm^2 and a torsional strain of 2.55×10^{-4} in./in. maximum shear strain had been applied, further tensile stress of 626 g/mm^2 caused a decrease in the decrement. A similar effect was found in the polycrystalline specimen after a tensile stress of 836 g/mm^2 and a torsional strain of 1.80×10^{-4} in./in. maximum shear strain. Increasing the tensile stress further, caused an increase in the decrement of the polycrystalline specimen. The same effect was found in the single crystal specimen after annealing at 25°C and applying further torsional strain of 0.72×10^{-4} in./in.

It was established that the decrement measured after the removal of the tensile stress was greater than that measured with the tensile stress applied.

IV. Discussion of Results

A. Double valued behavior

It is of interest to consider the behavior of an edge dislocation under the conditions of the internal friction measurement. The dislocation may be considered as pinned by dislocation intersections, points at which the dislocation line leaves the slip plane, and is surrounded by a maxwellian atmosphere of solute atoms. The concentration of solute atoms about the dislocation varies as $C = C_o e^{U/RT}$ where C_o is the average solute concentration and U is the interaction energy of the solute atom and the dislocation. At temperatures above $T_o = U_{max}/K \ln \frac{1}{C_o}$ the atmosphere has a maxwellian distribution.[40] Under the oscillating stress of the internal friction measurement, a stress of the order of

$$\tau_c = 1/2 \, c N \mu \epsilon r_s^3 \qquad (1)$$

is required to free the dislocation from the influence of its dilute atmosphere. (N is the number of atoms per unit volume, b is the Burgers vector, ϵ is the strain due to the solute atoms, r_s is the radius of the matrix atom and μ is the shear modulus.) Even if the dislocation is freed from the influence of its dilute atmosphere, it is still pinned by dislocation intersections, and by those points at which the dislocation leaves the slip plane. Its extent of motion is limited by these pinning points.

The type II behavior where no hysteresis was observed, may be due to the pinning of the dislocation by intersections, while the large increase in damping may be due to the freeing of the dislocation from its dilute solute atmosphere. Since the dislocation remains geometrically fixed in the crystal, the repinning time for the solute atmosphere is quite short. The large hysteresis loop of the type I behavior may be expected when the dislocation is freed from its pinning points and is displaced geometrically in the crystal. In order to reform the

solute atmosphere about the dislocation in this case, diffusion will have to occur over greater distances so the repinning time will be longer. Therefore, during the period of the internal friction measurement the specimen should exhibit a hysteresis behavior.

For the aluminum used in this experiments T_o is of the order of 0°K so that solute atmosphere may be considered dilute at all the temperatures considered. For this material A is 10^{-23} dyne cm^2 and C_o is 8.65×10^{-4}. The stress at which the double valued behavior occurred was 3.9×10^6 dynes/cm^2 at -196°C and 2.5×10^6 dynes/cm^2 at -147°C. The calculated stress for freeing the dislocation from its atmosphere is of the order of 4×10^5 dynes/cm^2.

For the sodium chloride crystals used in these experiments A is 6.2×10^{-21} dynes/cm^2 and C_o is 10^{-2}. T_o is calculated to be -100°C. The solute atom interaction energy with the dislocation is greater for the sodium chloride than for the aluminum crystals. The stress at which the double valued behavior was observed was of the order of 4×10^8 dynes/cm^2. The calculated stress required to free the dislocation from its dilute atmosphere is of the order of 14×10^8 dynes/cm^2. The large hysteresis found in the sodium chloride may be explained on the basis of the much larger stress amplitudes used for this crystal.

The probability if observing the double valued behavior appears to be greater in those specimens where loosely pinned dislocations have been produced by heat treatment or cold work, or in those materials in which the dislocation pinning is weak. If the dislocation density is increased by plastic deformation the dislocations may become more strongly pinned by dislocation intersections and the stress to produce the double valued behavior increases as shown in Fig. 2. The hysteresis behavior of crystals may also be suppressed by increasing the dislocation pinning by cold work.

B. Effect of Deformation

The slip systems in the F.C.C. crystals of silver, copper, and aluminum are the (111) [101]. There are four (111) planes in the crystal each of which contains three 101 slip directions, thus giving a total of 12 slip systems.(63) During the plastic deformation, those slip systems are utilized which have acting on them a resolved shear stress greater than a critical value. The extent of slip on each slip system is proportional to the resolved shear stress. In the case of compressional deformation, the planes of maximum shear stress lie 45° to the compressional axis, while for torsional deformation, there are two sets of maximum shear stress planes ie; the planes which contain the axis of torsion and those which lie perpendicular to it.

In terms of a dislocation mechanism, the compressional deformation may be described as the movement of dislocation rings along the slip planes on which the resolved shear stresses are the greatest. The manner of movement of these dislocation rings is such that the total deformation is in the slip directions in which the resolved shear stresses are the greatest. During the deformation new dislocation rings are generated at sources such as the Frank-Read source. In any local region of the crystal, the orientation of the crystal will determine whether slip will take place on one or on several slip systems. The geometric conditions are consistent with slip on a single slip system or slip on several slip systems.

The situation in the case of torsional deformation may be quite different. If we disregard the requirements of crystal structure, the torsional deformation may be described as the formation of a crossed grid of screw dislocation[64] on the planes perpendicular to the torsional axis which produces rotational slip, or as the formation of screw dislocations lying on the planes containing the torsional axis[41]. Neither of these mechanisms is compatable with the requirements of crystal structure except in case of special crystal orientations. The nature of torsional deformation

may be described as slip on those slip planes whose orientations are closest to the planes of maximum shear stress and in such directions so as to have the total deformation compatable with the crystal structure and with the geometric requirements of the torsional deformation. This may be accomplished by having slip occur in several of the permissable slip directions on each of the active slip planes and in such a manner that the average slip is equivalent to slip in a tangential direction. It can be shown that the tangential shear stress is given by an expression of the type[65]

$$\tau_t = \tau_o \frac{\cos\phi(1-\cos^2\theta\tan^2\phi)}{\left[1+\cos^2\theta\tan^2\phi\right]^{1/2}} \qquad (2)$$

where τ_t = tangential shear stress

τ_o = constant

ϕ = angle between the axis of torsion and the normal to the slip plane.

θ = angle between the slip direction projection on a plane perpendicular to the torsion axis and the semiminor axis of the ellipse formed by the intersection of the slip plane with the cylindrical specimen.

The value of τ_t is a maximum at $\phi = 0^\circ$ and for this orientation is a constant for all values of θ. For the case of $\phi \neq 0^\circ$ then τ_t is a function of θ, increasing as θ approaches 90°. For values of ϕ greater than 45°, τ_t is negative for a range of values of θ. It has also been shown experimentally that during the torsional deformation the plane normals of the crystal rotate about the axis of torsion rather than the normal to the slip planes.[65] Furthermore, it may be easily shown that the strain accompanying a torsional deformation increases linearly with distance from the center of the specimen.

The mechanism of torsional deformation may be described on the basis of the above ideas. As a torsional stress is applied, the deformation takes place at the surface of the crystal by the motion or generation of dislocations on those slip

planes which have the greatest resolved shear stress. The stress required for the deformation is given by the average critical tangential shear stress. The motion of dislocations is such that shear occurs in several of the slip directions and to such an extent that the total shear accomodates the torsional stress. The rotation of the shear planes about the torsion axis necessitates dislocation motion on slip planes which intersect the active torsional slip planes. Thus the final pattern of crystalline imperfections introduced by torsional deformation is quite complex and is a function of specimen orientation. In general, it may be stated that as the crystal orientation varies so that ϕ approaches 0°, the slip tends to be localized on a single slip plane and cross slip necessitated by the rotation of the slip planes diminishes. Thus we begin to attain the ideal case discussed by Frank[64]. In this ideal case where $\phi = 0^{\circ}$ the final density of dislocations produced on the slip plane by the torsional deformation is constant across the crossection.

Since the planes of maximum shear strain in compression and torsion lie at 45° to each other, the active slip systems in compression and torsion will in general intersect each other. Alternate compressional and torsional deformation will therefore produce a large amount of cross slip and dislocation intersections. It has been shown that this cross slip leads to rapid work hardening. This has been analyzed on the basis of dislocation jogs by Seeger[66]. In the decrement measurements utilizing an x- cut quartz, the active slip planes coincided with the active slip planes of the compressional deformation. Therefore, the dislocations introduced on the active slip planes of the torsional deformation lie on inactive slip planes during the decrement measurement. In general, however, the shear stress on these planes are not zero so some dislocation motion does take place under the action of the oscillating stress. The value of N considered in the following discussion does not include those dislocations which form small angle boundaries, as the restoring force on these would render them essentially immoble under the stress used in the

internal friction measurement. The extent of the dislocation motion under the compressional oscillating stress will be approximately proportional to a shear factor of $2 \cos\phi \sin\phi$ where ϕ is the angle between the slip plane and the specimen axis.

The experimental results may be qualitatively interpreted on the basis of the above ideas and the expression for the decrement caused by oscillating dislocations as determined by Koehler[23]. This expression is

$$\Delta = \frac{K_1 N \omega}{C^4} \left[1 + \frac{K_2 \omega^2}{C^2} + \frac{K_3 \omega^2}{C^4} \right] \qquad (3)$$

where C is the concentration of pinning points, N is the atomic lengths of active dislocation line/cm^3, K_1 K_2 K_3 are constants and w is the frequency of oscillation. This expression does not account for the restoring force of neighboring dislocations which would tend to decrease the decrement.

The concentration of solute atom pinning points is of the order of 1×10^{-3} as estimated by Koehler[23]. The concentration of dislocation intersections may be estimated at $10^{-12} N^{\frac{1}{2}}$ giving a total concentration of pinning points of $\frac{N_B}{N} + 10^{-12} N^{\frac{1}{2}}$ where N_B is the number of solute atom pinning points.

The effect of deformation on the internal friction may be examined on the basis of the above analysis. If the mode of deformation is such as to produce a dislocation pattern on slip planes for which the shear factor is small, then these imperfections will serve merely to pin the active dislocations on intersecting slip planes and will not contribute appreciably to the energy dissipation. Thus the effect of deformation would be to decrease the decrement and the amplitude dependence of the decrement. If the deformation produces slip on planes whose shear factor is appreciably greater than zero, these dislocations contribute to the energy dissipation as well as increasing the concentration of pinning points on intersecting dislocation lines.

Equation (3) may be written as

$$\Delta = \frac{K_1 N \omega}{\left(\frac{N_S}{N} + 10^{-12} N^{1/2}\right)^4} + \frac{K_1 K_2 \omega^3 N}{\left(\frac{N_S}{N} + 10^{-12} N^{1/2}\right)^6} + \frac{K_1 K_3 \omega^3 N}{\left(\frac{N_S}{N} + 10^{-12} N^{1/2}\right)^8} \qquad (4)$$

The observed variation of the decrement with N exhibits a rapid initial increase followed by a more gradual decrease. The shape of the Δ vs N behavior calculated from the above relation, is similar to that determined experimentally. The maximum value of the decrement is found to occur at a dislocation density of the order of 10^9 dislocation lines/cm^2 which is a reasonable value for a slightly worked specimen. The value of N at which the maximum decrement occurs will depend on the specimen orientation since the contribution of the dislocations introduced by deformation to the energy dissipation will be a function of the compressive shear factor. We may therefore expect different curves for the variation of Δ vs N for the torsional deformation and for the compressive deformation. This is shown experimentally in Figures (11, 12, 20) where compressional deformation causes an increase in the decrement although the maximum in the decrement vs. torsional deformation has been exceeded.

The behavior of the aluminum and silver specimens under alternate torsional and compressive deformation as shown in Figures (11, 12, 17, 20, 21) suggests that when the maximum value of N for one type of deformation has been exceeded, application of a second mode of deformation will shift the value of N_{max} so further deformation in the first mode will cause an increase in the decrement. Another possible explanation is that the deformation in a second mode causes the removal of some of the dislocations introduced during the first mode of deformation. This may be accomplished on the basis of the lattice plane rotations during deformation. In the compressional deformation the active slip planes tend to rotate to bring the axis of compression into a plane which is symetric with two slip planes, causing duplex slip. In the torsional mode of deformation the slip planes tend to rotate to a position where the resolved shear stress on one slip system is increased or to a position where the axis of torsion is symetrically oriented with respect to two slip systems. In general, the lattice rotation in these two cases will not be in the same directions and will have

components which oppose one another. On alternate compression and torsion, these rotations may be accomplished by the removal of some of the dislocations which caused the previous lattice rotations. In effect this removal of dislocations is a work softening and may decrease the dislocation density. A decrease in the dislocation density by the second mode of deformation would then allow the decrement to increase with further application of the second mode of deformation. This process may account for the observed experimental results.

On the basis of the above discussion, it is expected that on the initial torsional deformation of a crystal with a (111) slip plane at 90° to the torsional axis, the deformation required to obtain the maximum in the decrement vs. deformation curve would be less than for a crystal which does not have this orientation. This is observed in the date for Ag. 1 and Ag. 2 shown in Figures 6 and 8. It is also expected that the deformation required to obtain the maximum and the value of the decrement at the maximum will be less for a crystal deformed in torsion than in compression. This is observed in the date for Al HP 3a and Al HP 6 shown in Figures 17 and 22.

The behavior of the amplitude dependence of the decrement with deformation could not be determined on the basis of the available data. In the aluminum crystals the deformation caused an increase in the amplitude dependence irrespective of the mode of deformation. The copper crystals showed no appreciable effect of the deformation on the amplitude dependence and the silver crystals exhibited both a decrease in the amplitude dependence with deformation and no change.

In all of the crystals examined, low temperature annealing caused a large decrease in the decrement and in the amplitude dependence of the decrement. (Figures 9, 10, 11, 12, 18, 19). Since the final value of the decrement and the amplitude dependence was lower than for the original crystal, these results cannot be accounted for on the basis of solute atom diffusion to the dislocations. This is also indicated

by the fact that the relaxation time for the annealing process appears to be independent of the degree and mode of deformation. These results may be accounted for on the basis of the movement of dislocations to stable energy configurations in which they may be securely bound and would not contribute to the energy dissipation. The expression for the recovery of internal stresses in a worked metal developed by Cottrell and Aytekin[67] may be used to formally describe the change in decrement with time of annealing. The applicable expression is

$$\sigma = \sigma_0 - \frac{kT}{\beta} \ln \left(1 + t/t_0\right) \tag{5}$$

where σ = the internal stresses and t is the annealing time. β and t_0 are constants. If it is assumed that the decrement is proportional to the internal stresses the expression for the change of decrement with annealing time is

$$\Delta = k_1 \sigma_0 - k_2 \ln \left(1 + t/t_0\right) \tag{6}$$

An examination of the available data indicates that the annealing behavior is of this form. The mechanism of the recovery process of the decrement may be associated with the formation of stable dislocation configurations which decrease the number of effective dislocation lengths.

The effects of stress on the internal friction as measured by the torsion pendulum lends support to the above hypothesis of the effects of deformation on internal friction as measured by the piezo-electric method. The measurements were made at a temperature where the relaxation processes due to the grainboundaries should not contribute to the energy dissipation If the assumption is made that the dislocations contribute to the energy dissipation in these measurements the experimental results may be interpreted on the basis of the previous dislocation model.

The minimum in the variation of the decrement with tensile stress exhibited by the high purity copper and the C.F H.C. can be accounted for on the basis of the intersection of the active dislocations by those introduced by the tensile stress.

Since the initial dislocation density of these specimens are undoubtedly greater than in the single crystal specimens due to the differences in their preparation it is expected that the dislocation density may be greater than N_{max}. This viewpoint agrees with the observed initial decrease in the decrement. The observed increase in decrement with torsional deformation is also consistent with the above picture in that since the dislocation pattern in this case is produced on planes which are most active during the decrement measurement, the value of N_{max} for this mode of deformation is greater than for the tensile deformation. The behavior of the copper specimens under the alternate tensile and torsional deformation again indicates that the second mode of deformation decreases the dislocation density on the slip planes operative in the first mode. This can account for the alternate increase and decrease in decrement as the specimen is alternately deformed in torsion and tension.

The behavior of the aluminum single crystal and polycrystalline wires again lends credence to the postulated dislocation mechanism. The initial dislocation density in these wires were considerably less than in the copper wires due to the method of preparation and the fact that the aluminum polygonizes at a lower temperature than the copper. Therefore the increase in the decrement with initial tensile stress is consistent with the hypothesis that N_{max} must be exceeded for the particular mode of deformation before the decrement will decrease on further deformation. The partial recovery of the decrement when the measurements are made with the stress removed indicates a greater degree of freedom of the dislocations when they are not piled up against barriers. The amplitude dependence of the decrement which is observed after plastic deformation, and the observed decrease of this amplitude dependence with annealing time supports the hypothesis that the observed changes in decrement are due to changes in the dislocation configuration.

TABLE I

Specimens	Impurities									
	Fe	Si	Cu	Mn	Mg	Na	Ca	Al	Pb	Sb
Aluminum	.0004	.0006	.0022	.0002	.0004	.0001	.0002			
Copper H.P.				99.999 o/o						
Copper O.F.H.C.			Commercial Purity							
Silver				99.99 o/o						
Sodium Chloride	.00001	.0001			.001	.01	.1	.0001		

TABLE II

SPECIMEN	RESONANT FREQUENCY (KC)
NaCl 1	78.976
Ag 1	29.485
Al H.P. 1	32.140
Ag 2	80.424
Cu 1	30.000
Al H.P. 3b	69.208
Al H.P. 6	71.245
Al H.P. 4a	39.500
Cu H.P. 2	78.815
Al H.P. 4b	79.274

TABLE III

SPECIMENS	TREATMENT	DECREMENT $X10^3$
HP Cu #4	22 g/mm^2 tensile stress	1.85
Annealed at	66 g/mm^2 tensile stress	1.81
500°C for 24	110 g/mm^2 tensile stress	1.68
hours.	220 g/mm^2 tensile stress	1.75
	550 g/mm^2 tensile stress	1.73
	550 g/mm^2 tensile stress	
	$2.13x10^{-4}$ in./in. max. shear strain in torsion	2.43
	880 g/mm^2 tensile stress	2.48
	880 g/mm^2 tensile stress	2.38
	annealed 10 minutes at 25 C	
OFHC Cu #1	Initial	1.70
Annealed at	$1.31x10^{-4}$ in./in. max. shear strain in torsion	1.80
550°C for 5	$7.86x10^{-4}$ in./in. max. shear strain in torsion	2.30
hours	$14.4x10^{-4}$ in./in. max. shear strain in torsion	2.80
	$19.7x10^{-4}$ in./in. max. shear strain in torsion	3.20
	$25.9x10^{-4}$ in./in. max. shear strain in torsion	3.80
	$39.3x10^{-4}$ in./in. max. shear strain in torsion	5.00
	$66.8x10^{-4}$ in./in. max. shear strain in torsion	4.40
	119 x 10 in./in. max. shear strain in torsion	[illegible]

		[illegible]
[illegible]	[illegible]	1.40
[illegible]	[illegible]	1.34
[illegible]	[illegible]	1.12
[illegible]	[illegible]	1.07
	[illegible] tensile [illegible]	1.07
	[illegible] tensile [illegible]	1.25
	[illegible] tensile [illegible]	1.40
	[illegible] tensile [illegible]	2.22
	[illegible] tensile [illegible]	2.65
	[illegible] tensile [illegible]	3.05
OFHC Cu #3 annealed at 750°C for 4 hours	[illegible]	2.00
	[illegible] strain in torsion	2.42
	[illegible] tensile [illegible]	2.25
	[illegible] strain in torsion	3.28
	[illegible] tensile [illegible]	2.73
	[illegible] strain in torsion	3.60
	[illegible] tensile [illegible]	2.65
	[illegible] strain in torsion	3.55
	[illegible] tensile [illegible]	2.55
	[illegible] tensile [illegible]	2.26
	[illegible] strain in torsion	4.77
	[illegible] tensile [illegible]	4.30

TABLE IV

SPECIMENS	TREATMENT	DECREMENT $X10^{3}$
H.P. Al 2b Single Crystal	22 g/mm^2 tensile stress	1.26
	66 g/mm^2 tensile stress	1.44
	176 g/mm^2 tensile stress	1.67
	286 g/mm^2 tensile stress	1.96
	286 g/mm^2 tensile stress, annealed at 25°C for 15 minutes	1.57
	1.95×10^{-4} in/in max. shear strain in torsion 286 g/mm^2 tensile stress	1.94
	0.6×10^{-4} in/in max. shear strain in torsion 286 g/mm^2 tensile stress	3.84
	626 g/mm^2 tensile stress	3.21
	22 g/mm^2 tensile stress	3.54
	Annealed at 25°C for 24 hours 22 g/mm^2	2.10
	0.72×10^{-4} in/in max. shear strain in torsion 22 g/mm^2 tensile stress	5.54
	132 g/mm^2 tensile stress	6.24
	242 g/mm^2 tensile stress	6.67
	352 g/mm^2 tensile stress	6.67
	352 g/mm^2 tensile stress, annealed at 25°C for two hours	5.60
H.P. AL 10 Polycrystalline Annealed at 500°C for 5 hours	Initial	2.00
	22 g/mm^2 tensile stress	2.00
	66 g/mm^2 tensile stress	2.82
	176 g/mm^2 tensile stress	3.87
	1.05×10^{-4} in/in max. shear strain in torsion 176 g/mm^2 tensile stress	3.18

SPECIMENS	TREATMENT	DECREMENT
	836 g/mm^2 tensile stress	5.85
	0.75×10^{-4} in/in max. shear strain in torsion 1540 g/mm^2 tensile stress	4.44
	1650 g/mm^2 tensile stress	6.50
	1650 g/mm^2 tensile stress, annealed at 25°C for 10 minutes	4.40
	44 g/mm^2 tensile stress	5.56
	154 g/mm^2 tensile stress	5.03
	2.10×10^{-4} in/in max. shear strain in torsion 154 g/mm^2 tensile stress	5.23

1. Read, T. A. Phys. Rev. 58 (1940) 371

2. Frankl, D. R. Phys. Rev. 92 (1953) 573

3. Read, T. A. Trans. A.I.M.E. 143 (1941) 30

4. Nowick, A. S. Phys. Rev. 80 (1950) 249

5. Read, T. A. and Tyndall, E. Jnl. App. Phys. 17 (1946) 713

6. Wert, C. J. Jnl. App. Phys. 20 (1949) 29

7. Swift, I. H. and Richardson, J. E. Jnl. of App. Phys. 18 (1947) 417

8. Zener, C., Clarke, H. and Smith, C. S. Trans. A.I.M.E. 147 (1942) 90

9. Lawson, A. W. Phys. Rev. 60 (1941) 330

10. Hosiguiti, R. R. and Hirai, T. Jnl. App. Phys. 22 (1951) 1084

11. Weertman, J. and Koehler, J. S. Jnl. App. Phys. 24 (1953) 624

12. Maringer, J. Jnl. App. Phys. 24 (1953) 1525

13. Kunitomi, N. Sendai Univ. Science Reports 4 (1952) 386

14. Koster, W. Z. Arch. Eisinhattenw 14 (1940) 271

15. Boulanger, C. R. Acad. Sci. Paris 226 (1948) 1170

16. Cochardt, A. W. Jnl. App. Phys. 25 (1954) 670

17. Ke, T. S. Jnl. Metals 2 (1950) 575

18. Norton, J. Trans. A.I.M.E. 137 (1940) 49

19. Forster, F. and Koster, W. Z. Metallk 29 (1937) 116

20. Koster, W. Z. Metallk 32 (1940) 282

21. Koster, W. Z. Arch. Eisenhutlenw 14 (1940) 271

22. To be published

23. Koehler, J. S. Imperf. in Nearly Perfect Crystals (1952) P. 197

24. Eshelby, J. D. Proc. Roy. Soc. A 197 (1949) 396

25. Orowan, E. Proc. Phys. Soc. 52 (1940) 8

26. Nabarro, F.R.N. Proc. Phys. Soc A 209 (1951) 279

27. Nowick, A. S. Symp. on Plastic Deformation of Crystalline Solids (1950) P. 155

28. To be published

29. Taylor, G. I Proc. Roy. Soc. A 145 (1934) 362, 388

30. Orowan, E. Nature 147 (1941) 452

31. Mott, N F. Research 2 (1949) 162

32. Burgers, J. M. Second Report on Viscosity and Plasticity, Acad. Sci. Amsterdam (1938) 200

33. Kochendorfer, A. Zeitz, Physik 108 (1938) 244

34. Laurent, P. Rev. Met. 42 (1945) 79, 125, 156, 194, 230

35. Edwards, F. H. Washburn, J., Parker, E. R., University of Calif. Technical Report #8 Series 27 (1953)

36. Bainbridge, D. W., Li, C. H., Edwards, E. H. Acta. Met. 2 (1954) 322

37. Andrade, E. N. and Henderson, C. Phil. Trans. Roy. Soc. A 244 (1951) 177

38. Moddin, R., Mathewson, C. H. Hibbard, W. R. Trans. A.I.M.E. 175 (1948) 86, 185 (1950) 527

39. Lucke, K. and Large, H. Zeitz, Metall 41 (1950) 65

40. Rohm, F. und Kochendorfer, A. Zeitz, Metall. 41 (1950) 265

41. Paxton, D. W., and Cottrell, A. H. Acta. Met. 2 (1954) 3

42. Mott, N. F. Phil. Mag. 43 (1952) 912

43. Cottrell, A. H. Dislocations and Plastic Flow in Crystals Oxford Press (1953)

44. Lomer, W. M. Phil. Mag. 42 (1951) 1327

45. Cottrell, A. H. Prog. in Metal Physics 1 (1949) 77

46. Kuhlmann, D. Proc. Phys. Soc. A 64 (1951) 140

47. Cottrell, A. H. and Aytekin, V. Jnl. Inst. Met. 77 (1950) 389

48. Cahn, R. W. Prog in Metal Physics 2 (1950) 151

49. Heidenseich, R D. Jnl. App Phys. 20 (1949) 943

50. Mott, N. F. Proc. Phys. Soc. B 64 (1951) 729

51. Seitz, F. Advance in Physics 1 (1952) 43

52. Molenaar, J. and Aarts, W. H. Nature 166 (1950) 690

53. Bartlett, P. and Viennes, G. Phys. Rev. 89 (1953) 848

54. Mott, N. F. Imperfections in Nearly Perfect Crystals Wiley (1952)

55. Suzuki, H. Science Reports Sendai Univ. 4 (1952) 455

56. Zener, C. Elasticity and Anelasticity in Metals Univ. of Chicago Press (1948)

57. Ke, T. S. Phys. Rev. 78 (1950) 420

58. Ke, T. S. Trans. A.I.M.E. 176 (1948) 448

59. Pittenger, J. T. Navy Contract N 6 or 147 (1951)

60. Marx, J. W., Baker, G. S., and Sivertsen, J. M., Acta Met. 1 (1953) 193

61. Bordoni, P. G. La Ricerca Scientifica 19 (1949) 851

62. Quimby, S. Phys. Rev. 25 (1925) 558

63. Schmid, E. and Boas, W. Crystal Plasticity, J. Springer (1935)

64. Frank, F. C. Report of a Conference on the Strength of Solids Phys. Soc. (Lon) 1948

65. Hsu, S. S. and Cullity, B. V. Trans. A.I.M.E. 6 (1954) 305

66. Seeger, A. Phil. Mag. 45 (1954)

67. Cottrell, A. H. and Aytekin, V. Jnl. Inst. Met. 77 (1950) 389

68. Levy M. To be published

69. Zener, C. Trans. A.I.M.E. 152 (1943) 122

70. Wert, C. Acta Met. 1 (1953) 113

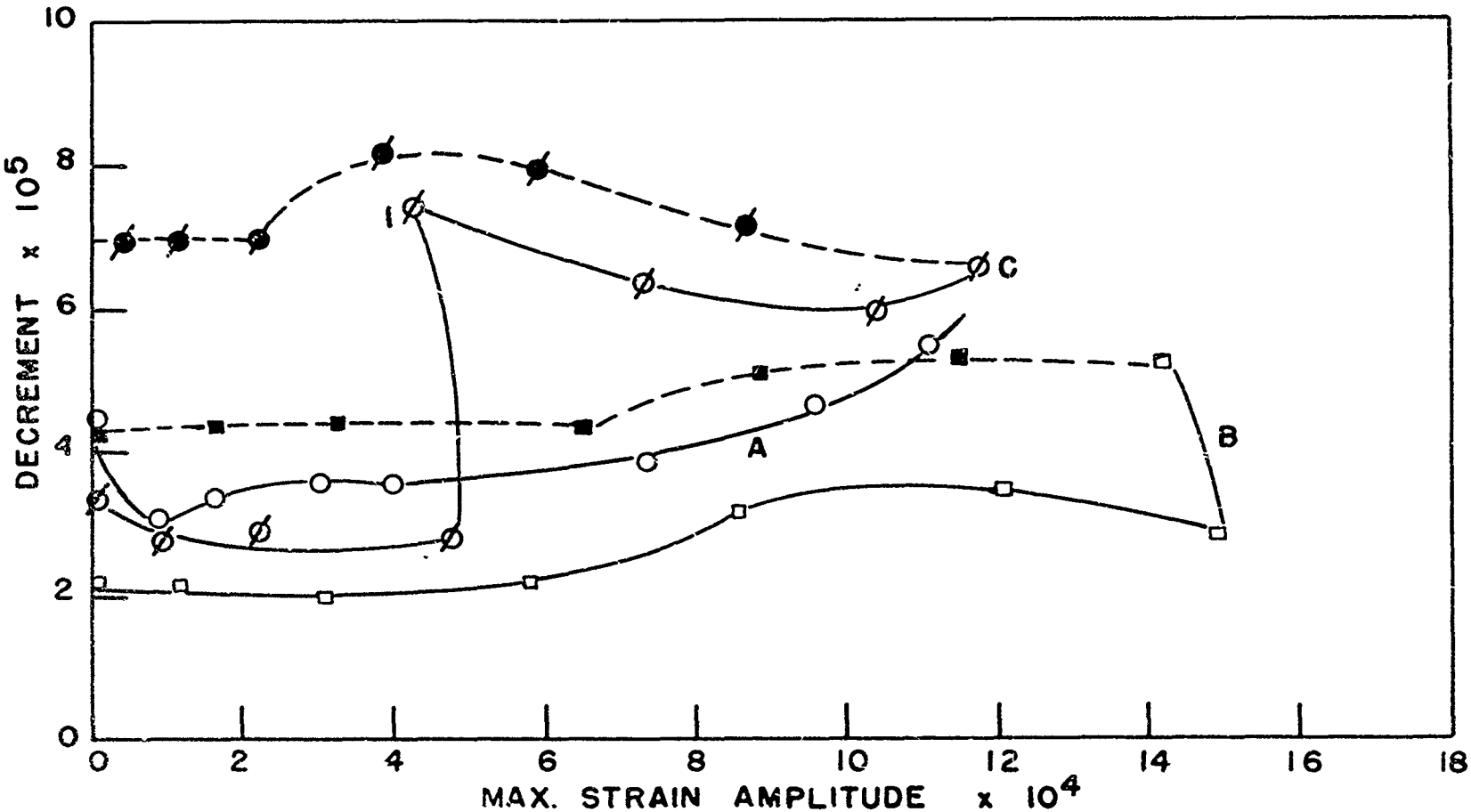

FIG. 2 EFFECT OF HEATTREATMENT ON INTERNAL FRICTION IN SODIUM CHLORIDE CRYSTALS

A 750° ANNEAL, COOLED AT 50° C PER HOUR

B 500° C ANNEAL, COOLED AT 300° C PER HOUR

C 19 HOURS AT 25° C

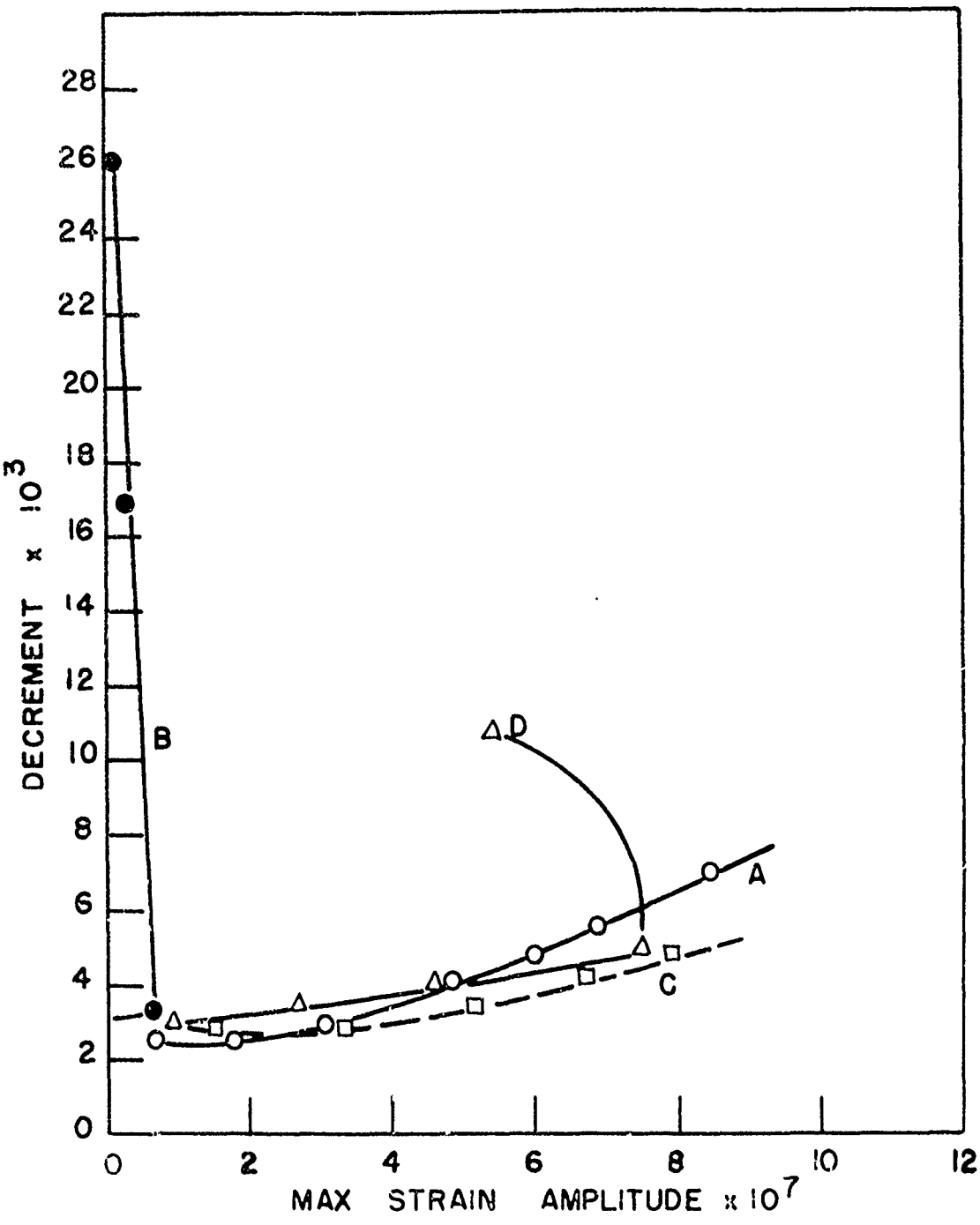

FIG. 3 VARIATION OF INTERNAL FRICTION WITH DEFORMATION OF Ag SINGLE CRYSTAL

A AS GROWN

B 4×10^{-4} in/in TORSIONAL STRAIN

C 12 HOURS AT 25° C

D 16×10^{-4} in/in TORSIONAL STRAIN

70 MINUTES AT 25° C

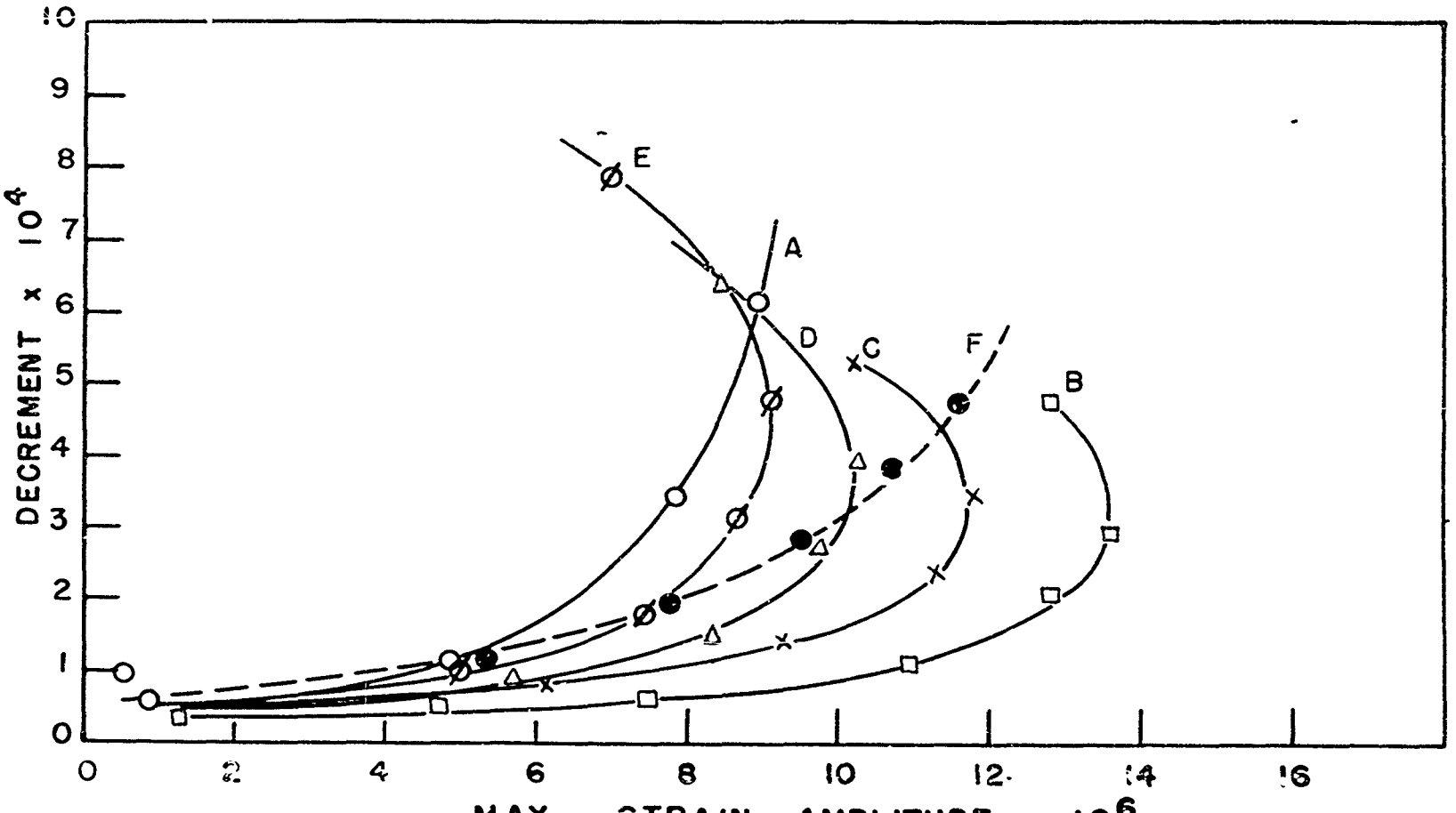

FIG. 4 VARIATION OF INTERNAL FRICTION WITH TEMPERATURE IN Al SINGLE CRYSTAL

A	28° C	D	-167° C
B	- 196° C	E	-147° C
C	- 186° C	F	-125° C

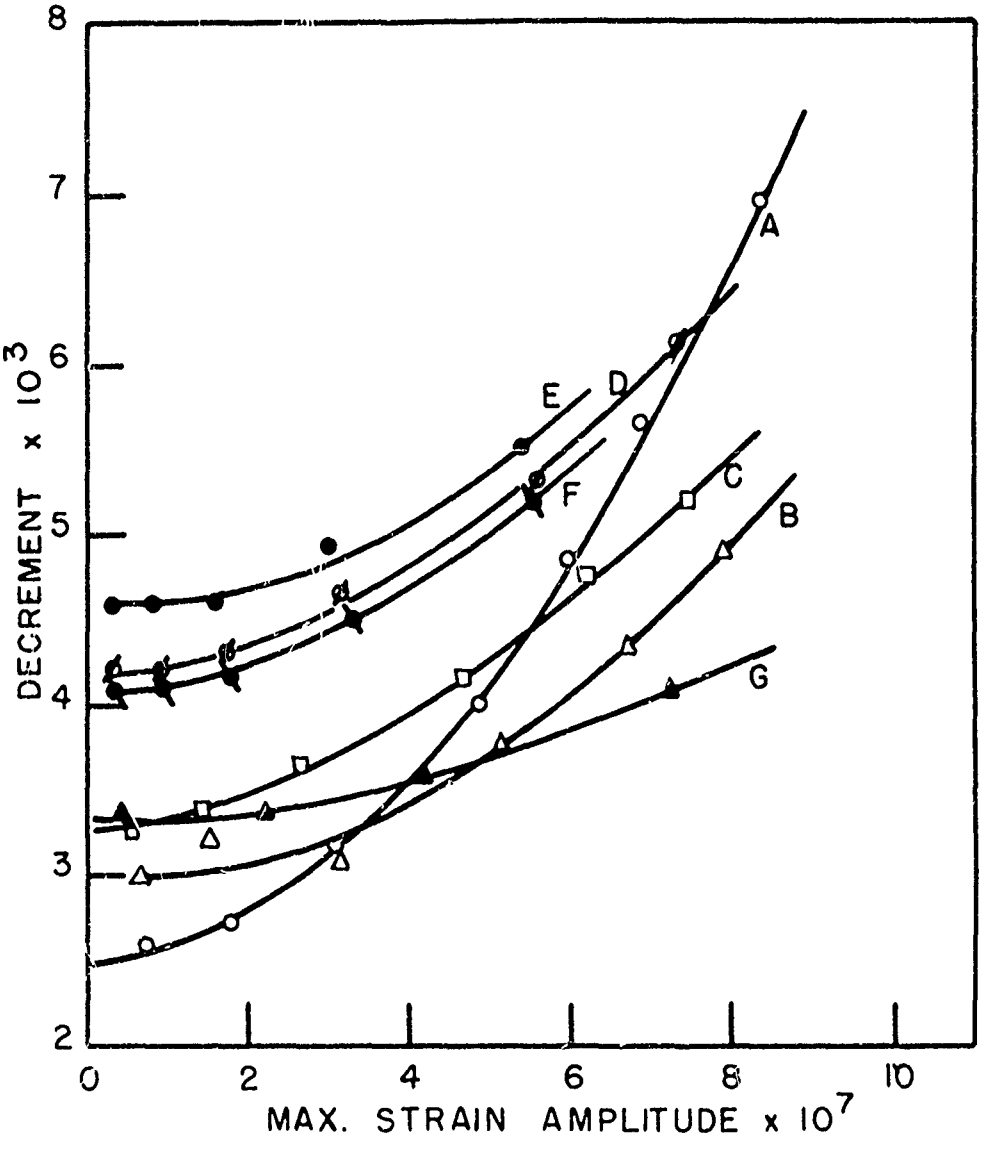

FIG. 5 EFFECT OF TORSIONAL STRAIN ON INTERNAL FRICTION

Ag 1

TOTAL TORSIONAL STRAIN

A AS GROWN

B 2.93×10^{-4} in/in

C 4.42×10^{-4} in/in

D 9.75×10^{-4} in/in

E 11.5×10^{-4} in/in

F 15.0×10^{-4} in/in

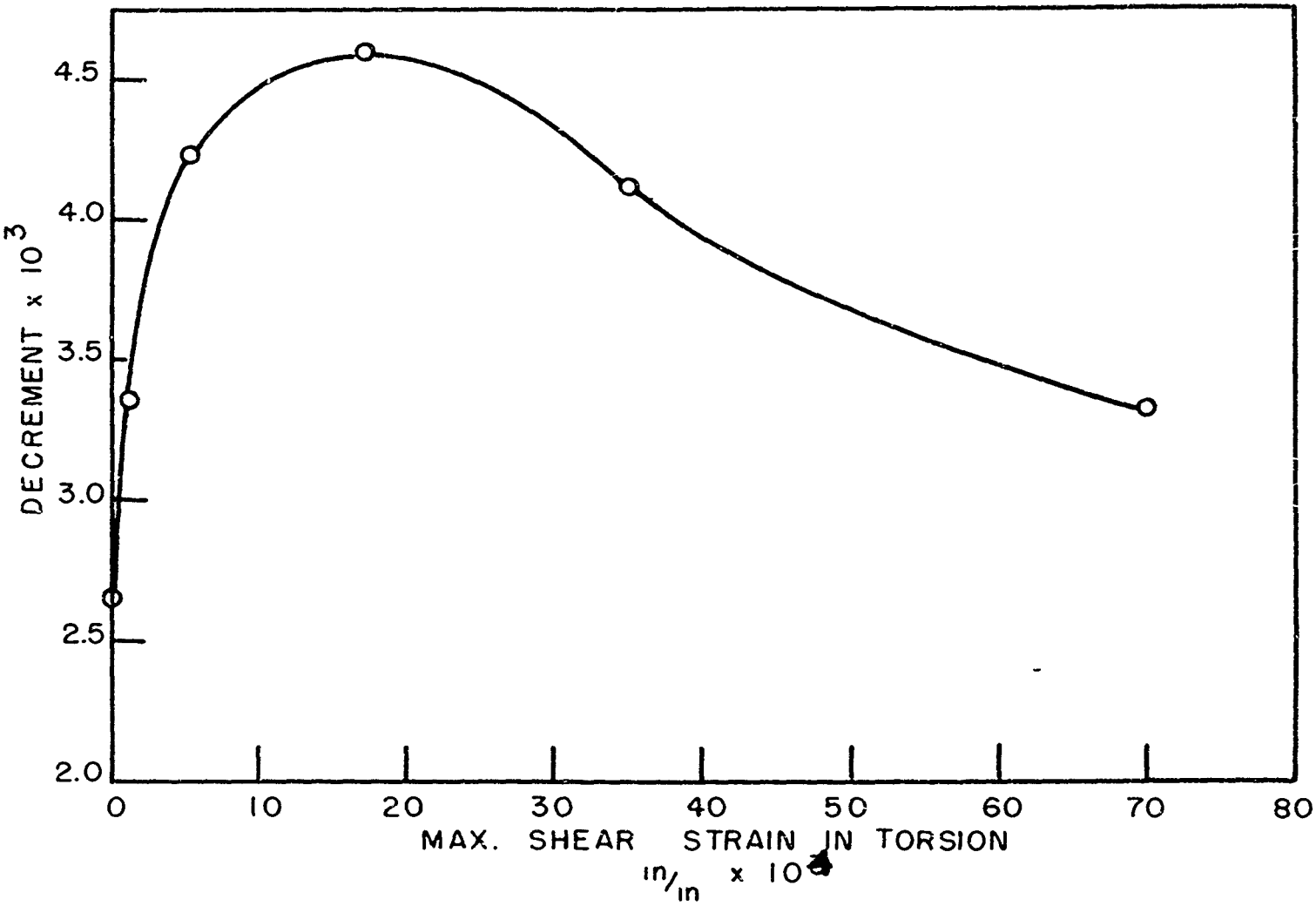

FIG. 6 EFFECT OF TORSIONAL STRAIN ON INTERNAL FRICTION

Ag 1 MAXIMUM STRAIN AMPLITUDE 1x 10^{-7} in/in

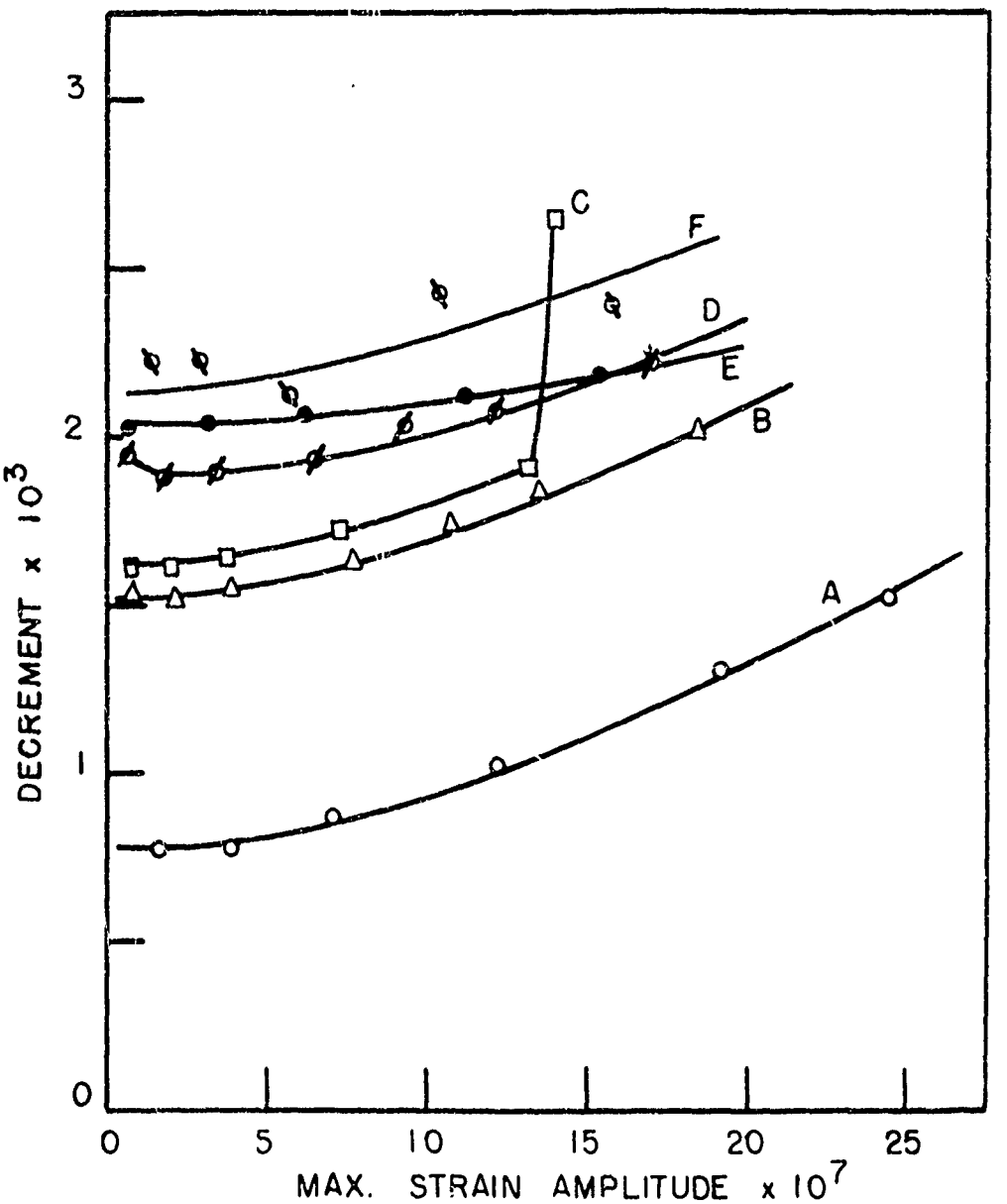

FIG. 7 EFFECT OF TORSIONAL STRAIN ON INTERNAL FRICTION

Ag 2

TOTAL TORSIONAL STRAIN

A AS GROWN

B 1.5×10^{-4} in/in

C 7.2×10^{-4} in/in

D 15.2×10^{-4} in/in

E 27.2×10^{-4} in/in

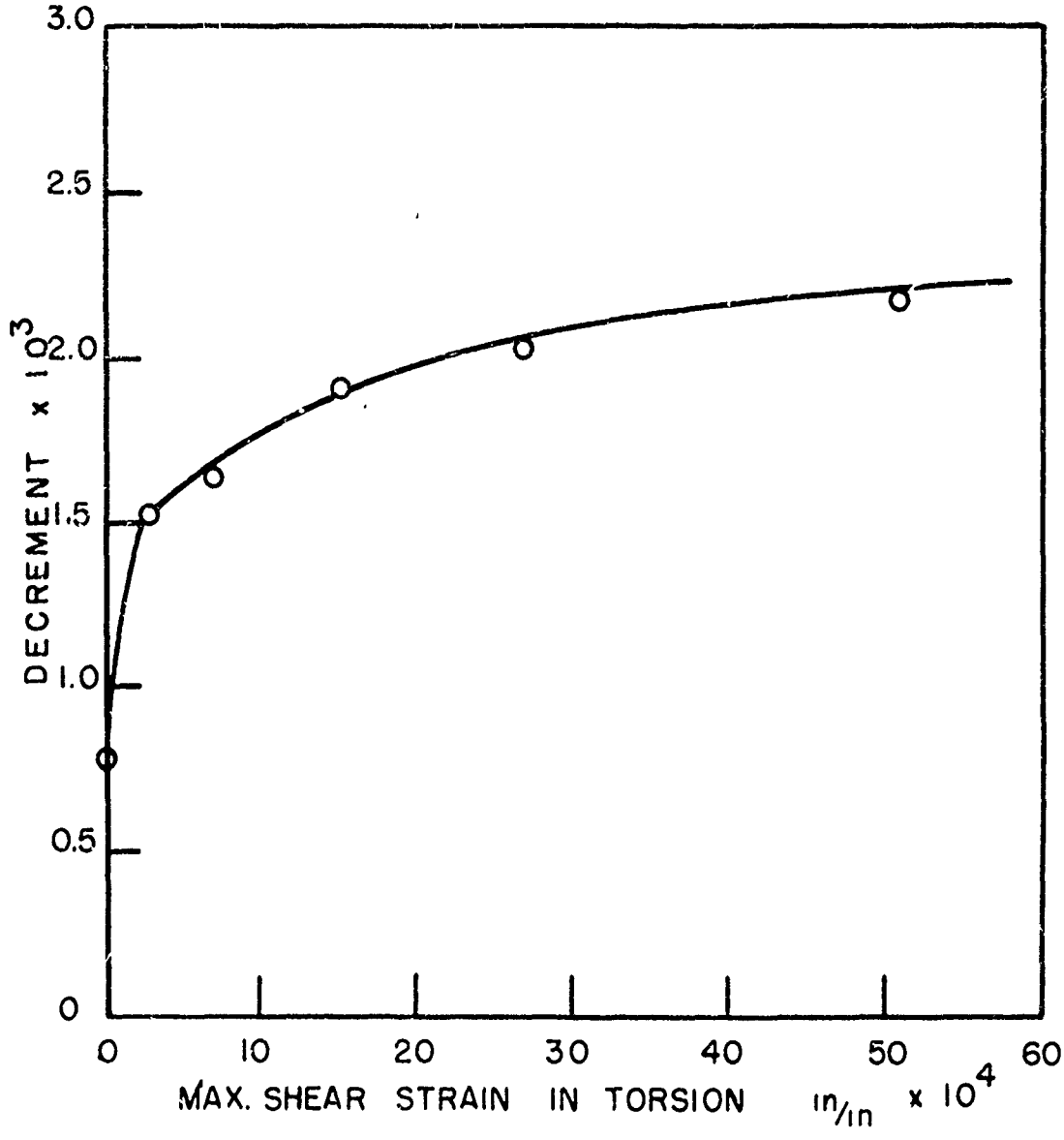

FIG. 8 EFFECT OF TORSIONAL STRAIN ON INTERNAL FRICTION

Ag 2 MAXIMUM STRAIN AMPLITUDE 1 x 10^{-7} in/in

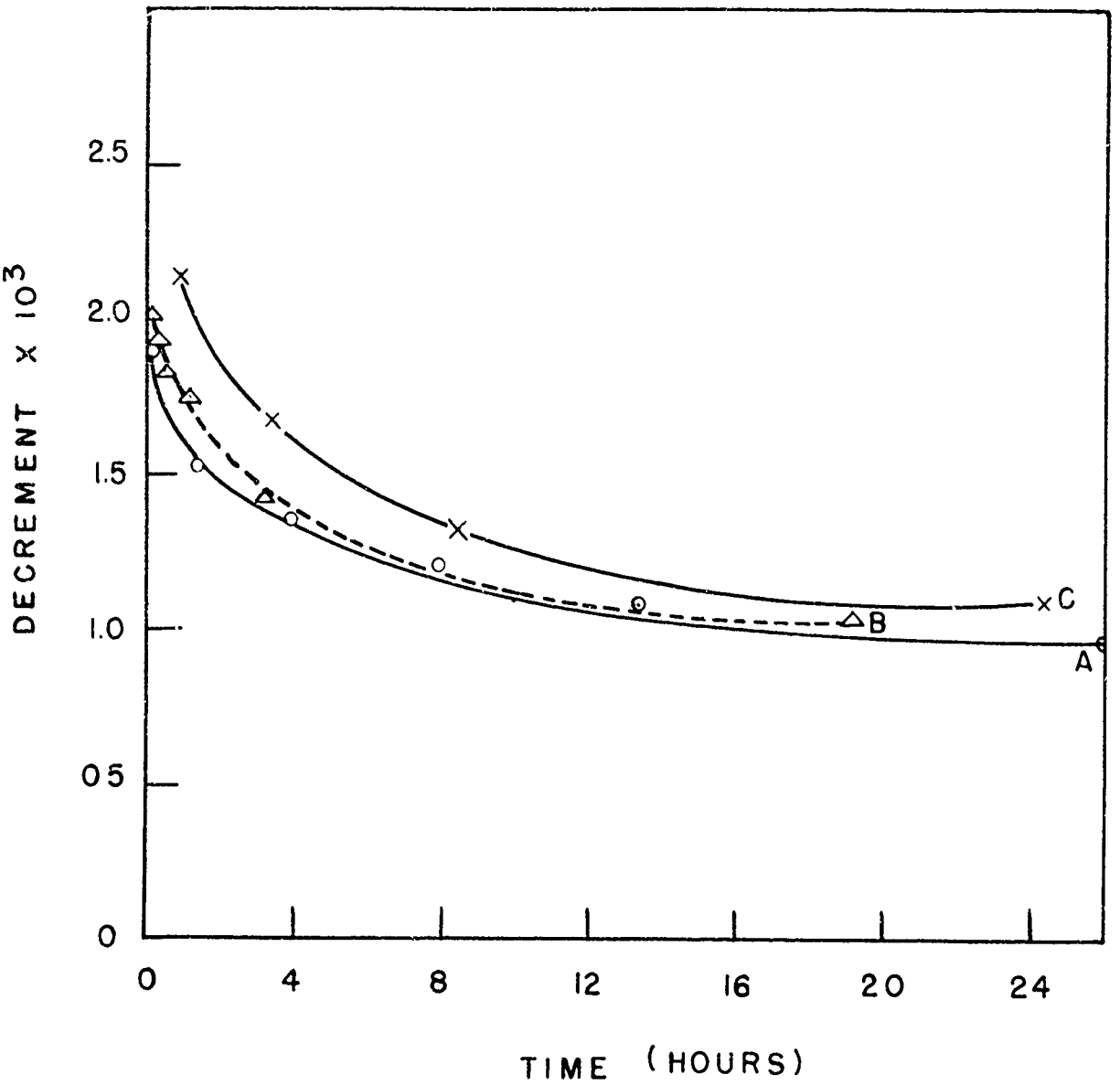

FIG. 9 EFFECT OF ANNEALING ON INTERNAL FRICTION

Ag 2

A DEFORMED 15.2 x 10^{-4} in/in TORSIONAL STRAIN

B DEFORMED 27.2 x 10^{-4} in/in TORSIONAL STRAIN

C DEFORMED 110 x 10^{-4} in/in TORSIONAL STRAIN,

2 Kg. COMPRESSIVE LOAD

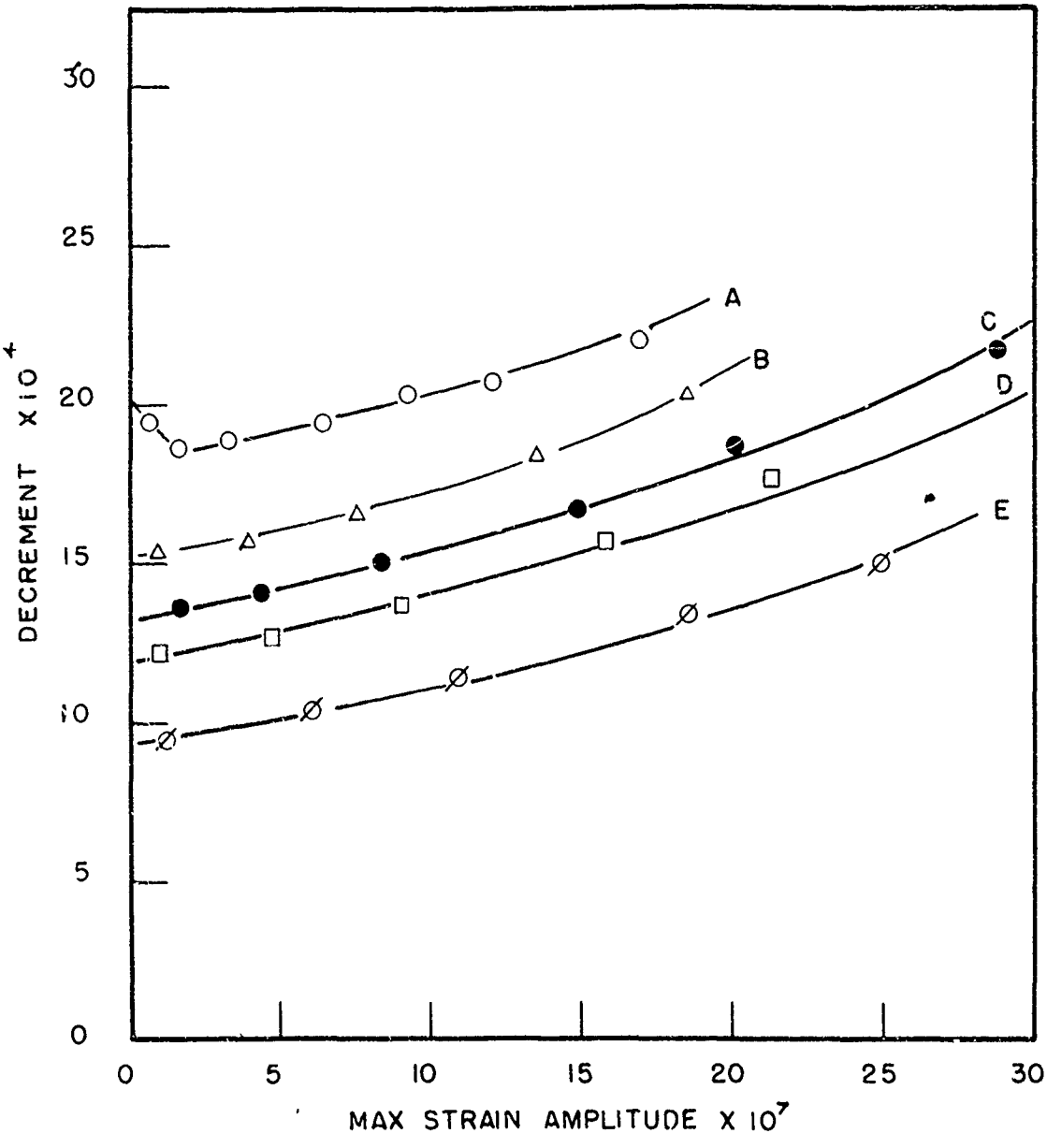

FIG. 10 EFFECT OF ANNEALING ON INTERNAL FRICTION

Ag 2 DEFORMED 15.2 x 10^{-4} in/in TORSIONAL STRAIN

A 13 MINUTES AT 25° C

B 90 MINUTES AT 25° C

C 240 MINUTES AT 25° C

D 480 MINUTES AT 25° C

E 1110 MINUTES AT 25° C

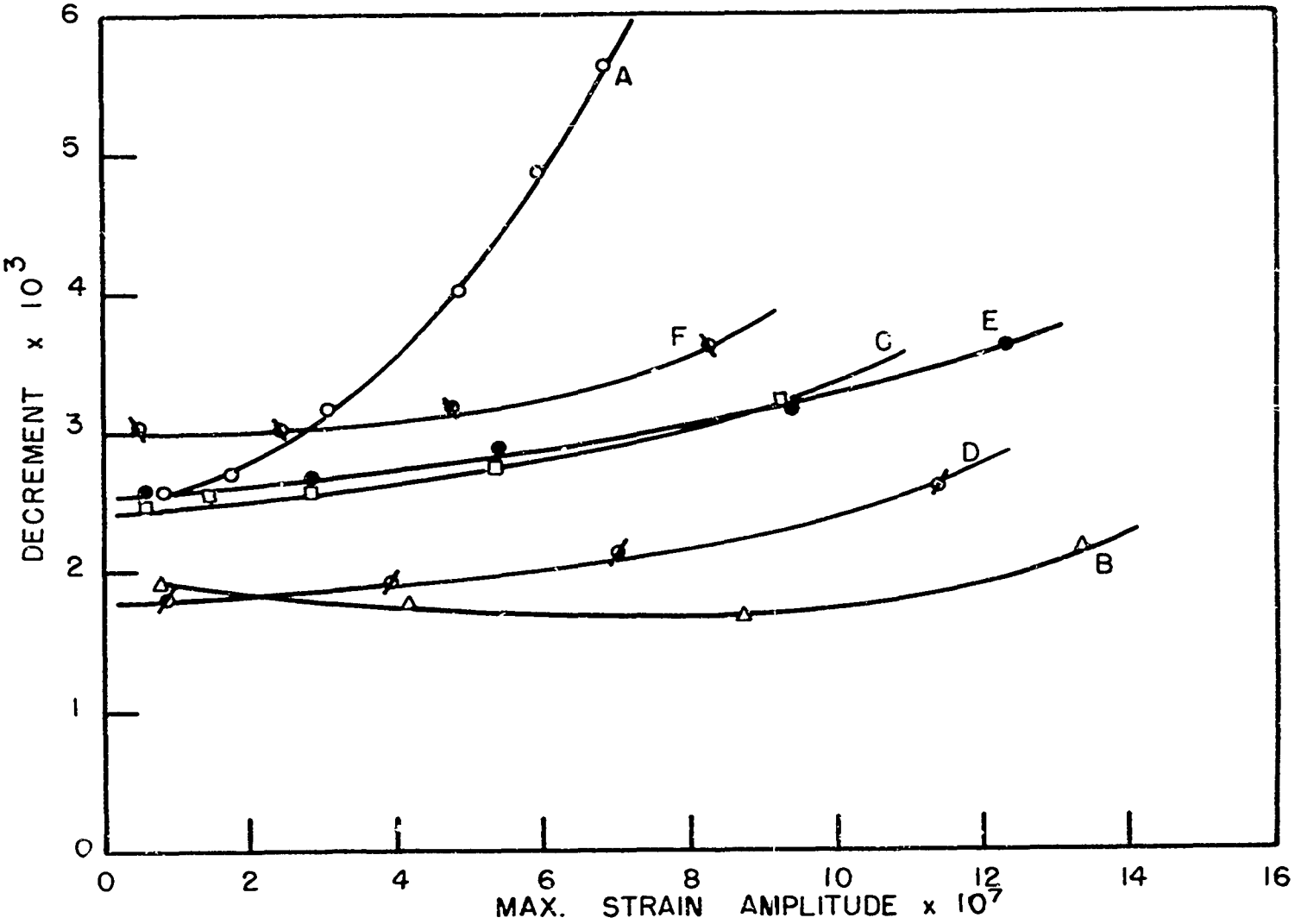

FIG. 11 EFFECT OF DEFORMATION ON INTERNAL FRICTION Ag 1

A AS GROWN.

B .12 in/in TORSIONAL STRAIN, 15 HOURS AT 25° C

C 2 Kg. COMPRESSIVE LOAD.

D 5.5 HOURS AT 25° C

E 4 Kg. COMPRESSIVE LOAD

F .01 in/in TORSIONAL DEFORMATION

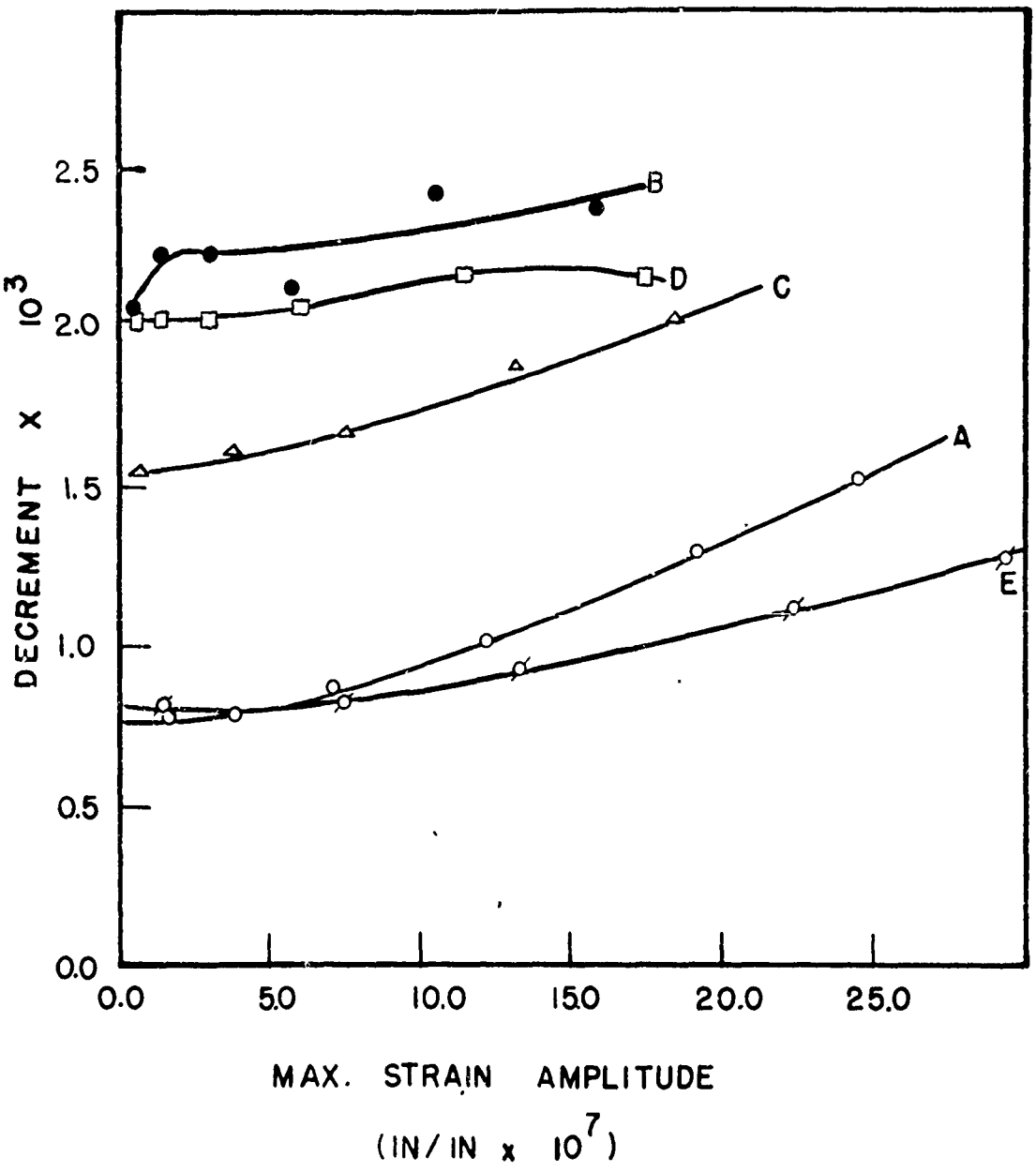

FIG. 12 EFFECT OF DEFORMATION ON THE INTERNAL FRICTION

Ag 2

A AS GROWN

B 51.2×10^{-4} in/in TORSIONAL STRAIN

C 150 MINUTES AT 25° C

D 2 Kg. COMPRESSIVE LOAD

E 24 HOURS AT 25° C

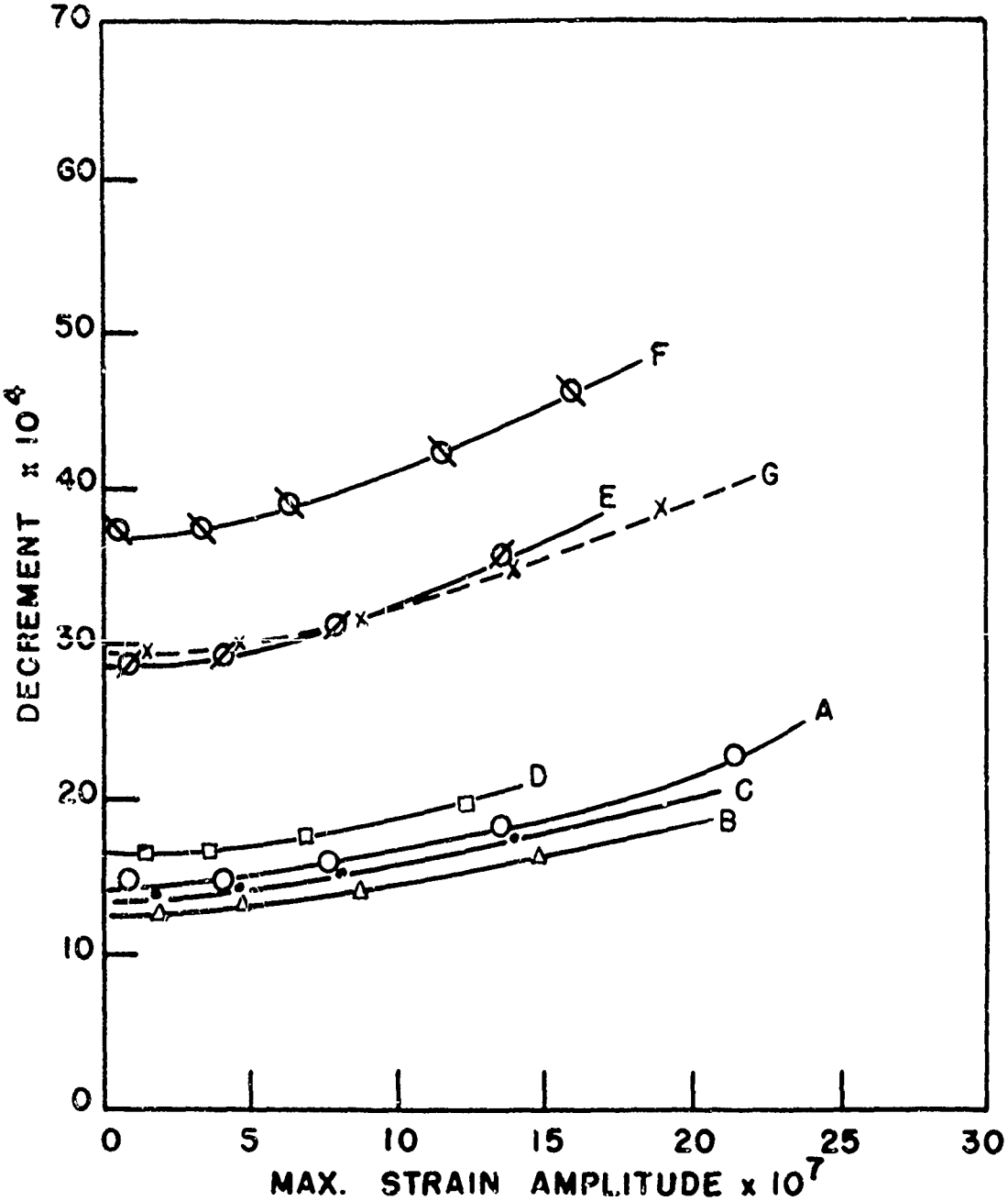

FIG. 13 EFFECT OF TORSIONAL DEFORMATION ON INTERNAL FRICTION

Cu 1 0.1 % Al

TOTAL TORSIONAL STRAIN

A AS GROWN
B 3.5 x 10^{-4} in/in
C 10.5 x 10^{-4} in/in
D 21.0 x 10^{-4} in/in
E 31.5 x 10^{-4} in/in
F 49.0 x 10^{-4} in/in
G 84.0 x 10^{-4} in/in

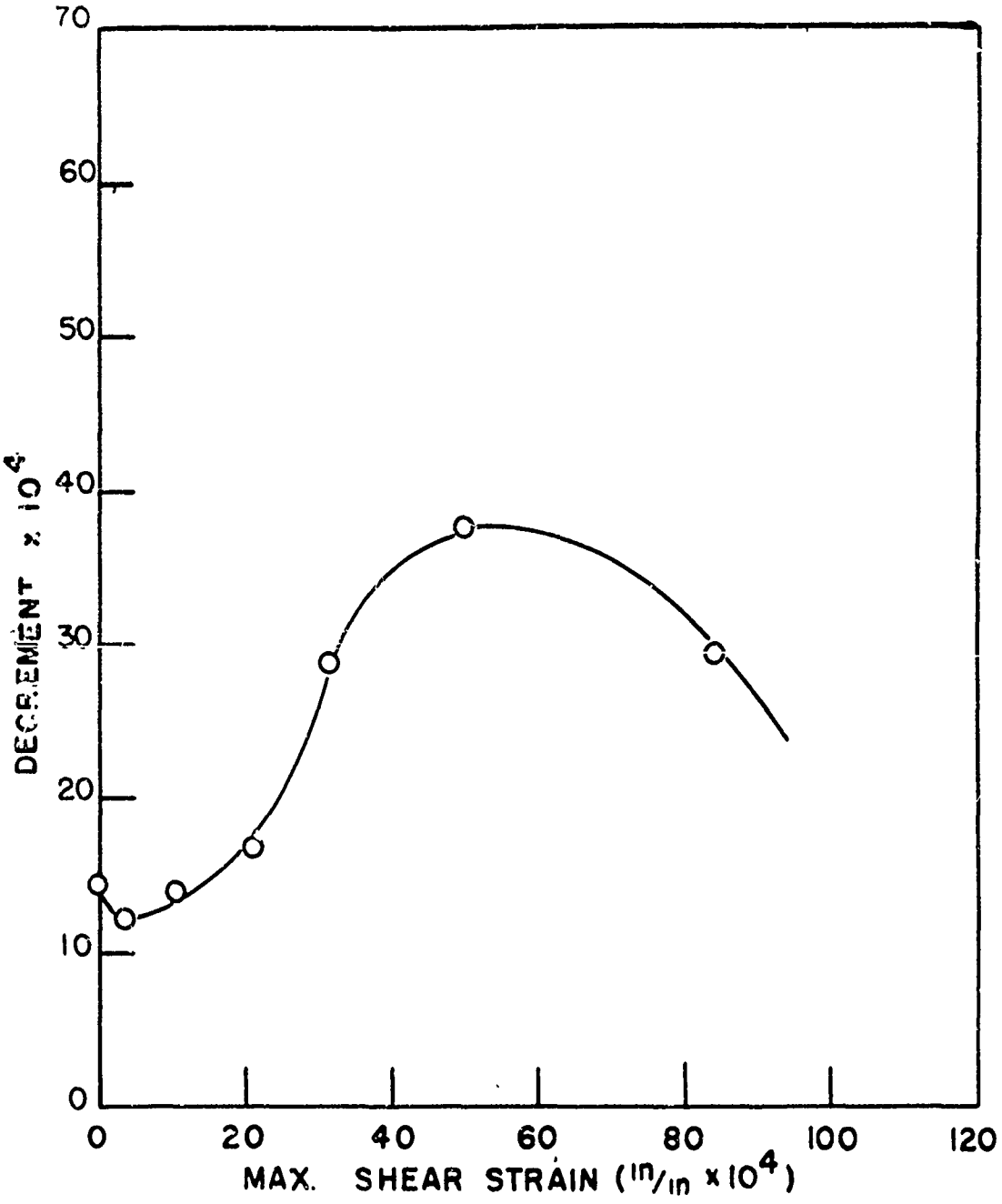

FIG. 14 EFFECT OF TORSIONAL DEFORMATION ON INTERNAL FRICTION

Cu 1 0.1 % Al

SPECIMEN INITIALLY UNDEFORMED

MAXIMUM STRAIN AMPLITUDE 2.5×10^{-7} in/in

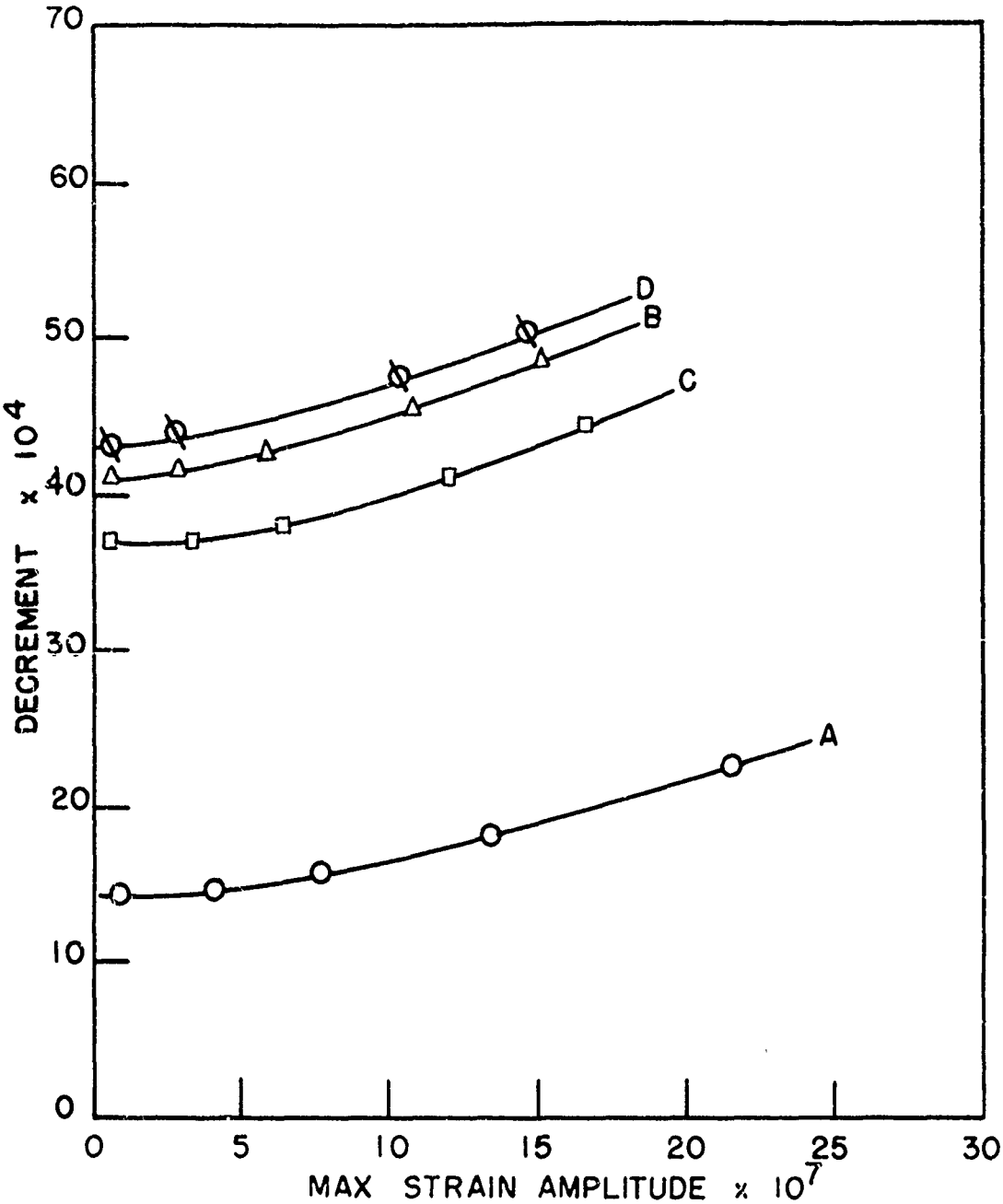

FIG. 15 EFFECT OF DEFORMATION ON INTERNAL FRICTION

A AS GROWN Cu 1 0.1 % Al

B 339 x 10^{-4} in/in TORSIONAL DEFORMATION,
9.2 x 10^{-4} in/in COMPRESSIONAL DEFORMATION

C 52 x 10^{-4} in/in TORSIONAL DEFORMATION

D 17.5 x 10^{-4} in/in TORSIONAL DEFORMATION

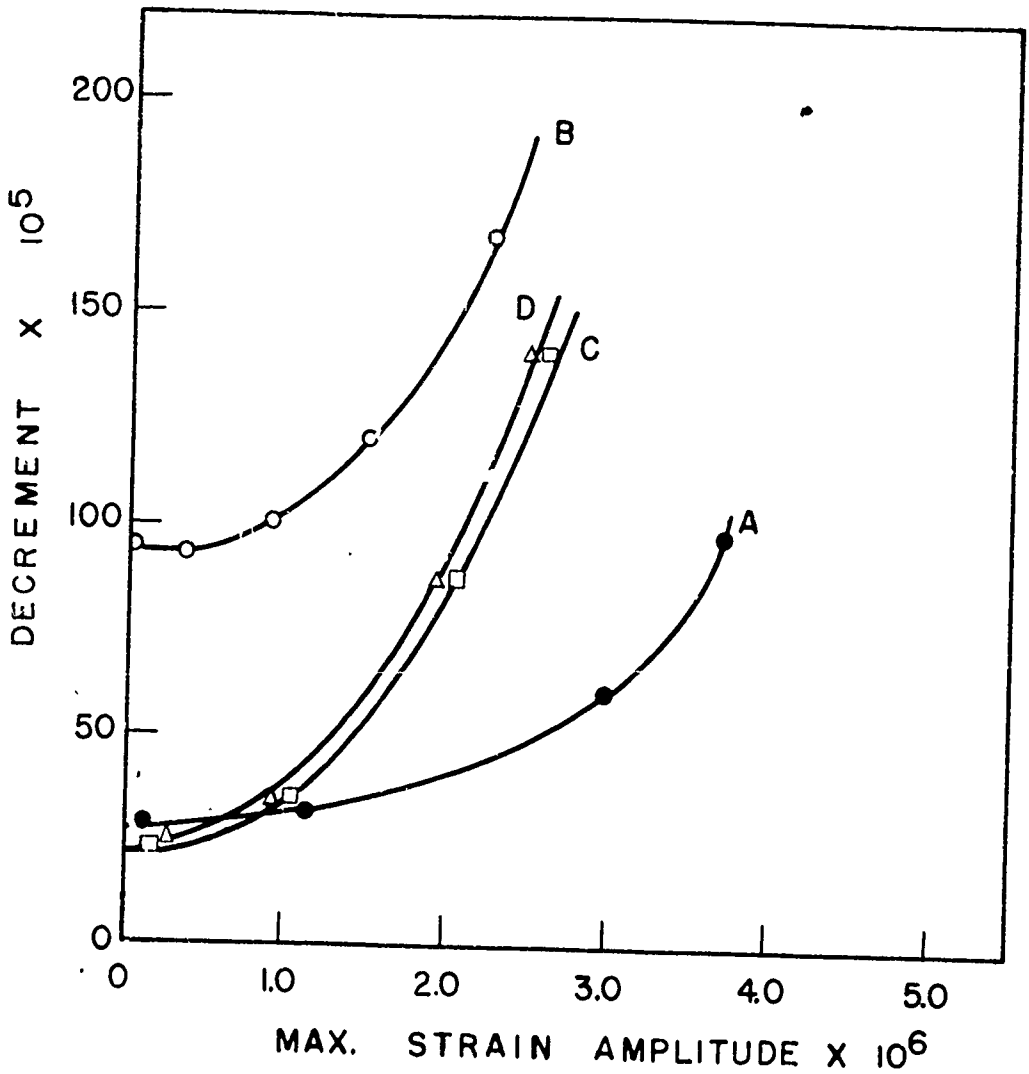

FIG. 16 EFFECT OF TORSIONAL STRAIN ON INTERNAL FRICTION Al H.P. 3b

TOTAL TORSIONAL STRAIN

A AS GROWN

B 1.71×10^{-4} in/in

C 5.81×10^{-4} in/in

D 8.89×10^{-4} in/in

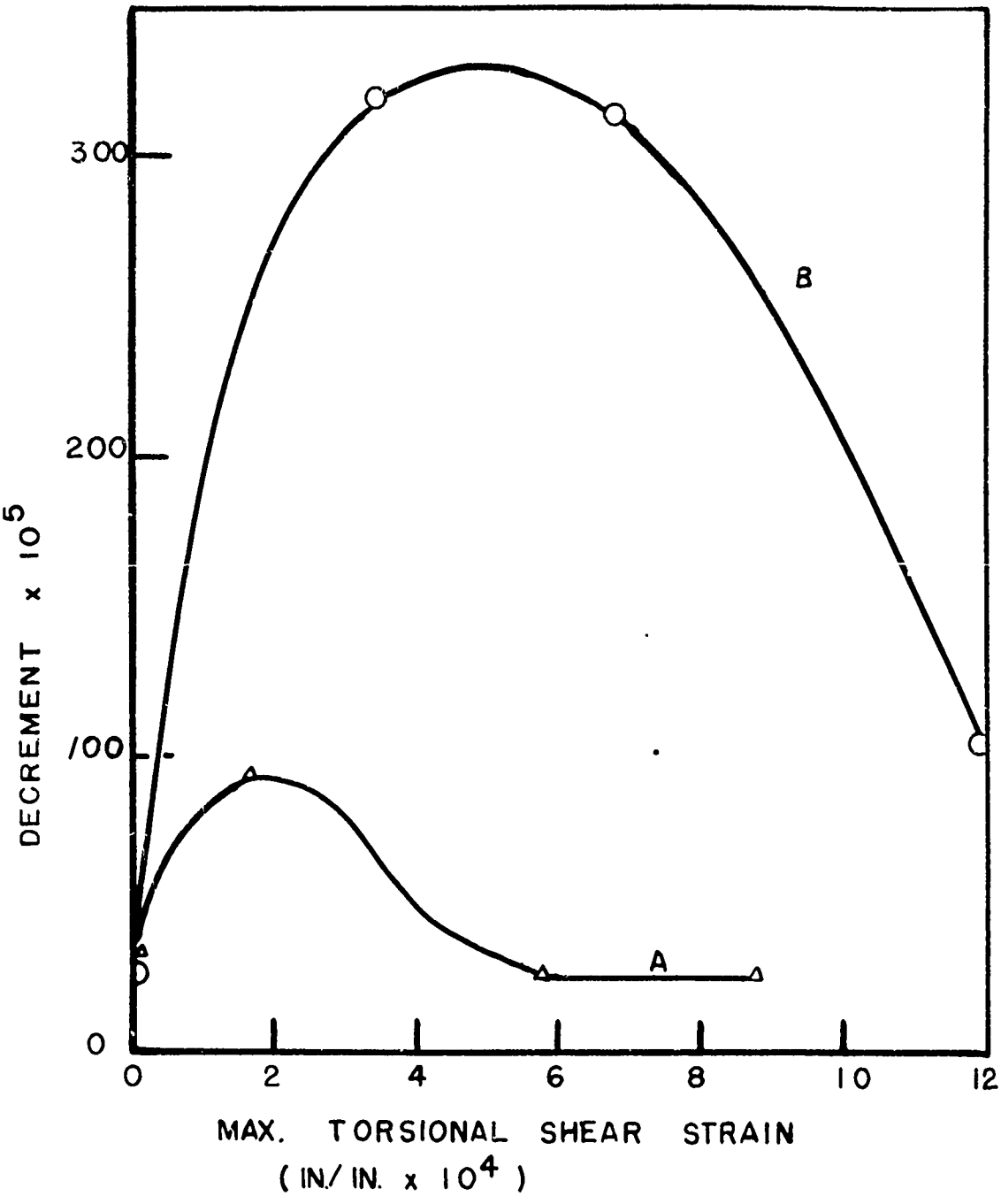

FIG. 17 EFFECT OF TORSIONAL DEFORMATION ON INTERNAL FRICTION Al H.P. 3b

A INITIALLY UNDEFORMED

B INITIALLY DEFORMED 15.7 x 10^{-4} in/in TORSIONAL STRAIN, 6 x 10^{-4} in/in COMPRESSIONAL STRAIN

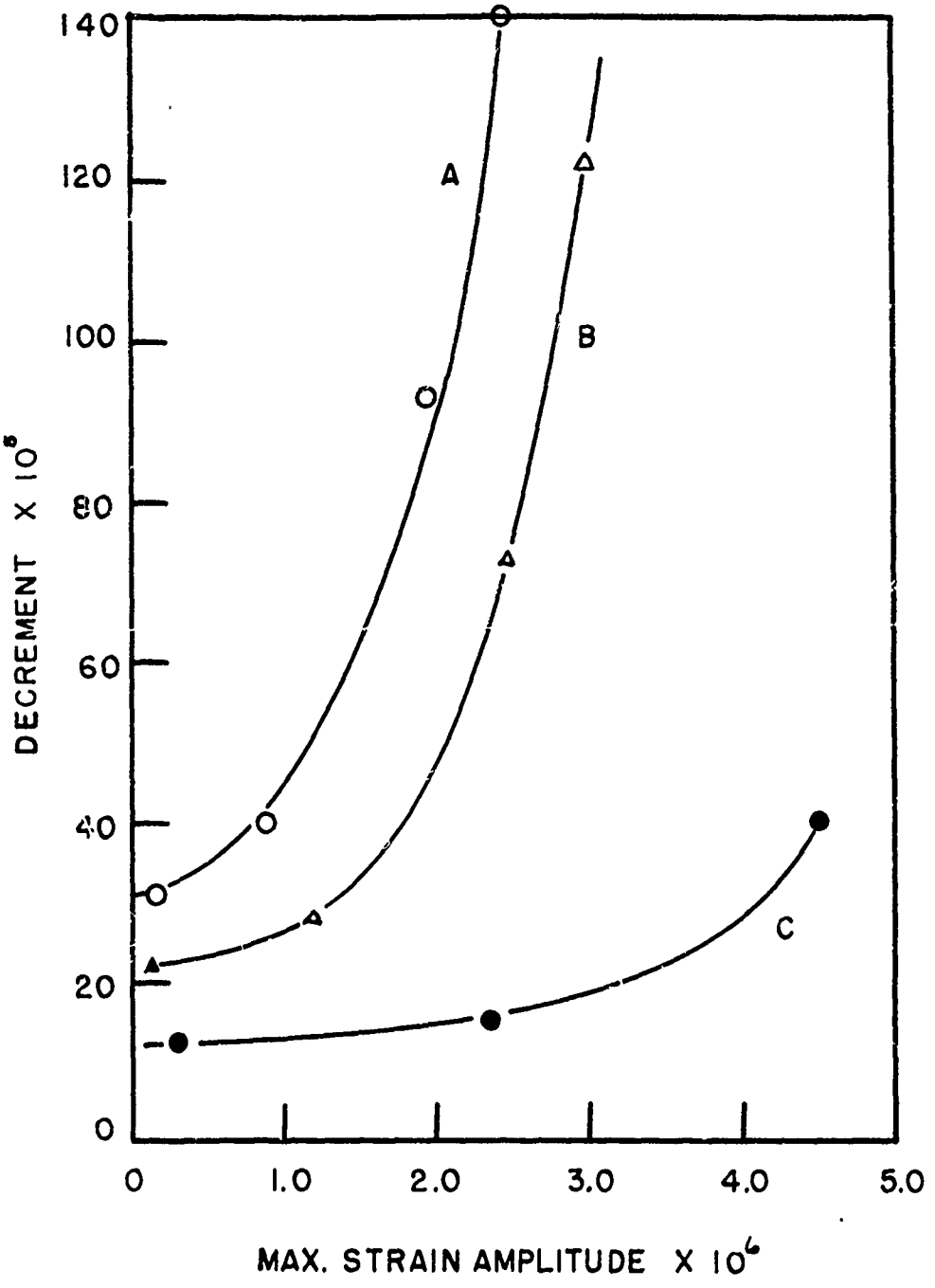

FIG. 18 EFFECT OF ANNEALING AT 25° C

Al H.P. 3b DEFORMED 16.7 x 10^{-4} in/in

TORSIONAL STRAIN, 3 x 10^{-4} in/in COMPRESSION

A 7 MINUTES AT 25° C
B 17 MINUTES AT 25° C
C 945 MINUTES AT 25° C

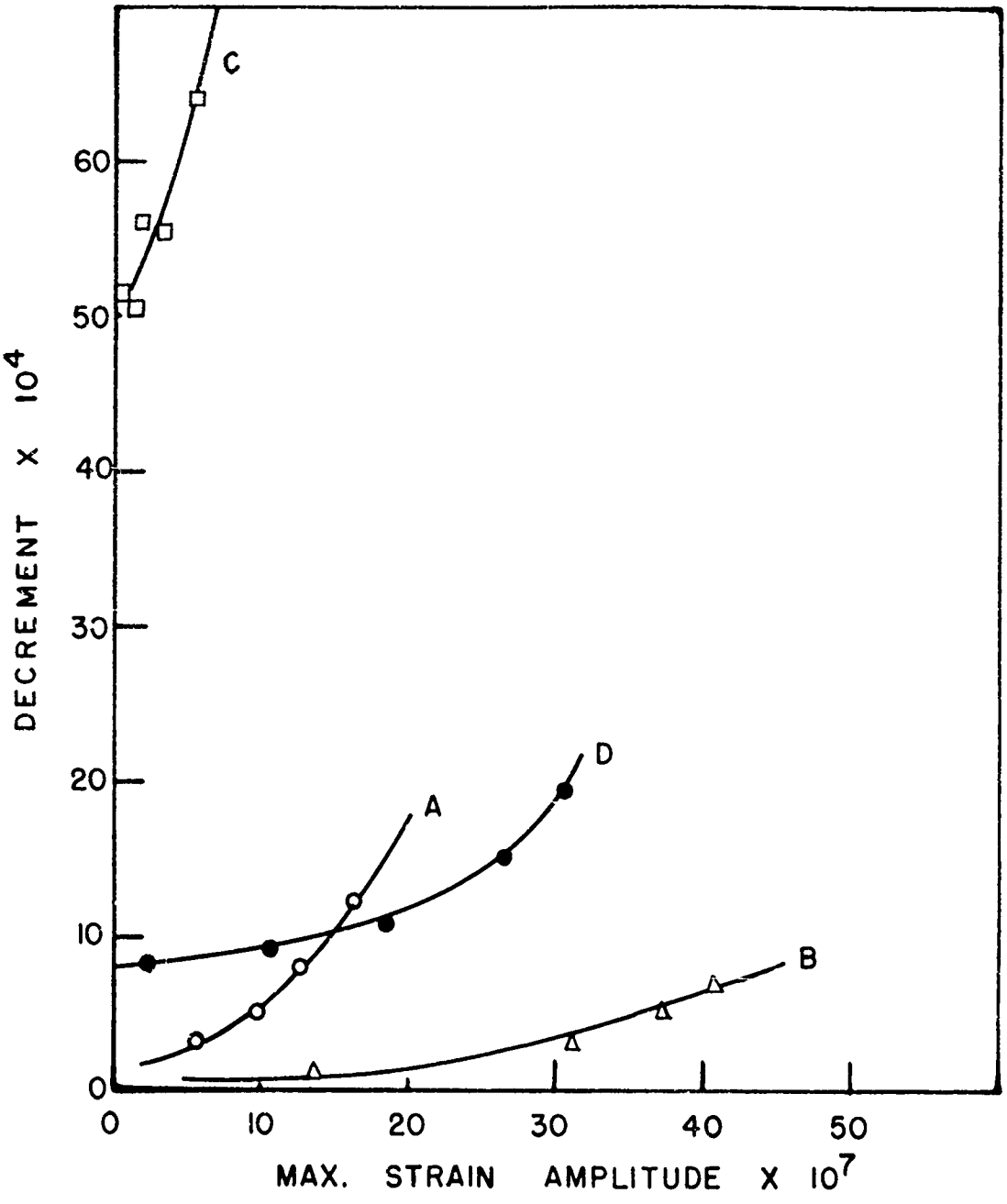

FIG. 19 EFFECT OF ANNEALING AT 25° C ON INTERNAL FRICTION

Al H.P. 6

A 11.1 x 10^{-4} in/in COMPRESSIONAL STRAIN

B 1100 MINUTES AT 25° C

C 40.7 x 10^{-4} in/in COMPRESSIONAL STRAIN

D 4320 MINUTES AT 25° C

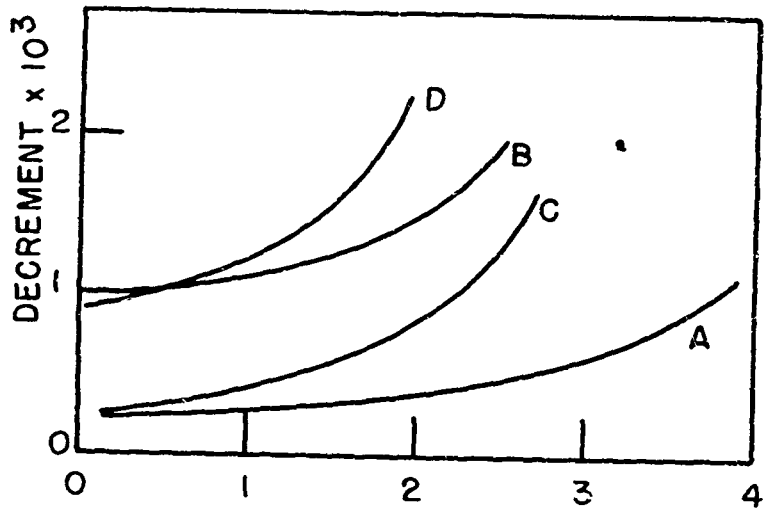

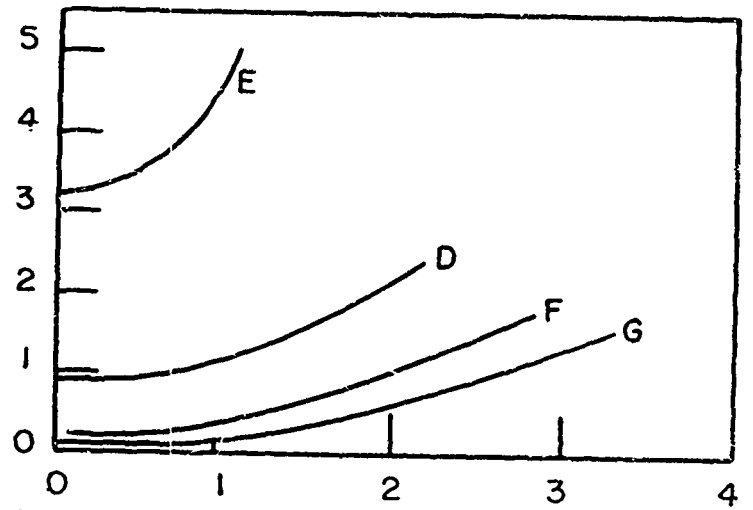

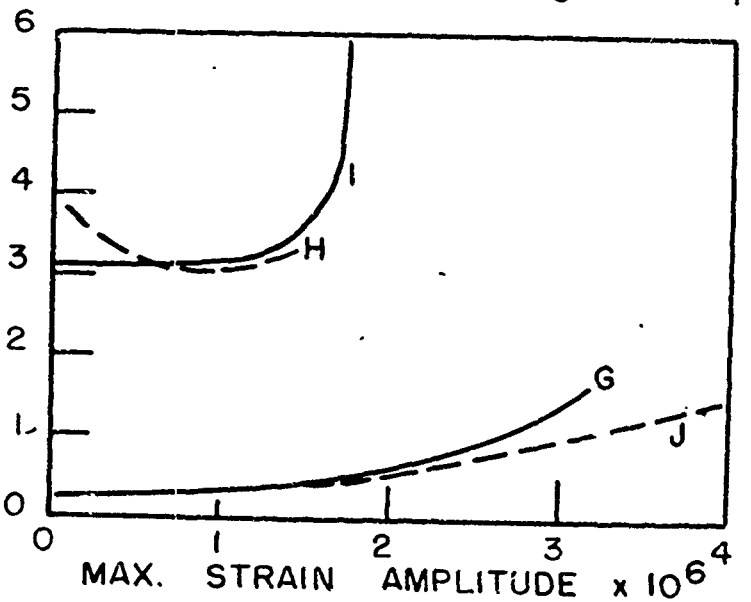

FIG. 20 Al H.P. 3b

A AS GROWN

B 1.71×10^{-4} in/in TORSIONAL STRAIN

C 8.89×10^{-4} in/in TORSIONAL STRAIN

D 3×10^{-4} in/in COMPRESSIONAL STRAIN

E 3.4×10^{-4} in/in TORSIONAL STRAIN

F 3.4×10^{-4} in/in TORSIONAL STRAIN

G 3×10^{-4} in/in COMPRESSIONAL STRAIN

H 3.4×10^{-4} in/in TORSIONAL STRAIN

I 3.4×10^{-4} in/in TORSIONAL STRAIN

J 6.8×10^{-4} in/in TORSIONAL STRAIN

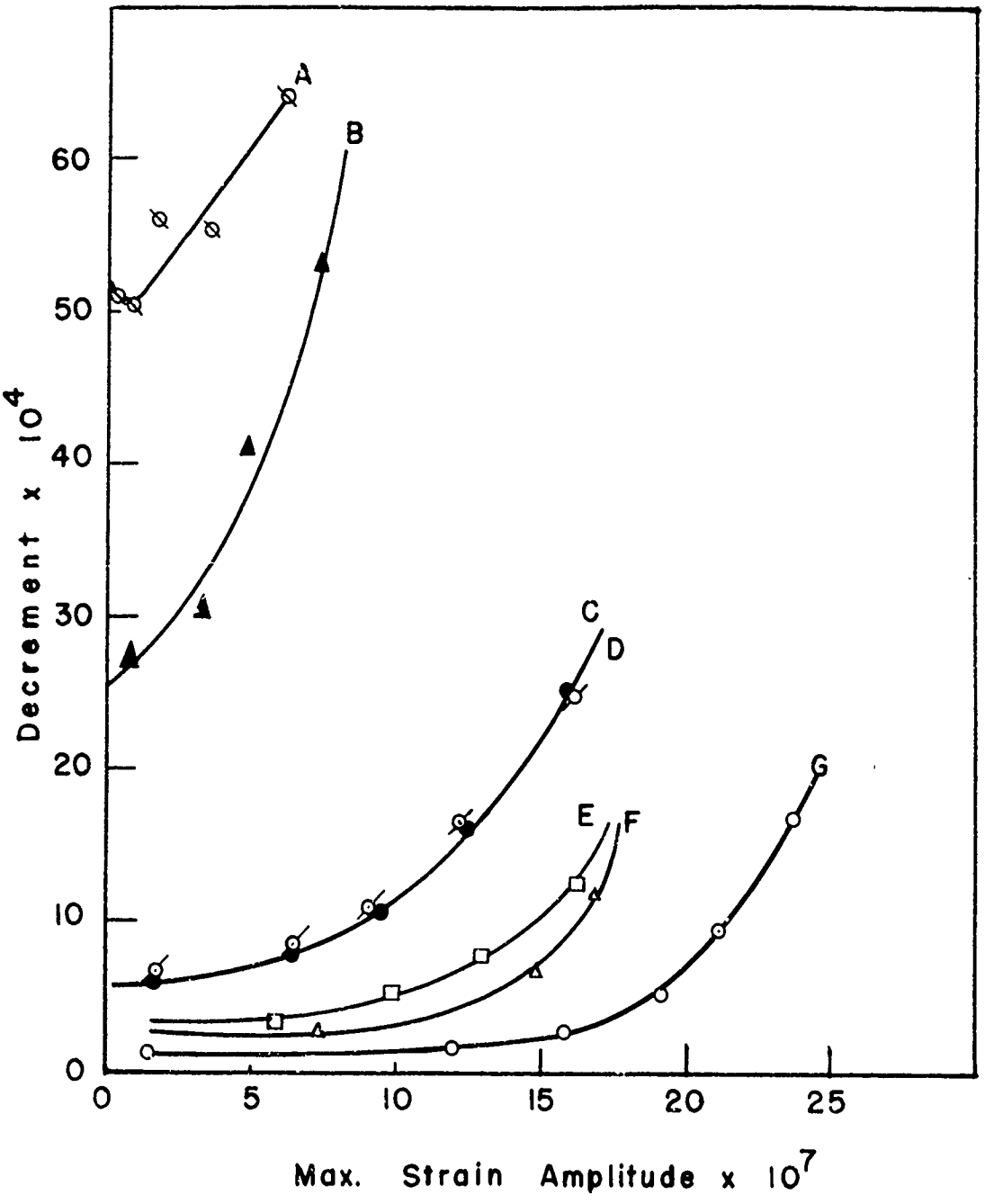

FIG. 21 EFFECT OF DEFORMATION ON INTERNAL FRICTION

Al H.P. 6

TOTAL DEFORMATION

A AS GROWN.

B 3.7 x 10^{-4} in/in COMPRESSIONAL STRAIN.

C 11.1 x 10^{-4} in/in COMPRESSIONAL STRAIN.

D 25.9 x 10^{-4} in/in COMPRESSIONAL STRAIN.

E 33.3 x 10^{-4} in/in COMPRESSIONAL STRAIN.

F 40.7 x 10^{-4} in/in COMPRESSIONAL STRAIN, 15 x 10^{-4} in/in TORSIONAL STRAIN.

G 40.7 x 10^{-4} in/in COMPRESSIONAL STRAIN, 30 x 10^{-4} in/in TORSIONAL STRAIN.

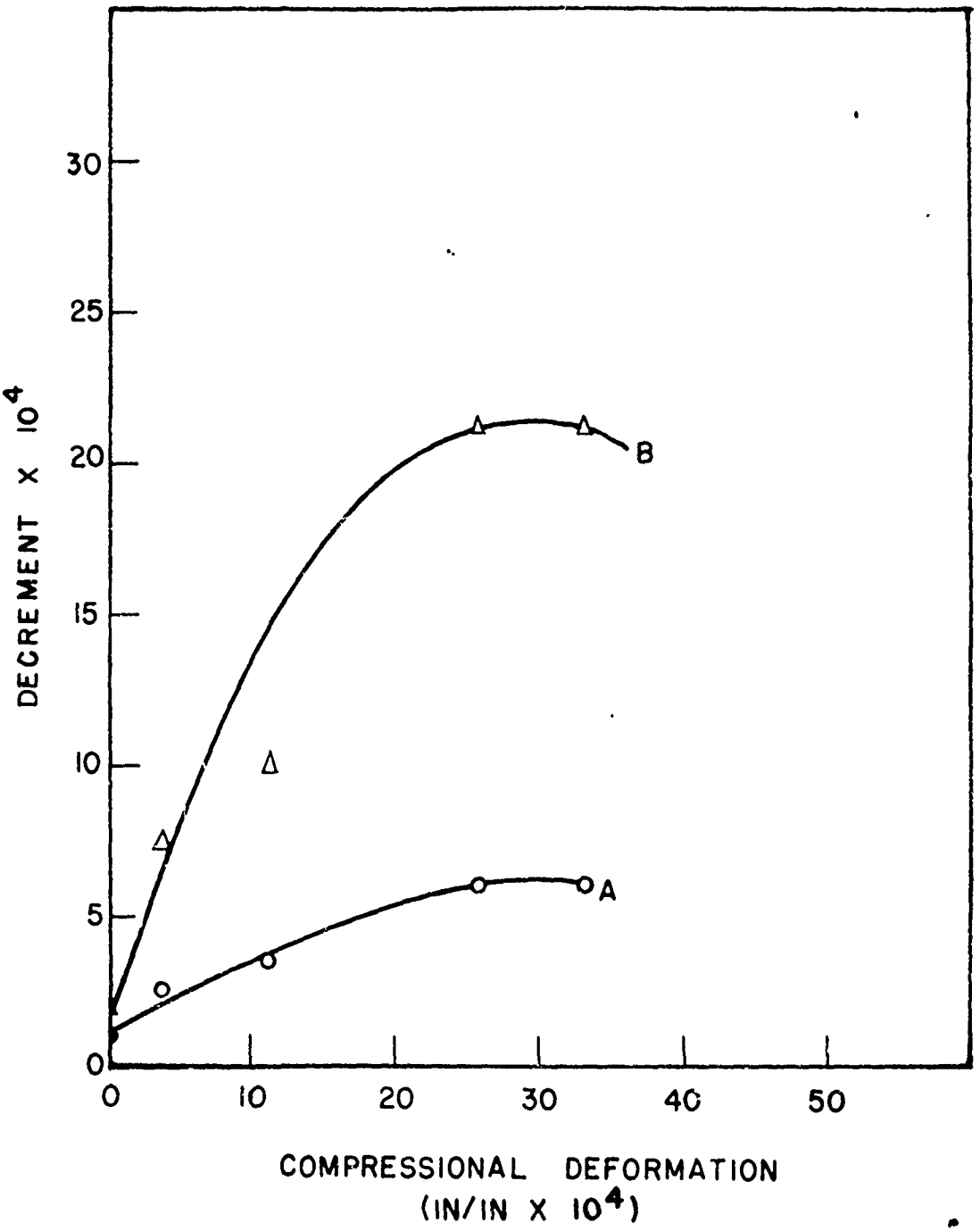

FIG. 22 EFFECT OF COMPRESSIONAL DEFORMATION ON INTERNAL FRICTION Al H.P. 6

A MAXIMUM STRAIN AMPLITUDE 2.5×10^{-7} in/in

B MAXIMUM STRAIN AMPLITUDE 15×10^{-7} in/in

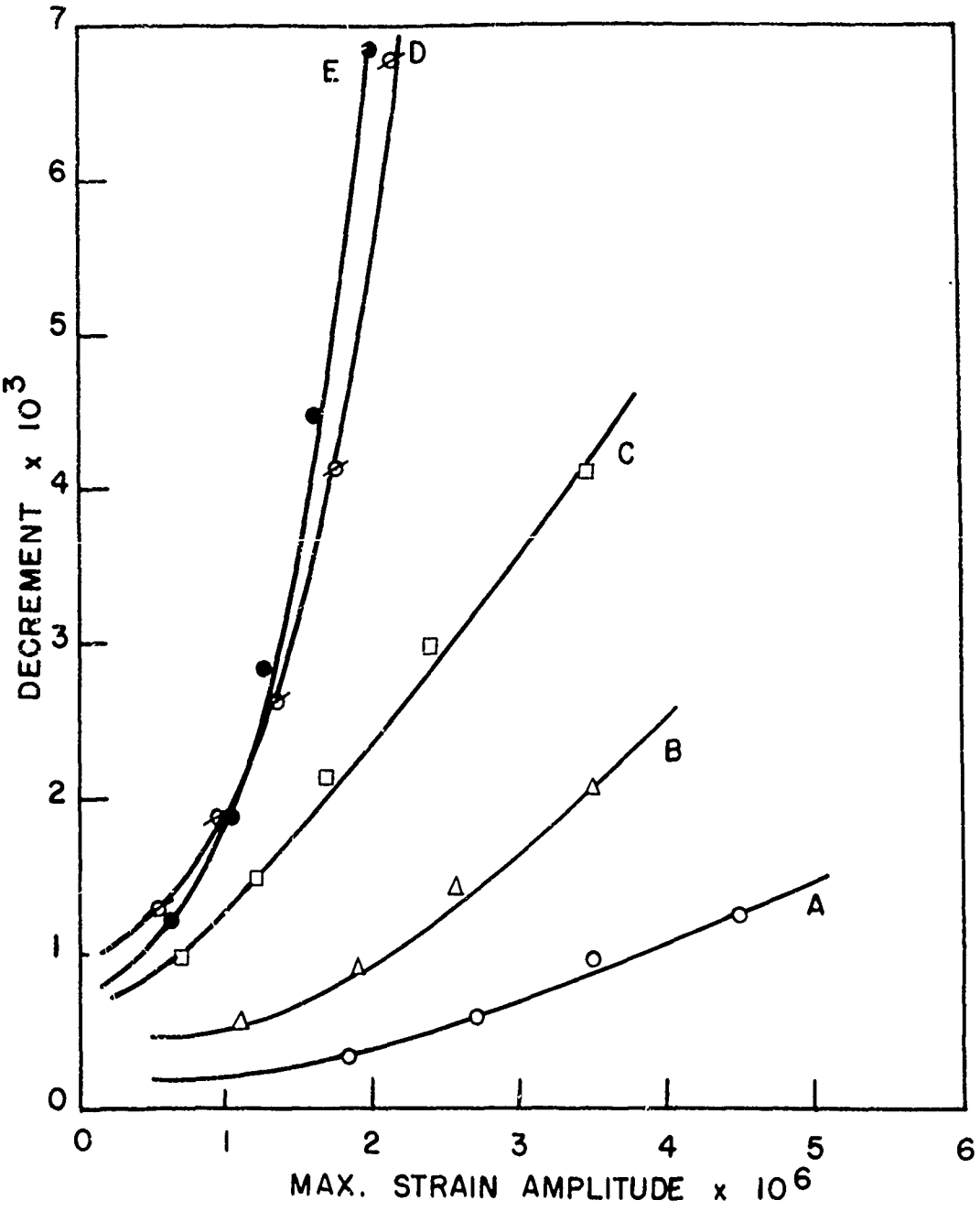

FIG. 23 EFFECT OF DEFORMATION ON INTERNAL FRICTION AS MEASURED BY A TORSIONAL QUARTZ

Al H.P. 4a

A AS GROWN

B 3×10^{-4} in/in COMPRESSIONAL STRAIN

C 6×10^{-4} in/in COMPRESSIONAL STRAIN

D 3.5×10^{-4} in/in TORSIONAL STRAIN

E 7.0×10^{-4} in/in TORSIONAL STRAIN

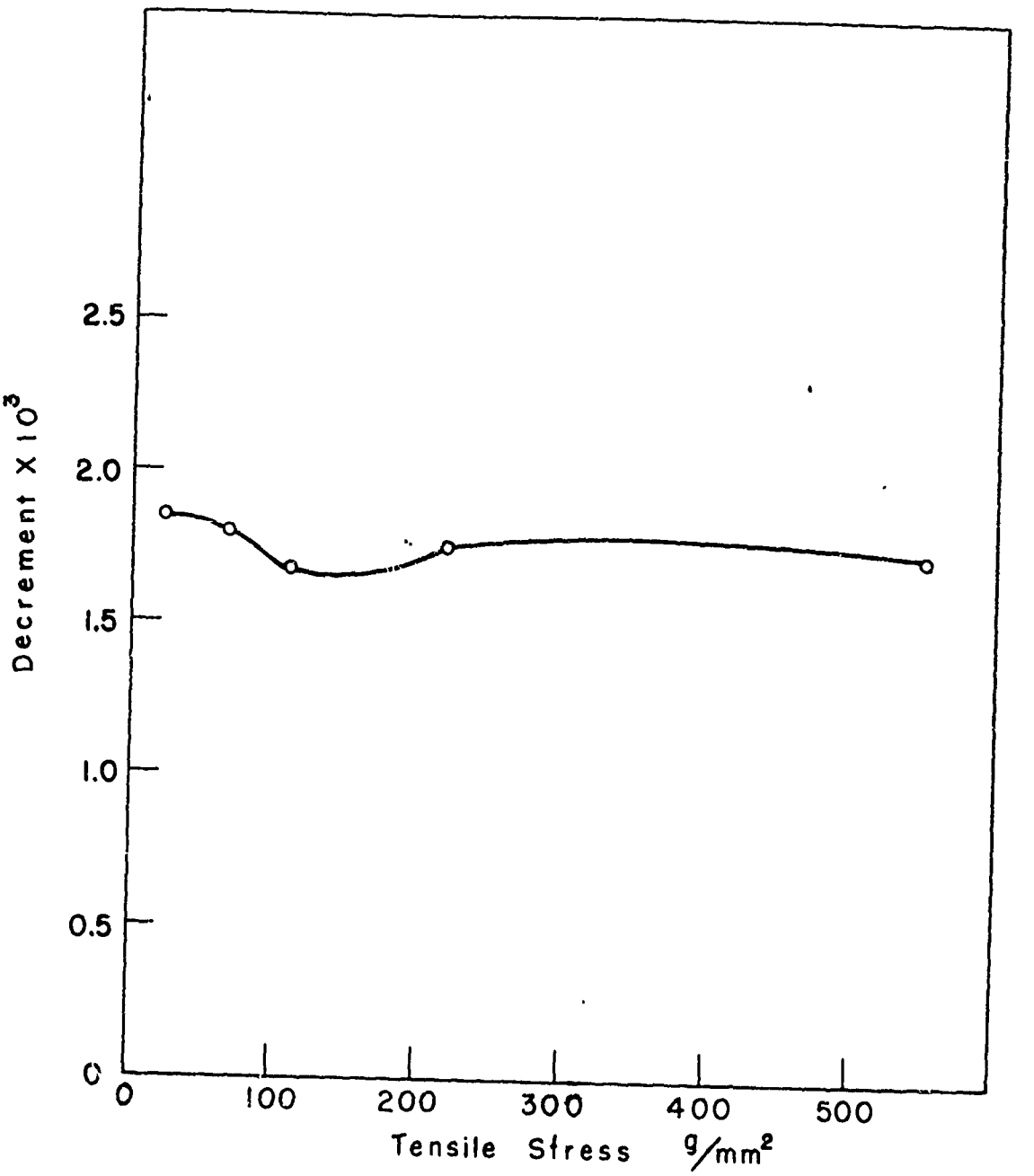

FIG. 24 EFFECT OF TENSILE STRESS ON INTERNAL FRICTION

Cu H.P. 4

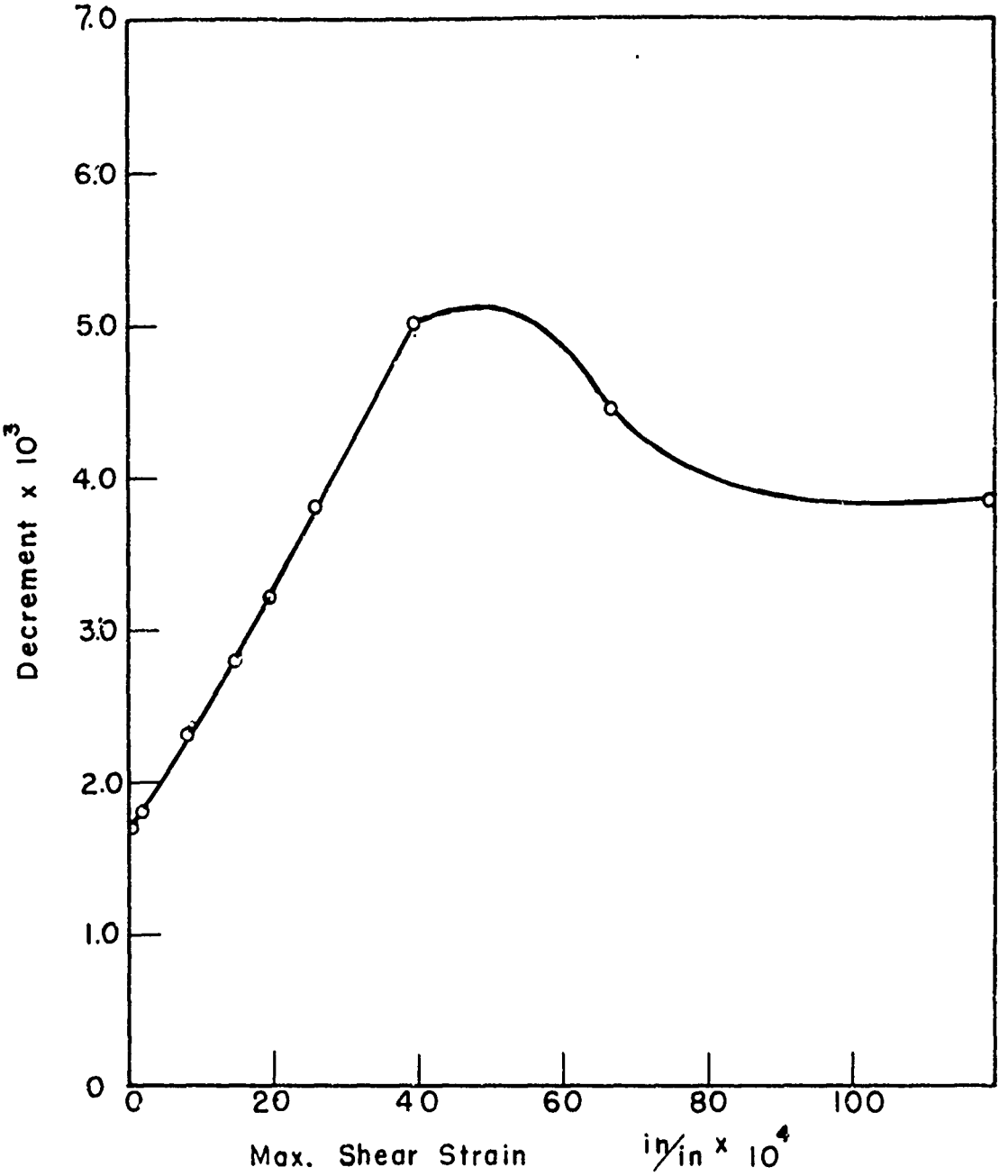

FIG. 25 EFFECT OF TORSIONAL DEFORMATION ON INTERNAL FRICTION

O.F.H.C. Cu 1

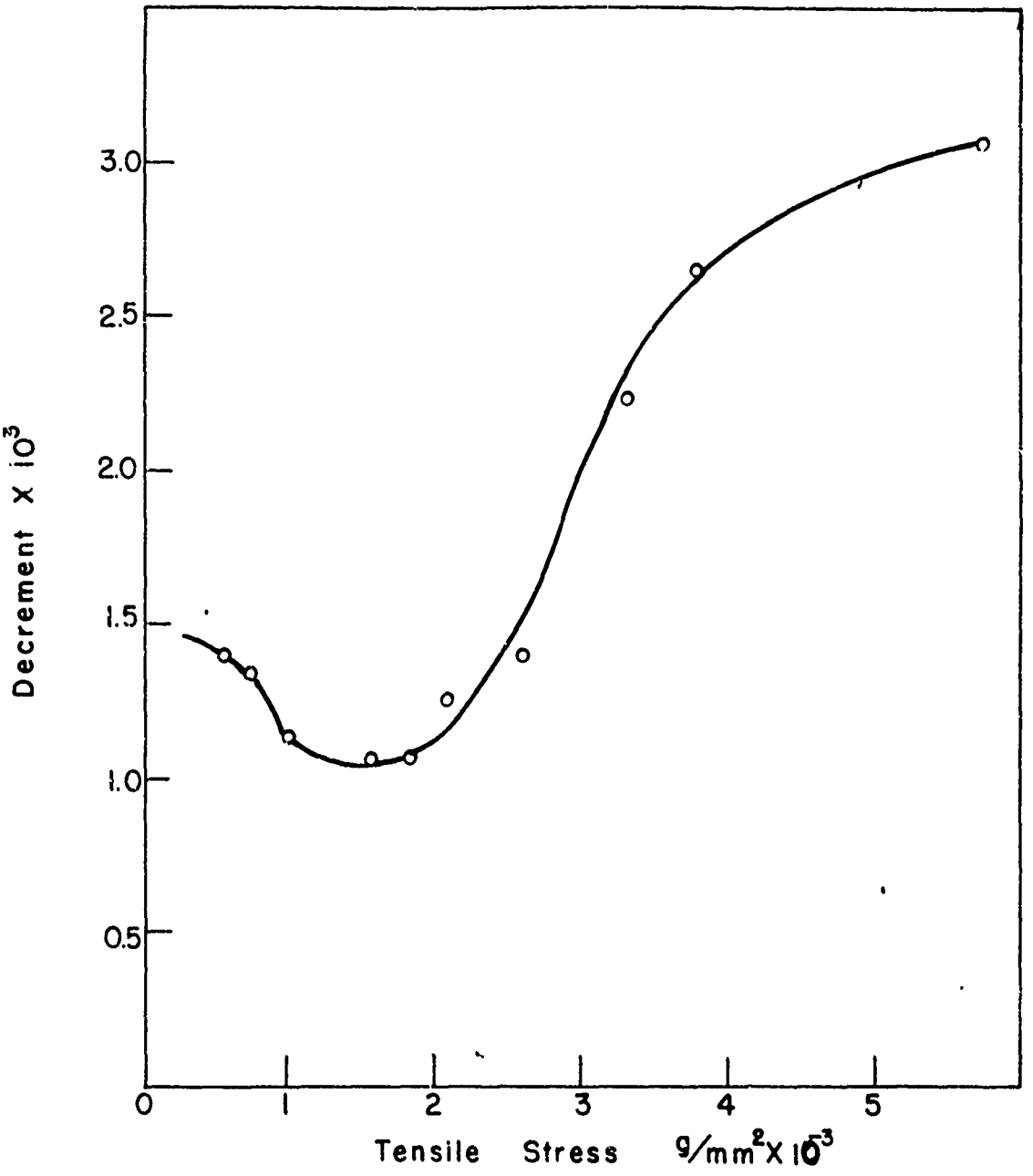

FIG. 26 EFFECT OF TENSILE STRESS ON INTERNAL FRICTION

O.F.H.C. Cu 2